ABSTRACT

Title of Dissertation: PHENOLOGY OF CYANOBACTERIAL BLOOMS IN THREE CATCHMENTS OF THE LAURENTIAN GREAT LAKES

Timothy Todd Wynne, Doctor of Philosophy, 2020

Dissertation directed by: Professor Raleigh R. Hood, Department of Marine Estuarine and Environmental Sciences

This dissertation discusses the cyanobacterial bloom phenology in three anthropogenically impacted regions of the Great Lakes: western Lake Erie, Saginaw Bay, and Green Bay. A detection algorithm was applied to ocean color satellite imagery, and a timeseries was constricted from each of the basins using either data from the MODIS sensor (Saginaw Bay), the MERIS sensor (Green Bay), or a combination of the two (western Lake Erie). The sensors have a high temporal resolution, collecting imagery several times a week. The algorithm used, the Cyanobacterial Index (CI), was applied to the imagery. The CI imagery was then sampled into fifteen 10-day composites throughout the bloom season (defined here as June 1 – October 31). Each of the five months will have three composites (each spanning ~10 days). From this point the bloom climatology is shown and the variability of each region is addressed. The interannual variability of the cyanobacterial blooms can be low (factor of ~2 in Saginaw Bay) or high

(differing by a factor of ~20 in Green Bay and western Lake Erie). Various ancillary datasets describing the physical environment of each region were assembled including: field data, modeled data, remotely sensed data, or some combination therein. Impacts of associated cyanobacterial biotoxins were addressed and statistical models were formulated to explain any variability. The dissertation will also cross compare the three basins with one another in an effort to determine the similarities as well as differences among the regions. Management recommendations are given at the end of each of the three subsequent chapters to deter potential detrimental impacts of the blooms and their associated toxins.

PHENOLOGY OF CYANOBACTERIAL BLOOMS IN THREE CATCHMENTS OF THE LAURENTIAN GREAT LAKES

by

Timothy Todd Wynne

Dissertation submitted to the Faculty of the Graduate School of the
University of Maryland, College Park, in partial fulfillment
of the requirements for the degree of
Doctor of Philosophy
2020

Advisory Committee:
Professor Raleigh R. Hood, Chair
Christopher W. Brown
Victoria J. Coles
Andrew Elmore
Richard P.Stumpf

FOREWORD

In this dissertation are three unique research chapters. I am the principal author of each of the chapters, however, all chapters were a collaboration with other scientists. All chapters have been published or will be published shortly. At the conclusion of each chapter co-authors and collaborators will be acknowledged. Chapter 2 has been published. Citation is: Wynne, T.T. and R.P. Stumpf. 2015. Spatial and temporal patterns in the seasonal distribution of toxic cyanobacteria in western Lake Erie from 2002-2014. *Toxins.*7:1649-1663. Chapter 3 has been submitted. Citation is: Wynne, T.T., R.P. Stumpf, R.W. Litaker, and R.R. Hood. 2020. Cyanobacterial bloom phenology in Saginaw Bay from MODIS and a comparative look with Lake Erie. *Harmful Algae*. Chapter 4 will be submitted shortly.

DEDICATION

I would like to dedicate this dissertation to my wife, Rebecca and my three children; Aaron, Henry, and Madelyn. I'd also like to dedicate this to my parents, Doug and Nancy Wynne, as well as to my late mother-in-law, Lea Wait, for their encouragement and support.

Furthermore, I would like to also dedicate this dissertation to Wayne Litaker who was very much responsible for me completing this. Without his encouragement, guidance, time, availability, and near insistence on its completion, this document would not have happened.

ACKNOWLEDGEMENTS

First I would like to thank my adviser, Dr. Raleigh Hood who has had infinite patience for me over the years that it has taken for this to complete this dissertation. His optimism, guidance, and encouragement were very much appreciated. I would also like to thank my four other committee members: Christopher Brown, Victoria Coles, Andrew Elmore, and Richard Stumpf, whose patience, time, support, and mentorship has allowed this to unfold.

I would like to acknowledge institutional support from NOAA, as well as from my various supervisors over the nine years that this has taken: Gunnar Lauenstein, John Christensen, Mark Monaco, Terry McTigue, Peter Thompson, Sherri Fields, Greg Piniak, Wayne Litaker, and Marc Suddleson. Finally, I would like to thank Rick Stumpf for his mentorship over the past 18 years, and Kris Holderied who was an early source of inspiration in this process.

TABLE OF CONTENTS

LIST OF TABLES

Table 3.3.

Correlations between the discharge volumes from Saginaw and Maumee Rivers and the annual maximum 10-day integrated CI values.

Chapter 4

Table 4.1.

Shown here is the 10-day composite numbering system used for each year.

Table 4.2.

Shown here is the data downloaded by NASA's Giovanni dataset that will be used for model development.

Table 4.3.

The 10-day composite periods (dates in parentheses) exhibiting the highest mean, median, and mode integrated CI values during the 10-year MERIS time series. Details on how values were calculated are given in section 2.3.

Table 4.4.

Shows the correlation statistics between the average CI_{cyano} between Green Bay and Lake Winnebago. Four scenarios were considered, a lag of 0 days, 10days, 20 days and 30 days. The correlation decreased with each lag period indicating that the blooms from Green Bay co-occur with blooms in Lake Winnebago as opposed to the blooms in Green Bay being transported from Lake Winnebago.

Table 4.5.

Shows the results of the Maximum annual CI and the Minimum annual CI between Green Bay, Lake Winnebago, western Lake Erie and Saginaw Bay.

LIST OF FIGURES

Figure 2.6.

The spatial pattern of percentage frequency of severe cyanobacteria (> 10^5 cells mL^{-1}, CI >0.001) for each 10-day period during all years from 2002-2014.

Figure 2.7.

Same as figure 5 for only years with blooms (percentage frequency of detectable cyanobacteria).

Figure 2.8.

Same as figure 6 for only years with blooms (percentage frequency of severe cyanobacteria).

Figure 2.9.

Frequency of severe blooms during the 2002-2014 record at the approximate location of selected water treatment intakes from Figure 2. Except for Toledo station (station 1), the data from the other stations were taken 2 pixels (~2 km) into the center of the lake to obtain valid data without land contamination or masking.

Chapter 3

Figure 3.1.

(A) Map showing the bathymetry and other relevant features of Saginaw Bay. (B) Map showing the geographic location of Saginaw Bay and the WLEB relative to one another. The Saginaw River, which supplies a majority of the nutrients to Saginaw Bay, and the Maumee River, which similarly supplies a majority of nutrients to the WLEB are also shown. (C) Map showing the bathymetry and other relevant features of the WLEB.

Figure 3.2.

(A) Regression analysis of the relationship between annual volume of water from the Saginaw River and total annual phosphorus load from the 1974- 1991 (MDEQWB, 2010) (B) Same as for (A) except for the 2001-2005 time period (MDEQWB, 2010). The slope of the regression line in (A) compared to that in (B) is consistent with phosphorus abatement strategies begun in the 1970s having successfully reduced TP loading into Saginaw Bay from the Saginaw River.

Figure 3.3.

Regression analysis of the CI from the Stumpf et al. (2016) model on western Lake Erie against the CI from the MODIS data used in the current study. The slope (m) and the slope intercept (b) of the relationship shown here was used to adjust equation 6.

Figure 3.4.

(A)The maximal cumulative cyanobacterial index (CI) values from every 10-day composite (see Table 1) available for Saginaw Bay for 2000-2019. (B) The maximal commutative CI values for the WLEB (light bars) and Saginaw Bay (dark bars) allowing comparison of relative differences in the biomass of the cyanobacterial blooms in the two systems. The vertical black lines delimit the bloom season for each year, which starts on June 1 –June 10 and ends October 20-October 31 (See Table 1). Each bloom year was divided into the same 15, 10-day composite periods.

Figure 3.5.

Relationship between the maximal annual CI value (*) and the total volume of water discharged from the Saginaw River per water year (October previous year to September of the current year - o; corresponds to period from demise bloom previous September to start of bloom decline in the current year), March – June (+) current year and March – July (x) current year.

Figure 3.6.

(A) Mean and standard deviation for monthly discharge from the Saginaw River from 2000-2019. The data are plotted from October 1 to September 30 to correspond to the end of the bloom the previous year and the decline of the bloom the following September. (B) Same data for the Maumee River processed as detailed in A.

Figure 3.7.

(A) March - June discharge from the Saginaw and Maumee Rivers versus the corresponding maximal 10-day Cyanobacterial Index in Saginaw Bay (*) and the WLEB (o) respectively. (B) March - June total phosphate loading from the Saginaw and Maumee Rivers versus the corresponding maximal 10-day Cyanobacterial Index in Saginaw Bay (*) and the WLEB (o) respectively.

Figure 3.8.

(A) Observed annual maximum 10-day, Cyanobacterial Index (CI) value vs modeled maximal CI based on total phosphorus (TP) input from the Maumee (o) and Saginaw (*) Rivers. (B) Observed annual maximum CI value vs modeled maximal CI value based on dissolved reactive phosphorus (DRP) input from the Maumee (o) and the Saginaw (*) Rivers. The models used for predicting CI from TP and DRP input were originally developed using data available for the WLEB (Stumpf et al. 2016).

Figure 3.9.

Relationship between the flow weighted mean concentrations of total phosphorus (TP) and dissolved reactive phosphorus (DRP) from the *in situ* dataset from the National Center for Water

Quality Research for the Maumee, Sandusky, and Cuyahoga Rivers. The Saginaw River TP data was from the Cha et al (2010) dataset. These data were graphed and the linear equation was used to convert the TP values available from the Saginaw River into an estimated average flow weighted DRP concentration.

Figure 3.10.

Time series showing maximal CI values for every pixel in Saginaw Bay for each of the 15, 10-day periods. The composited images for each 10-day period were arranged in chronological order to show development and decline of the bloom. Data for each image were determined by extracting the maximal CI values for the same pixel in every corresponding 10-day period from all 20 years and then averaging those data to provide an average pixel value for a given 10-day period. The center of the bay has lower concentrations relative to the shoreward areas, due to prevailing circulation within the bay. The inner bay has higher concentration relative to the outer bay. Warmer colors indicate higher levels of cyanobacteria, while cooler colors indicate lower levels.

Figure 3.11.

(A) The percent of time a pixel exceeds a Cyanobacterial Index (CI) exceeded 0 in each of the 15 10-day periods between 2000 and 2017 in Saginaw Bay. (A) CI=0 is estimated to be ~20,000 cells mL^{-1} (Stumpf et al., 2012). This provides a probability estimate of a cyanobacterial bloom being present in a given location in each of the 15 of the 10-day periods (Table 1) from June 1 to October 31. (B) Same as A except it is percent of time the CI value of a ≥ 0.001, which is equivalent to a concentration of 10^5 cells mL^{-1}.

Figure 3.12.

(A) Saginaw Bay was subdivided into 5 regions to examine geographic variation in bloom intensity. The cumulative maximal CI values for each 10-day composites from each of these five regions was then plotted as time series from 2000 to 2019. (B) Map showing the different subregions of the Bay. (C) The average of the cumulative maximal CI values for each subregion over all 20 years years of the study normalized to surface area. Region 1, closest to the primary nutrient source, the Saginaw River, had the highest CI value. The inner bay (R2, R3), had a higher CI value than the outer bay subregions (R4, R5). Values for the eastern shore subregions (R3, R5) were higher than the corresponding ones on the eastern shore (R2, R4).

Chapter 4

Figure 4.1.

Map of the Study area showing locations mentioned in Chapter 4.

Figure 4.2.

Illustration of how the CI is parsed out into two separate quantities based on Equation 3 in the text. The CI is equal to the sum of the CI_{cyano} and the $CI_{noncyano}$.

Figure 4.3.

Shows the relationship between the CI and the CI_{cyano}. Each point represents the integrated quantity over a 10-day period during the bloom season (June – October) from 2002-2011. Panel A shows the relationship in western Lake Erie. Panel B shows the relationship in Saginaw Bay

and Panel C shows the relationship in Green Bay. The point circled show where the CI says there should be a bloom but the CI_{cyano} determined that there was no bloom present.

Figure 4.4.

Panel A shows all 69 samples where there was at least one pixel in a 9x9 box around the sampling point. The median of the 9x9 block pixels was taken. Panel B shows the subset of Panel A where the CI_{cyano} is positive.

Figure 4.5.

Shows the linear regression between the cyanobacterial biovolume and the CI_{cyano}. This relationship is much stronger that the relationships shown in figure 5 indicating that the CI_{cyano} satisfactorily estimates cyanobacterial biovolume.

Figure 4.6.

Shown here is the climatology of the CI_{cyano}. Each 10 day composite is the mean of the 10 of the MERIS data (2002-2011).

Figure 4.7.

Shows the timeseries over the 10 years of the study for both Lake Winnebago (shown in blue) and Green Bay (shown in Green). There exists a high degree of interannual variability. The CI_{cyano} values in Lake Winnebago nearly always exceeds Green Bay.

Figure 4.8.

Panel A shows the results from the Principal Components Analysis (PCA) in using three parameters to discern Green Bay, western Lake Erie, and Saginaw Bay. The parameters used

were the night sea surface temperature (nsst), the river discharge (river_Q) from three respective rivers (Maumee River, Saginaw River, and Fox River), and the combine gelbstoff absorption and phytoplankton absorption (adg + aph). Panel B shows the separation using just nsst and adg + aph.

Figure 4.9.

Shows the monthly timeseries of the gelbstoff absorption (Panel A) for Green Bay (Green line), Saginaw Bay (Black line) and western Lake Erie (blue line). Each point represents a month. Panel B shows the phytoplankton absorption for the same regions over the same timeseries.

Figure 4.10.

Panel A shows the separation between bloom years (gray) and non-bloom years (black) for Green Bay using a PCA. The five input parameters were particulate backscatter (bbp), gelbstoff absorption (adg), the meridional wind speed (vgrd), sensible heat flux (shtflsfc), and latent heat flux (lhtflsfc). Panel B shows the unsatisfactory separation of the bloom years form non-bloom years in western Lake Erie using the same five parameter PCA presented in Panel A.

Figure 4.11.

Panel A shows the separation between bloom years (gray) and non-bloom years (black) for western Lake Erie using a PCA. The three input parameters were river discharge (river_Q), sensible heat flux (shtflsfc), and latent heat flux (lhtflsfc). 2004 had the sixth highest CI out of the timeseries and was classified as a bloom in earlier work (Stumpf et al., 2012). It was not in this context as operationally the top 5 CI years were classified as a bloom and the bloom 5 CI values were classified as non-bloom. Panel B shows the unsatisfactory separation of the bloom

years form non-bloom years in Green Bay using the same three parameter PCA presented in Panel A.

Figure 4.12.

Panel A uses the eight parameters used in other PCAs (figures 9, 11, and 12) to separate 2009 and 2010 from the other years in Green Bay. 2009 and 2010 had virtually no bloom at all in Green Bay. Panel B shows the PCA when only two parameters are used. Acceptable separation is still achieved, and this illustrates that the adg + aph and temperature are the driving factors in determining when no bloom forms.

Figure 4.13.

Shows the annual CI_{cyano} from western Lake Erie, (WLE), Saginaw Bay (SB), Green Bay (GB), and Lake Winnebago (LW). The annual CI_{cyano} was calculated by taking the mean of the highest three sequential 10 day composites of the CI_{cyano}.

Figure 14.14.

Panel A shows the night time sea surface temperature from the monthly NASA Giovanni Data from Green Bay (Green o), Saginaw Bay (blue +), and western Lake Erie (black *). Panel B shows the Latent Heat Flux from the monthly NASA Giovanni Data from Green Bay (Green o), Saginaw Bay (blue +), and western Lake Erie (black *). Panel C shows the Sensible Heat Flux from the monthly NASA Giovanni Data from Green Bay (Green o), Saginaw Bay (blue +), and western Lake Erie (black *).

INTRODUCTION

1.1 Overview

Cyanobacteria are globally ubiquitous. They may be credited with being the oldest organism on Earth (Banack, et al., 2012) at 4.5 billion years. There is some evidence that cyanobacteria caused the formation of the early atmosphere of the Earth (Schirrmeister et al., 2015). Which has been supported by the work of Thomas et al. (2005) who have shown that common cyanobacteria of the genus *Synechococcus* and *Anabaena* (now called *Dolichospermum*) are able to grow in an atmosphere composed entirely of CO_2.

There are both marine and freshwater species of cyanobacteria. The marine species of cyanobacteria are responsible for a large percentage of the ocean's primary productivity. *Prochlorococcus* and *Synechococcus*, two dominant species of cyanobacteria have been hypothesized to make up a significant portion of the world's marine primary production, and will increase with a changing climate (Flomaum et al., 2013). Some species of cyanobacteria are diazotrophs, which are capable of fixing atmospheric N_2 (diazotrophs may be either freshwater or marine). This ability allows diazotrophic cyanobacteria to grow when fixed nitrogen concentrations in the water are depleted.

This dissertation focuses on freshwater blooms of cyanobacteria. These blooms generally occur in eutrophic environments where anthropogenically derived nutrient sources empty into a shallow warm basin. There are numerous species of freshwater cyanobacteria, with some of the common genera being: *Microcystis*, *Dolichospermum* (formerly *Anabaena*), *Planktothrix*, *Cylindrospermopsis*, *Nodularia,* and *Aphanizomenon*. Of the most compelling reasons to study blooms of these ancient organisms is that they are capable of producing biotoxins collectively

referred to as Cyanotoxins. There are 3 separate types of toxins associated with cyanobacteria: neurotoxins, hepatotoxins and dermatoxins. Neurotoxins include saxitoxin and Anatoxin-a, that can cause paralysis and respiratory failure. Hepatotoxins include microcystin which affects the function of the liver and kidneys. The most common dermatoxin is lynbyatoxin, which is produced by the cyanobacterium *Lyngbya,* and can cause skin irritation and gastrointestinal distress (Chorus and Bartram, 1999).

1.2 Causes of Cyanobacteria Blooms

Cyanobacteria blooms are promoted by eutrophication. The main nutrients that are needed for primary production are Nitrogen (N) and Phosphorus (P). In marine systems N is generally the limiting nutrient, while P is generally the limiting nutrient in freshwater systems. Therefore, over enrichment of P will often cause cyanobacteria blooms in freshwater environments. Furthermore P comes in two general forms; dissolved and particulate. The most important type of dissolved P is the biologically available, Soluble Reactive Phosphorus (SRP) which is a dissolved inorganic form of phosphorus that is readily available to the algal community. The most commonly measured phosphorus, is Total Phosphorus, which is any form of phosphorus (including SRP), which can be inorganic, organic, dissolved or particulate. Generally total phosphorus is around 10% SRP. Other physical factors can also play roles in limiting, or sustaining cyanobacteria blooms. Temperature is one of the key drivers, as cyanobacteria have an affinity for warm water (Paerl and Huisman, 2008). They prefer a warm stable environment so well mixed areas are not prone to cyanobacteria blooms. Various methods have been demonstrated to be effective in controlling cyanobacteria, e.g., mixing devices can be installed in smaller lakes and ponds in an effort to limit cyanobacteria growth, but these are typically applied to smaller sized water bodies and are not appropriate for large catchments (see review by Lurling et al., 2016.) In natural

systems wind is usually the primary mixing force, although quickly flowing rivers can also supply turbulence needed to keep cyanobacterial blooms from forming. Additionally light availability is a factor as cyanobacteria have an affinity for high light environments.

1.3 Economic Impacts

Cyanobacteria are one of the most visible signs of an impaired aquatic ecosystem. Cyanobacteria can form surface scums which are aesthetically unappealing. Wind can often cause cyanobacteria to accumulate along shorelines and in harbors where they will most likely be seen by the public. The public tends to have a general perception of the water being polluted as a result (Ibelings et al., 2003). Large persistent blooms of cyanobacteria can have adverse effects on property values (Steffenson, 2008). Cyanotoxins can cause further economic ramifications by killing livestock and other domestic animals as well as wildlife. Additional economic impacts can be felt through adverse effects in both the secondary production (Larson et al., 2017) as well as in fisheries (Ludsin et al., 2001).

1.4 Public Health Impacts

While not the most pressing public health concern, the most common public health complaint associated with cyanobacteria is through recreational exposure to dermatoxins which results in gastroenteritis and allergic reactions such as skin rashes, respiratory symptoms, and eye irritation (Graham et al., 2009). Health ramifications associated with Cyanotoxins vary with the concentration of toxins in the water. The world Health Organization has set up guidelines for public health exposure. These are listed in table 1.

Table1: Public health exposure guidelines from the World Health Organization (Chorus and Bartram, 1999; Graham et al., 2009).

Probability of health impacts	Chlorophyll-a concentrations (μ L^{-1})	Cyanobacteria (cells ml^{-1})	Microcystin (μ L^{-1})
Low	< 10	< 20,000	< 10
Medium	10-50	20,000 – 100,000	10-20
High	50-5,000	100,000 – 10,000,000	20-2,000
Very High	> 5000	> 10,000,000	> 2,000

Perhaps the largest public health impact is also the largest economic impact, and that is the contamination of drinking water. These health effects come from the hepatotoxins: microcystin and cylindrospermopsin. These toxins are highly heat stable and will not be destroyed through the boiling process. Furthermore, they will not be removed from municipal water supplies through conventional filtering. There is a guideline of 1part per billion (ppb) in finished drinking water (Jetoo et al., 2015). If microcystin is present above 1 ppb, the water must be flushed out and treated with nanofiltration or other techniques (EPA, 2020). All known methods of removing intercellular or extracellular (dissolved) cyanotoxins are expensive and are not routinely done by municipal water suppliers. In August, 2014 the city of Toledo, Ohio issued a "Do Not Drink" proclamation on the water supply, when the drinking water reached a microcystin concentration exceeding 1 ppb (Jetoo et al., 2015). This left several hundred thousand people without drinkable municipal water for several days in the summer, which had vast economic and public health effects and altered public perception of the pollution levels of Lake Erie. This was not the only time there has been a large scale water outage in municipal water supplies. In September of 2013 Carroll Township in Ohio issued a "do not drink" order to its 2,000 customers when microcystin concentrations exceeding 1 ppb were detected in the drinking water supply (NPR, 2017).

1.5 Laurentian Great Lakes

Collectively, the Laurentian Great Lakes contain five of the world's 15 largest lakes, and collectively have been estimated to contain 21% of the world's fresh surface water (Table 2). The five Great Lakes were all pristine areas prior to European colonialism. Since then the Great Lakes have undergone various stages of degradation, with Lake Superior being the least impacted and Lake Erie being the most heavily impacted by anthropogenic activities. The western side of Lake Erie is the Maumee River watershed. The Maumee River is the largest input of nutrients into Lake Erie. Nearly the entire watershed, the largest watershed of Lake Erie, was once covered in a vast wetland referred to as the Great Black Swamp. The Great Black swamp was drained for agricultural activities in the mid nineteenth century. With much of the wetlands removed combined with the industrial revolution, western Lake Erie went through a period of eutrophication. Cyanobacteria blooms became common place and were associated with extremely high levels of chlorophyll which led to anoxic and hypoxic conditions (Scavia et al., 2014).

Perhaps the defining moment of western Lake Erie was when the Cuyahoga River caught fire in Cleveland, Ohio on June 22, 1969. This was generally thought to be the impetus of the Clean Water Act, which was passed three years later in 1972. After this point there was a series of measures that were undertaken to limit the eutrophication of Lake Erie, which were quite successful. Particularly relevant to removing cyanobacterial blooms were the wide scale phosphorus abatement strategies that were mandated by the Great Lakes Water Quality Agreement (GLWQA). These drastically decreased phosphorus loads into Lake Erie (as well as Saginaw Bay and Green Bay). The cyanobacterial blooms were essentially eradicated from the basins. However, since the mid-1990s Lake Erie has been going through a period of re-eutrophication, which has brought back cyanobacteria blooms. The cause of this re-

eutrophication has been potentially brought about by increases in Soluble Reactive Phosphorus (SRP) load, even while Total Phosphorus (TP) has been below the GLWQA goal of 11,000 MTA (Scavia et al., 2014). It has also been suggested that the invasive mussels of the genus *Dreissena* have contributed to changes in water quality that has led to the reoccurrence of cyanobacteria blooms in the Great Lakes (Juhel et al., 2006; Budd et al., 2001).

Table 2:

Listed here are some statistics for the Great Lakes. Primary Production numbers come from Fahnenstiel et al., 2016.

Lake	Average depth (m)	Dissolved Inorganic Carbon (μM)	Dissolved Organic Carbon (μM)	Primary Production (Tg/yr)	Surface Area (km^2)
Superior	147	1	100	8.1	82,000
Michigan	85	2.3	400	6.3	58,000
Huron	59	1.7	400	5.3	60,000
Erie	19	2.2	400		25,700
Ontario	86	2.2	400		7,340
Coastal Oceans	~100	~2	~100		

1.6 Cyanobacteria in the Great Lakes

The three primary areas in the Laurentian Great Lakes that are routinely affected by Harmful Algal Blooms are: the western basin of Lake Erie, Saginaw Bay, and Green Bay. All three basins share similarities. They are all fed by one principal river that supplies much of the phosphorus needed to drive cyanobacteria blooms within the system. They are all relatively shallow and warm basins which are anthropogenically impacted. However, each basin has very different bloom dynamics and phenology. My primary goal for this thesis is to compare and contrast the bloom phenology of the three basins.

1.7 Aims and Objectives

Chapter 1

In this chapter investigate western Lake Erie, a well-studied body of water, especially pertaining to cyanobacteria blooms. The emphasis of this chapter is on the relationship of the cyanobacteria blooms with the water intake facilities that supply water to various municipalities. The frequency and average cyanobacterial biomass is estimated and the likelihood of each water facility encountering severe, mild or no bloom conditions will be calculated based on 10-day periods. This chapter was motivated by the city of Toledo, Ohio issuing a “do not drink” order for its municipal water supply in August of 2014 due to having microcystin concentrations (exceeding 1 ppb) in finished drinking water. I calculated the frequency of severe bloom occurrence in six of the primary municipal water intake areas and made inferences on when, where and how often drinking water supplies would be effected by microcystin.

Chapter 2

I investigate the bloom phenology of Saginaw Bay. Specifically, I examine when blooms occur, the severity of the blooms, and the interannual variability of blooms. Relationships between the blooms and river discharge are considered. The chapter concludes with a comparative look at Lake Erie blooms and how the two systems act differently. This is comparison is important. Until a wet climatological phase in 2008 the two basins had similarly sized blooms, with some years Saginaw Bay actually having higher biomasses than Lake Erie. However since the wet phase began in 2008 the blooms in western Lake Erie have far surpassed Saginaw Bay, while the blooms in Saginaw Bay have remained approximately the same size. Determining differences in the two systems provides insights that can be used to help manage Saginaw Bay to avoid the fate of western Lake Erie where there are now massive annual cyanobacterial blooms. Conversely, these insights can potentially be used to more effectively manage the Lake Erie blooms. The two primary differences that can work to help reduce bloom impacts are a reduction in agriculture and restoration of wetland and riparian buffers.

Chapter 3

In chapter 3 I investigate the phenology of cyanobacterial blooms in Green Bay. Green Bay is fundamentally different from Saginaw Bay and western Lake Erie in that the summertime blooms are not monospecific *Microcystis* blooms, and instead co-occur with diatoms and green algae. Relationships between the blooms and a variety of different physical parameters is examined to determine which of them contribute to bloom formation. The eutrophic Lake Winnebago drains into Green Bay and Lake Winnebago has much more cyanobacterial bloom mass than does Green Bay. I test the hypothesis that blooms in Green Bay originate in Lake Winnebago. The chapter concludes with and examination of differences between Green Bay, western Lake Erie, and Saginaw Bay. The motivation behind this chapter was to explore linkages

between Lake Winnebago and Green Bay and determine what physical parameters govern bloom dynamics in Green Bay.

Spatial and Temporal Patterns in the Seasonal Distribution of Toxic Cyanobacteria in Lake Erie

2.1 Abstract

Lake Erie, the world's tenth largest freshwater lake, has had recurring blooms of toxic cyanobacteria for the past two decades. These blooms pose potential health risks for recreation, and impact the treatment of drinking water. Understanding the timing and distribution of the blooms may aid in planning by local communities and resources managers. Satellite data provides a means of examining spatial patterns of the blooms. Data sets from MERIS (2002-2012) and MODIS (2012-2014) were analyzed to evaluate bloom patterns and frequencies. The blooms were identified using previously published algorithms to detect cyanobacteria, as well as a variation of these algorithms to account for the saturation of the MODIS ocean color bands. Images were binned into 10-day composites to reduce cloud and mixing artifacts. The 13 years of composites were used to determine frequency of presence of both detectable cyanobacteria and high risk (>100,000 cells mL-1) blooms through the bloom season (defined here as June 1 – October 31). Maps show the pattern of development and areas most commonly impacted. Frequencies during years with significant blooms were examined as well. With the annual forecasts of bloom severity, these frequency maps can provide public water suppliers and health departments with guidance on the timing of potential risk.

2.2 Introduction

Lake Erie (Figure 2.1) has experienced a recurrence of blooms with potentially toxic cyanobacteria this century (Stumpf et al., 2012), with six of the last seven years having significant blooms (NOAA, 2014). The dominant species of cyanobacteria in Lake Erie is

Microcystis aeruginosa (henceforth referred to as *Microcystis*). *Microcystis* typically forms dense monospecific (single species) blooms, although *Anabaena* spp. and other genuses of cyanobacteria may sometimes appear. These blooms have a variety of detrimental impacts, such as: taste and odor issues in municipal water supplies, potential human health issues, mortalities in domestic and wild animal populations, and adverse economic impacts in local communities (Backer, 2002; Davenport and Drake, 2011). Contamination of drinking water is a potential hazard, given the number of intakes around the western lake. In September, 2013, Carroll Township, Ohio (Station 4 on Figure 2.2), which supplies water to several thousand people, shut down its municipal water supplies for two days (Henry, 2013) owing to microcystin, the toxin found in *Microcystis*, concentrations greater than the World Health Organization recommendation of 1 $\mu g\ L^{-1}$ (Chorus and Bartram, 1990). In August, 2014 microcystins reached the same risk level in the processed water of the city of Toledo, resulting in a two-day "do not drink" statement from its municipal water suppliers (station 2 on Figure 2.2) to approximately half a million customers (Fitzsimmons, 2014).

NOAA has routinely issued short-term (<1 week) forecasts in Lake Erie since 2009 (Wynne et al., 2013b; NOAA, 2014). The demand for these forecasts has been high. The subscriber list for the Lake Erie forecast has experienced an annual growth rate of approximately 250% from its inception in 2009. More recently, NCCOS has started issuing seasonal forecasts (NOAA, 2012; NOAA 2013; NOAA 2014) of cyanobacteria based on models presented by Stumpf et al. (2012). A determination of the frequency of blooms over the 13 years of satellite data will provide a better understanding of timing and distributions of these potentially toxic blooms.

These frequencies may allow for spatial-temporal forecasts, which may be beneficial in both a micro and macroeconomic scale. The results could support planning by managers of public water

suppliers and parks. They may also ultimately aid the public in avoiding coming into contact with potentially toxic (and unaesthetic) cyanobacteria.

2.3 Methods

The delineation and detection of these blooms has been well-documented with satellite ocean color data (Wynne et al., 2008; 2010; 2011; 2013a; 2013b; Stumpf et al., 2012; NOAA, 2014). The Medium Resolution Imaging Spectrometer (MERIS) on board the Envisat-1 satellite provided data for the summers from 2002-2011. On April 8, 2012 Envisat failed, resulting in a cessation of MERIS data. The Moderate Resolution Imaging Spectroradiometer (MODIS) was used for 2012-2014. MERIS level 2 reflectance (R; with sr^{-1} units) data sets from the second reprocessing were obtained from the European Space Agency (ESA). MODIS was obtained as level 0 data from the National Aeronautics and Space Administration (NASA) and processed to Rayleigh corrected bi-directional reflectance (ρ_s; which is dimensionless) using NASA's SeaDAS package, with the "rhos_s" option in SeaDAS l2gen. Products were processed in equal area Sinusoidal projection, with 1.1 km pixel scale through 2013, and were processed to Albers 1.1 km equal area projection in 2014. All sinusoidal images were reprojected to the Albers equal area projection for all analysis (as all future analyses in our group will use the Albers projection).

Both data sets were then processed with equivalent spectral shape (second derivative) algorithms, based around 680 nm (Wynne et al. 2008; 2013a). With MERIS bands the equation is:

$$(1)\quad S_{2d}(681) = R(681) - R(665) - \{R(709) - R(665)\}\frac{(681-665)}{(709-665)}$$

where R is the reflectance and the values are the band centers. For MODIS, Wynne et al., 2013a adjusted the MERIS algorithm to the MODIS Aqua sensor to yield:

$$(2)\ S_{2d}(678) = \rho_s(678) - \rho_s(667) - \{\rho_s(748) - \rho_s(667)\}\frac{(678-667)}{(748-667)}$$

where ρ_s is Rayleigh corrected bi-directional reflectance.

For MERIS, the cyanobacterial index (CI) is found from (Wynne et al., 2008):

$$(3)\ CI = -S_{2d}(681)$$

and for MODIS the conversion to match MERIS (Wynne et al., 2013a) is:

$$(4)\ CI = -S_{2d}(678) \times 1.3$$

Where the CI has units of sr^{-1}.

The timeseries shown here extends from 2002- 2014. The portion of the timeseries covering 2002-2011 used MERIS imagery, and the portion covering 2012 – 2014 used MODIS imagery. MERIS produced superior results with less noise than MODIS and no saturation. MODIS saturates for bright pixels, which can result from glint, haze, and turbid water (Franz et al., 2007; Wang et al., 2007; Wang and Shi, 2007). These conditions can occur during severe algal blooms during the summer (Wynne et al., 2013b), resulting in failure of the CI calculation expressed in equation 4. While the time-series from 2012 showed a bloom, the imagery was not overly turbid and the MODIS bands used in equation 2 did not saturate in bloom areas, so the MODIS saturation was not an issue. However, the 2013 and 2014 blooms were more intense and highly

reflective, resulting in some saturation. A mechanism was needed to quantify the biomass under saturation. The "land" bands in MODIS are calibrated in such a way that they will not saturate even under the most turbid water conditions, and have been recommended for use when the nine bands commonly used for ocean color from MODIS (covering 412-869 nm) have saturated (Franz et al., 2006). Cyanobacterial blooms are detectable as bright water, which can provide an estimate of presence and quantity of biomass (Budd et al., 2002; Kahru et al, 1997). The near-infrared (NIR) bands on the MODIS Aqua sensor were used to calculate a reflectance proxy for the CI for MODIS.

(5) $CI_{sat} = 0.5 * [\rho_w(859)]^{0.5}$

with

(6) $\rho_w(859) = \rho_s(859) - \rho_s(1240)$

where the 1240 band is used as a nominal atmospheric correction (Wang and Shi, 2007). The derivation of equation 5 was empirically tuned with a simple root relationship to overlap the retrieved CI values around saturated pixels. Slight errors in the tuning of equation 5 are not important to the study, as it would apply when conditions are well above the "severe bloom" threshold discussed below. While scum or algae floating on the surface can produce saturation in the MODIS bands, saturation also occurs in areas without surface scums. As a result, using other metrics like the "floating algae index" (Hu, 2009) would still require yet another algorithm (like equation 5) to provide coverage of all saturated areas.

When saturation did not occur, the standard CI solution (equation 4) is used; for the conditions when saturation occurred within a bloom, the CI_{sat} from equation 5 was applied. A tuning of reflectivity to biomass would probably vary between years, depending on the bloom characteristics, like cellular chlorophyll content. Resuspended sediment is uncommon during the summer in Lake Erie, and only the saturated pixels contained within blooms (areas of CI) were used. In 2014, the scattering appeared slightly milder, so the correction of equation 6 was reduced proportionately.

CI varies linearly with biomass, with a value of 10^{-3} sr^{-1} corresponding to 10^5 cells mL^{-1} (Stumpf et al., 2012), which is the World Health Organization's (WHO) threshold of significantly increased risk for human health (Chorus and Bartram, 1999). The minimum detection of the CI is still being assessed, however, a CI of 2×10^{-4} sr^{-1} produces consistent retrievals of the bloom edge over multiple images for both sensors, indicating that the minimum detection is less than 20,000 cells mL^{-1}, which is also the recommended threshold for avoiding irritative effects (Chorus and Bartram, 1999).

Clouds were masked and 10-day composites were made for each year during the bloom period using the maximum value of the CI at each pixel. There are several advantages to utilizing maximum value composites. The first advantage is that the composite reduces cloud interference, reducing the data to a systematic set of generally cloud-free images. The second key advantage is to estimate areal biomass. When winds are strong (> 7.7 m s^{-1}, or stress of 0.1 Pa), the bloom is mixed through the water column, diluting the surface concentration (Hunter et al., 2008; Wynne et al., 2010). Under calm winds, however, *Microcystis* floats upward with dense accumulations visible on the lake (Aparicio-Medran et al. 2013). The surface concentration (CI) estimated from satellite during calm conditions then represents the *Microcystis* that is present in the water

column (Wynne et al., 2010), however, the concentration detected during high winds underestimates true biomass. Typically, during any 10-day period in the summer, there is a period of calm clear weather (Wynne et al., 2013b), allowing this estimate. The cells return to the surface within 24-48 hours after a wind event. The bands used for the algorithm quantify concentration within 1 m of the surface in the clearest water (Pope and Fry, 1997), less as turbidity increases (usually because of the bloom). Finally, using a 10-day composite makes biological sense as the doubling time for *Microcystis* is as low as 10 days in the Great Lake region (Fahnensteil et al. 2008).

Blooms in Lake Erie generally occur in the summer when water temperatures exceed 15° C, although blooms can persist in cooler waters once established (Wynne et al., 2013b). As a result, the bloom season considered here is defined as 1 June through 31 October following conventions from Stumpf et al. (2012). Fifteen separate 10-day composites covering the bloom year (1 June to 31 October) were constructed from methods detailed in Stumpf et al. (2012). The final 10-day composite actually consists of 13 days to complete October (to October 31; See Table 1).

Table 1: Shows how the 10-day composites were created.

Composite Number	Start Date	End Date	No. Days
1	01 June	10 June	10
2	11 June	20 June	10
3	21 June	30 June	10

4	1 July	10 July	10
5	11 July	20 July	10
6	21 July	30 July	10
7	31 July	9 August	10
8	10 August	19 August	10
9	20 August	29 August	10
10	30 August	8 September	10
11	9 September	18 September	10
12	19 September	28 September	10
13	29 September	8 October	10
14	9 October	19 October	10
15	19 October	31 October	13

With the 10-day composites in hand, several climatological data sets were generated. The means for each of the 15 separate 10-day composites were made from the averages of all the years.

Frequency maps were made across two sets of conditions: (1) all years or bloom years, and (2) all detectable (measurable CI) and CI>0.001. As noted previously, CI = 0.001 corresponds to the

WHO significantly increased risk threshold of 10^5 cells mL^{-1}. The lower threshold indicates presence of cyanobacteria at a level that poses some (but slight) risk. Bloom years are those that had significant blooms. Stumpf et al., (2012) detected negligible blooms in 2002 and 2005-2007 (see also Bridgeman, 2013). While 2012 had a small bloom (NOAA, 2014), it was locally dense and nearly equivalent to the 2004 bloom, and is included. As a result, the frequency maps were calculated just for years containing defined blooms (2003, 2004, 2008-2014). These frequency maps were made based on all bloom types during just the bloom years.

Spurious pixels due to satellite misnavigation, cloud edges, and mixed land-water pixels were removed from analysis. It should be noted that the two pixels adjacent to the coastline in the southern shore of Lake Erie had to be masked due to somewhat severe land interference issues. These were caused mostly by misnavigation, although in the case of MODIS, slow sensor response as the sensor scanned from land, where it always saturated, onto water was the cause. In individual MERIS scenes that do not have these issues, the nearshore, masked, pixels appear to have similar concentrations to the offshore pixels. Still, the concentration can vary nearshore, particularly with light winds moving surface scums.

2.4 Results

Frequency Maps

The mean concentration over the 13 years (Figure 2.3) shows the pattern of high concentration through the season. (The color scale is logarithmic, so the orange-red colors have 10-fold greater concentration than cyan colors.) Sandusky Bay has the highest consistent concentration, with little change through the season. This is typically a bloom from the cyanobacterium, *Planktothrix* (Millie et al., 2008). The Maumee Bay and southwestern area of the western Lake Erie basin

(WLEB) have the next highest mean concentration, with rapid increase between July 21 and Aug 09. In contrast, the northwest area, in the plume of the Detroit River, does not have a detectable concentration. Away from the Detroit River, low concentration may be present along the Ontario coast in early season, increasing somewhat into September.

The central basin shows two events; presence of cyanobacteria in July (Jul 01-10) and in early October. The July mean was produced by blooms that occurred in 2012 and 2013. The October mean owes to the severe bloom of 2011 (see the frequency discussion below).

Accumulating the biomass across lake, including Sandusky Bay (Figure 2.4), provides a measure of the timing of the bloom development. The minimum value on June 1 reflects the presence of a bloom in Sandusky Bay, which persists through the season. The variability above this value captures the average bloom growth in the lake proper. Early July shows the short-lived bloom in the central basin. In the WLEB, development starts by July 22 on average, and peaks in area and biomass between Aug 30 and Sep 18. Overall, the peak lasts for 40 days (i.e., four 10-day periods) before decreasing rapidly in October.

The frequency distribution maps (Figures 2.5-2.8) capture key aspects of bloom development. Sandusky Bay has a bloom throughout the entire period practically, which is typically of the genus *Planktothrix*. Generally, the western basin blooms start in Maumee Bay, with high frequencies in the southwest corner of the WLEB at the beginning of July. The frequency is greatest in the west, with high frequency expanding eastward over the season. The greatest extent of cyanobacteria presence is from August 30 to Sep 18. The cyanobacteria then become slightly less prevalent during the next 30 day period, before experiencing a relatively sharp decline in

abundance during the 19 September – 28 September period. For all intents and purposes, cyanobacteria are gone over the entire western basin of Lake Erie after 18 October.

In detail, the bloom is most common first along both the west (Michigan) and south (Ohio) shorelines. However, on the Michigan coast, blooms do not occur north of Monroe (Station 2 on Figure 2.2). This area is under the influence of the Detroit River, the large volume of water (57th largest in the world; Wikipedia, 2015) keeps the bloom back near the Maumee River.

Eastward movement is not uniform. Detectable concentrations occur relatively early along the Ohio coast to Marblehead (early July). Later in the season, the pattern changes and the greatest frequency of detectable or intense blooms is near the islands in September. Ottawa County (Fig 2, station 5) has about half the frequency of blooms as do the islands. Generally, the chances of encountering cyanobacteria are less than 50% until August for the island region, while the peak frequency occurs between 9 September and 18 September for the western islands (i.e. Bass), and between 19 September and 28 September for the eastern islands (i.e. Pelee Island).

Ontario Shoreline:

The northern shoreline (Ontario) as a general rule is much less impacted relative to the southern shore (Ohio). The area east of Pelee Point is generally unaffected by cyanobacteria, with the only incident in the area occurring in the possibly unprecedented bloom of 2011 (Michalak et al., 2013). The area between Pelee Point and the Detroit River Plume is more regularly affected and, like the Ohio shoreline, blooms are more likely to be encountered from 20 August though 28 September.

Drinking Water Supplies:

As most intakes are within 1 km of the shore, I examined the frequency patterns of CI > 0.001 at 3 km offshore near several intakes. These water intake facilities covered a relatively large disparate area of western Lake Erie, with one station in Ontario, one in Michigan, and the remaining five in Ohio. The timing of risk for water suppliers varies (Figure 2.9). Toledo has the highest frequency, with 60 days having 5-6 years of intense blooms. Monroe, in Michigan, is on the edge of the influence of the Detroit River plume. While Monroe has occasional blooms in July, like Toledo, they are less frequent. Moving eastward, there is a difference with the mainland when compared to the islands. Carroll and Ottawa County have early blooms, while Put-in Bay (in the Bass Islands) has less frequent blooms in early August, with a short peak of high frequency at the end of August.

2.5 Discussion

Creating two frequency maps based on bloom years and all years is based on the value of the seasonal predictions issued by NOAA (NOAA, 2012; NOAA, 2013; NOAA, 2014). In these seasonal predictions, NOAA predicts whether a bloom of cyanobacteria is to be expected in Lake Erie based on a statistical model using discharge of total phosphorus concentration from the Maumee River as outlined in Stumpf et al. (2012). If a bloom is to be expected, the frequency map using just the bloom years would be more likely to be an accurate assessment of the probability map of the bloom relative to the frequency map using all years.

Distinguishing between bloom and non-bloom years allows for application of the annual forecasts (NOAA 2012, NOAA, 2013; NOAA, 2014b). Stumpf et al. (2012) detailed a method to calculate summer peak *Microcystis* biomass using spring discharge from the Maumee River.

This has been used as the basis of a forecast issued annually by NOAA since 2012. The previous year's forecast is validated prior to the new forecast being issued. Thus far the accuracy of the forecast has been well received (Dierkes, 2012), and the forecast will continue to be issued.

The maps can help natural resource managers as they plan on mitigation for the blooms. The municipalities that use Lake Erie for drinking water can make plans to avoid intake issues during times and places that are likely to have a bloom, or to plan for supplies to treat water to mitigate the risk to drinking water. Sampling of parks and public beaches for toxins can be made more strategically, as well. Even the public can use the maps to plan recreational activities to gain maximum use of the lake, while reducing risk. This could have positive impacts to the local economy as it would encourage repeat visitors if negative experiences can be avoided. Furthermore, actual mitigation of blooms may become possible if it is known when and where they will occur.

The distribution has provided insight into the patterns of the blooms. The contrast between the area near the Maumee River and the Detroit River is striking. Stumpf et al. (2012) showed that the phosphorus load from the Maumee River drives the plumes. The results here show that the plumes are located in most years in the area of the Maumee River. In contrast, the blooms do not occur near the Detroit River. The pattern in the center of the WLEB, which has relatively high frequency of blooms, likely results from the transport of the bloom around the Detroit River plume. The blooms do not make landfall on the northern Ontario coast until far east of the Detroit River. The large difference in nutrient concentration between the Detroit River and Maumee River explains this difference; the Detroit River has about 1/10 of the mean concentration of phosphorus as does the Maumee River (OEPA, 2010).

The forecast could also be useful for educational purposes by informing the public when and where blooms may occur and what causes them. The blooms have a tendency to congregate in harbors and on beaches where they are more likely to be encountered by the public (Ibelings et al., 2003). These areas would be easier for short term mitigation of the blooms relative to the large open areas of the Lake. Mitigating the inshore areas affected by blooms would partially alleviate the local economic impacts from the blooms. The public also perceives the Lake as being polluted when it encounters blooms of cyanobacteria, and by applying short term mitigation techniques it may be possible to raise the public perception of the Lake ecosystem.

Ecologically speaking, these frequency maps serve another purpose. Cyanobacteria blooms are common in western Lake Erie. The analysis in Figure 2.4 shows that the maximum intensity (biomass) of the blooms occurs between 9 September and 18 September. These maps give a spatiotemporal timeframe on the initiation and senescence of the blooms, which was not previously available. Furthermore, it gives a likelihood of where the bloom will likely next spread once it is underway. For instance, it seems highly probable that the blooms start in Maumee Bay, and will spread from there. In nearly all years, the bloom was essentially gone by 31 October, with the exception of Sandusky Bay.

2.6 Conclusions

The methods used here give an approximation of the spatiotemporal cyanobacterial quantification for western Lake Erie. The frequency maps can be updated as more years of data are available from MODIS. In 2015, the European Space Administration is planning on launching the replacement for MERIS, the Ocean Colour Land Imager (OLCI) sensor, on board the Sentinel-3 satellite. The accumulation of data will lead to increased statistical power of the

frequency maps and allow for evaluation of them as tools for predicting bloom position and timing.

2.7 Acknowledgements

MERIS imagery was provided by the European Space Agency (Category-1 Proposal C1P.3975). Funding was provided by the NASA Applied Science Program announcement NNH08ZDA001N under contract NNH09AL53I.

2.8 Figures

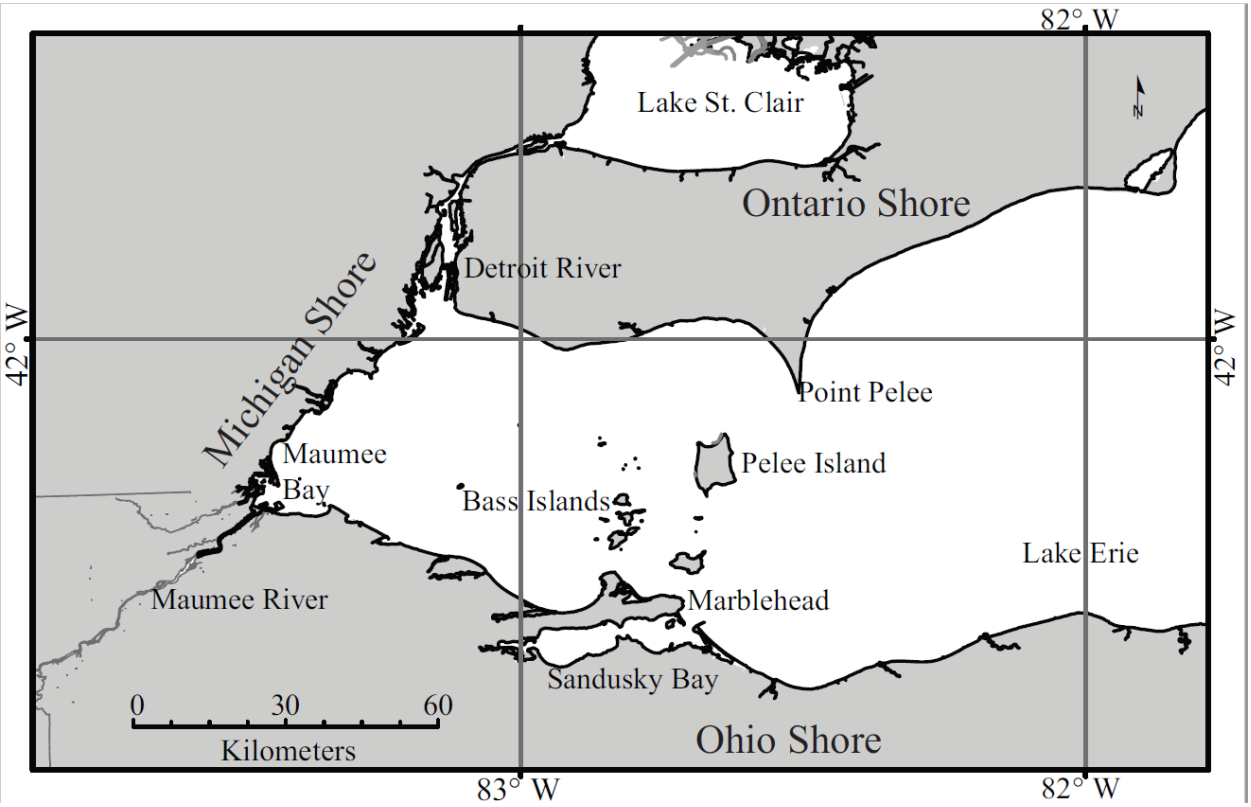

Figure 2.1. Study area and geographic features described in the text.

Figure 2.2. Location of Lake Erie municipal water intakes numbered as follows: 1.) Toledo PWS; 2.) Monroe; 3.) Carroll Water and Sewer; 4.) Ottawa County Regional; 5.) Put-In-Bay Village PWS; 6.) Marblehead Village PWS; 7.) Union

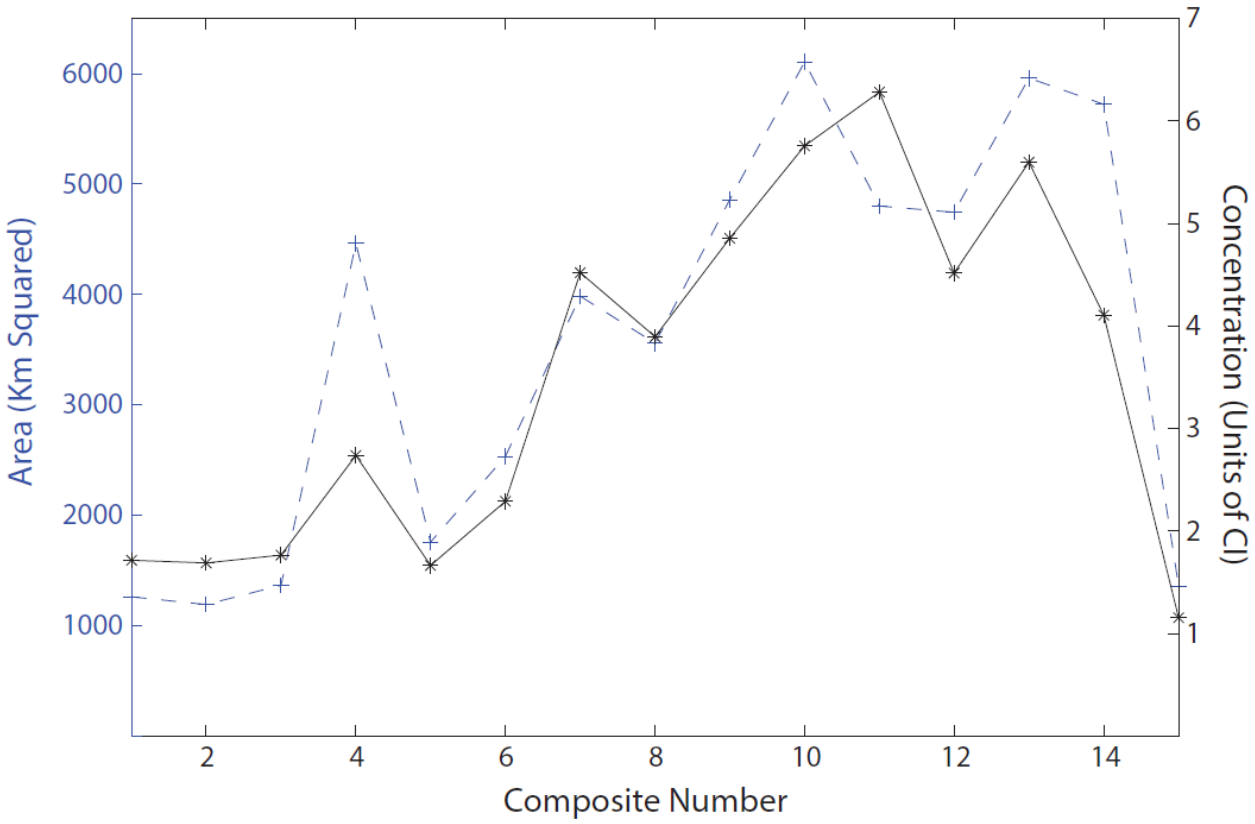

Figure 2.3. The 13-year average of the area and biomass in Lake Erie flagged by the satellite imagery. Area is shown in blue, average biomass is shown in black. The biomass is the accumulated biomass across the entire lake following method of Stumpf et al. (2012). 1 CI is nominally 10^{20} cells.

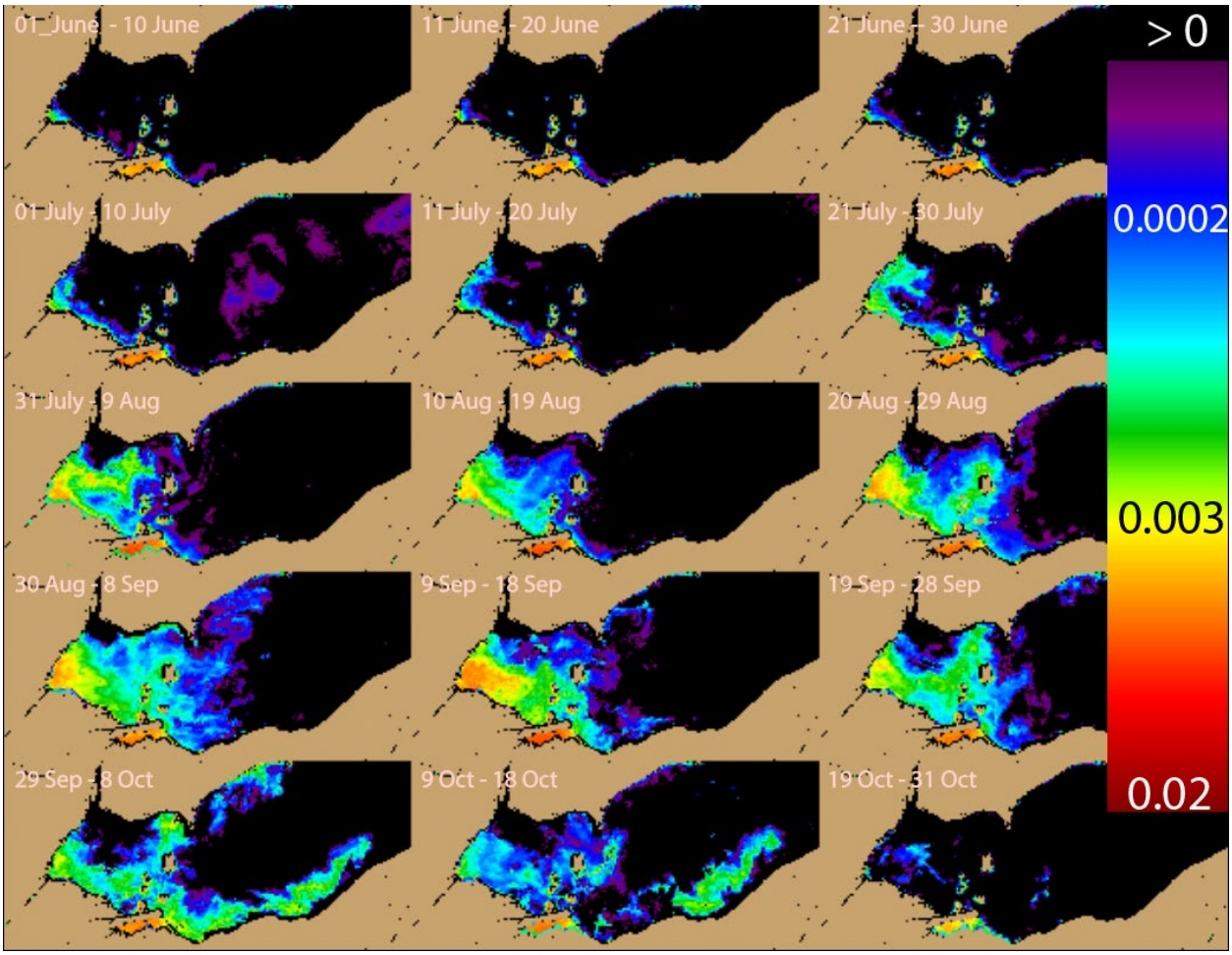

Figure 2.4. Shown here is the area and the average Cyanobacterial Index concentration of the 13 years (log scaled) for each 10-day period. Cell concentration can be estimated from the CI by Cells (mL^{-1}) = 10^8*CI (Wynne et al., 2010; Stumpf et al., 2012). CI > 0.001 exceeds the WHO (Chorus and Bartram, 1990) threshold of 10^5 cells mL^{-1}.

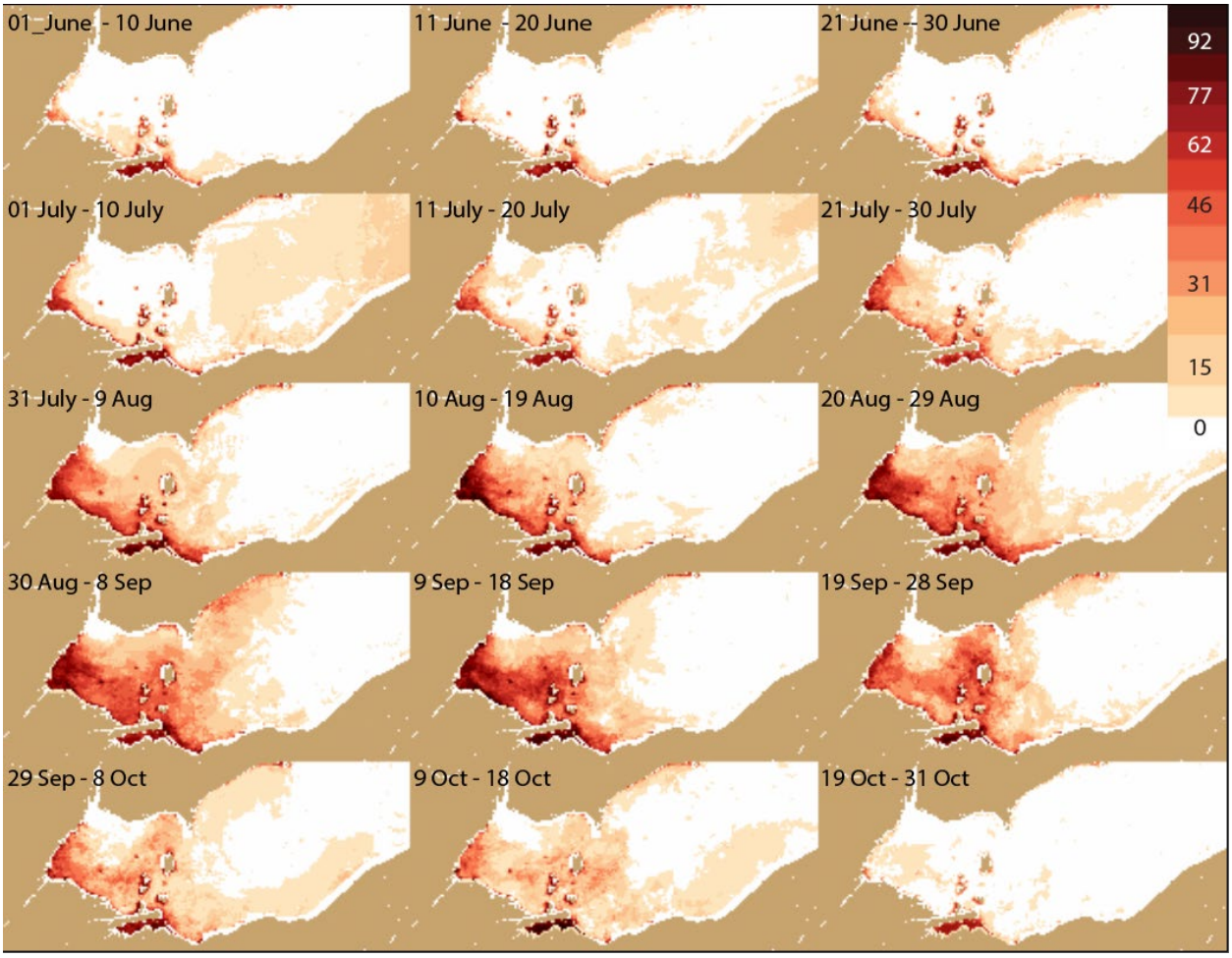

Figure 2.5. The spatial pattern (by pixel) of percentage frequency of detectable cyanobacteria. Analysis for each 10-day period during all years from 2002-2014.

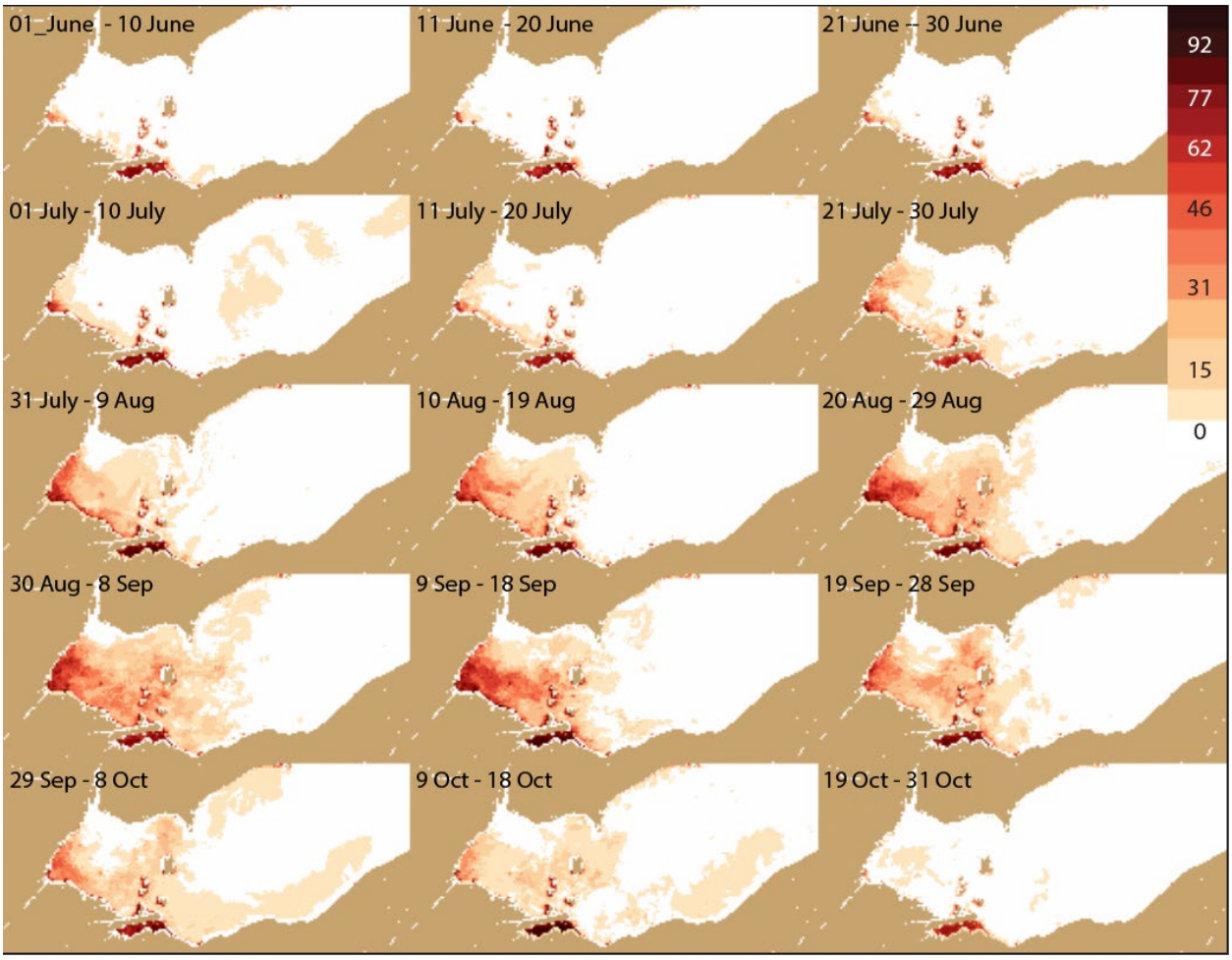

Figure 2.6.The spatial pattern of percentage frequency of severe cyanobacteria (> 10^5 cells mL^{-1}, CI >0.001) for each 10-day period during all years from 2002--2014.

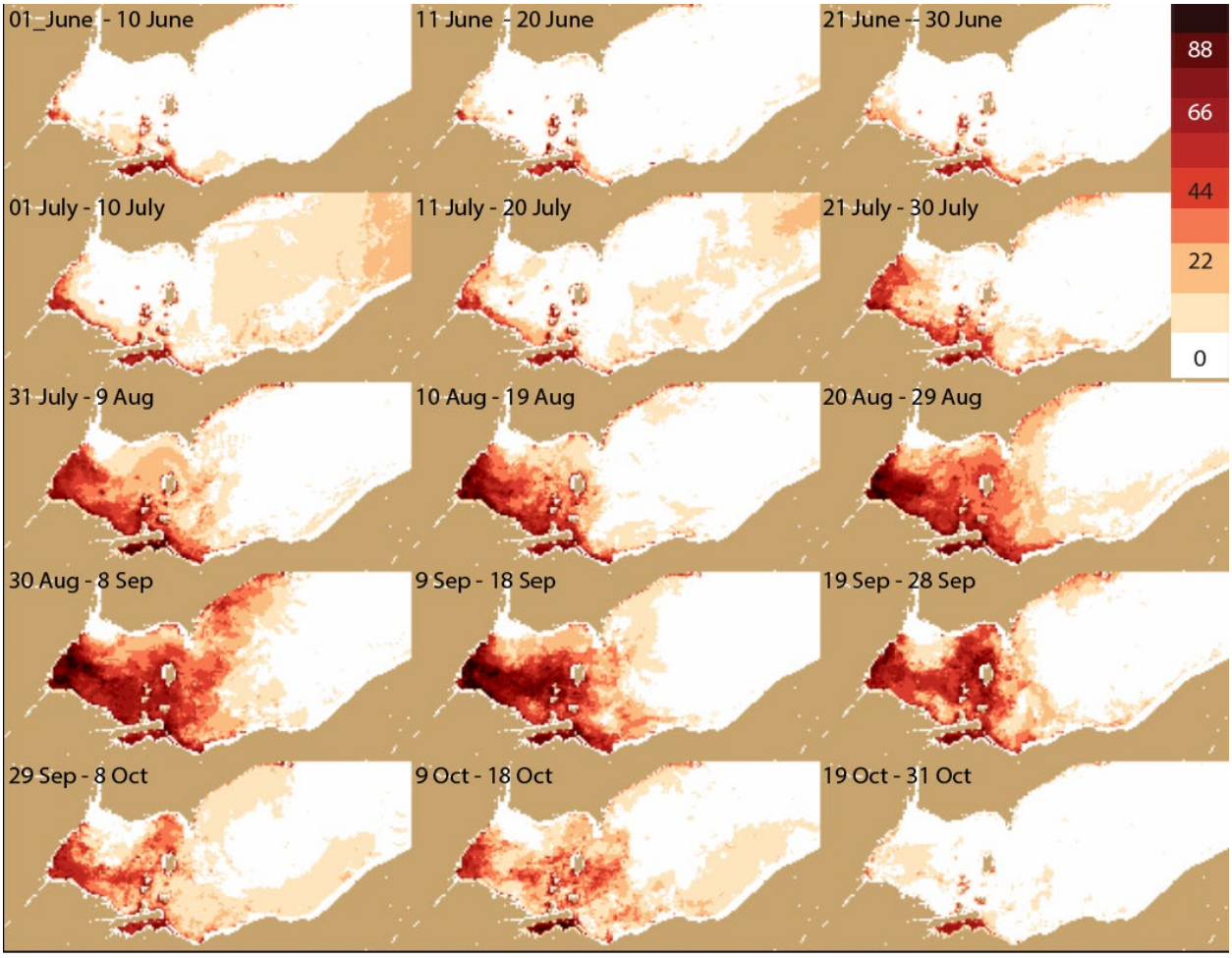

Figure 2.7. Same as Figure 2.5 for only years with blooms (percentage frequency of detectable cyanobacteria).

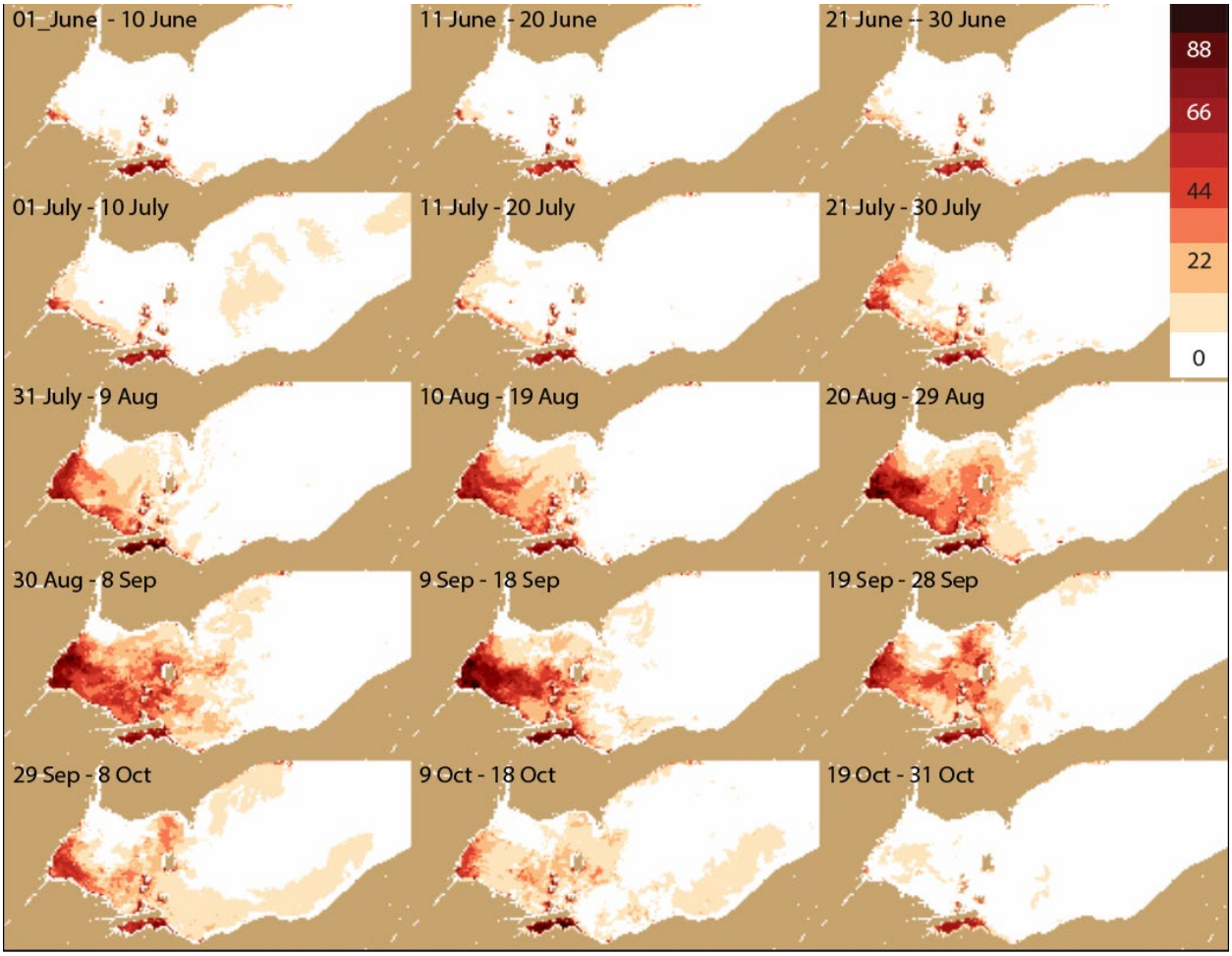

Figure 2.8. Same as Figure 2.6 for only years with blooms (percentage frequency of severe cyanobacteria.

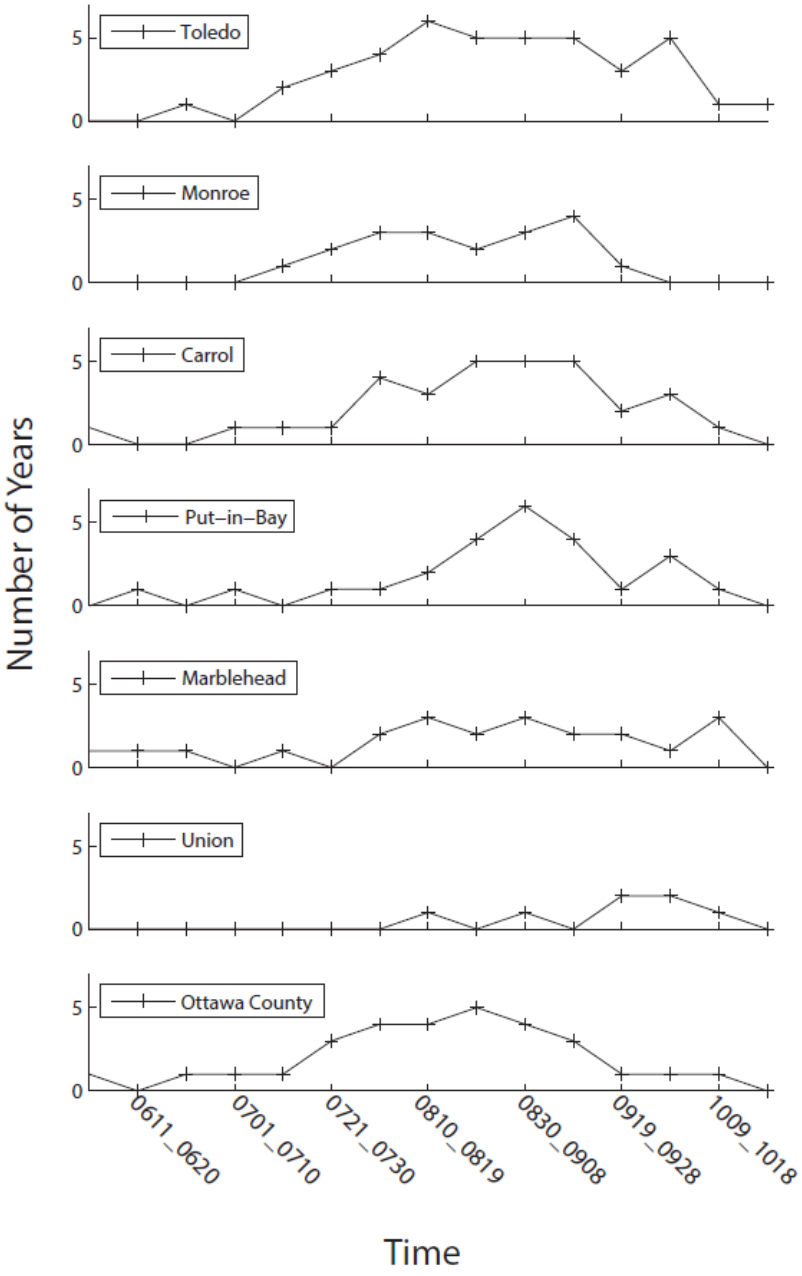

Figure 2.9. Frequency of severe blooms during the 2002-2014 record at the approximate location of selected water treatment intakes from Figure 2. Except for Toledo station (station 1), the data from the other stations were taken 2 pixels (~2 km) into the center of the lake to obtain valid data without land contamination or masking.

Cyanobacterial Bloom Phenology in Saginaw Bay from MODIS and a comparative look with Lake Erie

3.1 Abstract

Saginaw Bay and western Lake Erie basin (WLEB) are eutrophic catchments in the Laurentian Great Lakes that experience annual, summer-time cyanobacterial blooms. Both basins share many features including similar size, shallow depths, and equivalent sized watersheds. They are geographically close and both basins derive a preponderance of their nutrient supply from a single river. Despite these similarities, the bloom phenology in each basin is quite different. The blooms in Saginaw Bay occur at the same time and place and at the same moderate severity level each year. The WLEB, in contrast, exhibits far greater inter annual variability in the timing, location, and severity of the bloom. Phosphorus inputs are the primary driver of blooms in both systems. The WLEB has greater and more variable P-inputs than does Saginaw Bay. Data from Saginaw Bay indicates that if inputs of P into the WLEB were reduced to between 450 and 500 metric tons per year, which the most severe blooms would be abated. Above 500 metric tons P input, blooms increase non-linearly indicating any reduction in P-input at the highest inputs levels currently occurring in the WLEB, particularly of dissolved reactive phosphorus, would yield disproportionately large reductions in cyanobacterial bloom intensity. Any future shifts in the Saginaw Bay watershed toward higher agriculture uses and additional loss of wetlands will substantially increase the risk of more intense cyanobacterial blooms than what are currently occurring.

3.2 Introduction

Harmful Algal Blooms (HABs) are increasing worldwide (Smayda, 1990; Hallegraeff, 1993; Paerl and Paul, 2012; Ho et al., 2019). In freshwater systems these blooms are dominated by cyanobacteria, which adversely affect public health, water quality, and the normal food webs found in healthy aquatic ecosystems (Brooks et al., 2016). In the Great Lakes, cyanobacteria frequently produce potent hepatotoxins, such as microcystins (Watson et al., 2008; Brooks et al., 2016). Additionally, they can make organic compounds, such as geosmin, that cause taste and odor issues in municipal water supplies. Residents that rely on Lake Erie (USA/Canada) for drinking water have sporadically suffered drinking water advisories due to cyanotoxins, most notably in 2014, when the metropolitan area of Toledo, Ohio went several days under a "Do not drink" order (Steffen et al., 2017). Cyanotoxins can also cause mortalities in domestic animals as well as wildlife, primarily through ingestion of cyanobacterial scums (Hilborn and Beasley, 2015). The cyanobacterial blooms in the western basin of Lake Erie (WLEB) have been the focus of many studies in the primary literature (Wynne et al. 2008, 2010; Michalak et al., 2013; Obenour et al., 2014; Stumpf et al. 2016). In contrast, relatively few recent studies have focused on Saginaw Bay (Michigan, USA), especially from a remotely sensed perspective (Budd et al., 2001; Sayers et al., 2016).

Given this lack of information on bloom phenology in Saginaw Bay and the lower intensity blooms relative to the WLEB, whose watersheds share many morphological similarities, the current study was undertaken to address two primary objectives. The first was to detail the bloom phenology of Saginaw Bay using remotely sensed satellite data. The second was to compare the remotely sensed bloom phenology in Saginaw Bay with that of the more intensively studied WLEB to determine if the same or different environmental and anthropogenic factors govern the magnitude and timing of cyanobacterial blooms in both systems.

3.2.1. Saginaw Bay characteristics

Saginaw Bay (Figure 3.1) is a large catchment in the southwestern portion of Lake Huron in the Laurentian Great Lakes encompassing approximately 2,650 km^2. The Saginaw Bay watershed is primarily drained by the Saginaw River. This watershed is the largest in the U.S. state of Michigan and includes one of America's most extensive contiguous freshwater wetland systems. Fifteen percent of the land in Michigan lies within the Saginaw Bay watershed, and is home to approximately 1.5 million people. The land use within the watershed consists of 45% agriculture, 22% forest, 16% open water/wetland, 10% residential, 6% grassland, and 1% high density residential. Nearly the entire shoreline of the bay is lined with dense stands of three square bulrush, (*Schoenoplectus pungens*). The bathymetry of the bay is complicated (Figure 3.1), and makes for a complex circulation pattern. The water enters Saginaw Bay from Lake Huron on the western side of the basin and mixes with output from the Saginaw River before flowing along the eastern side of the bay and returning to Lake Huron. This predominant flow is reinforced by a small island located in the south central portion of the Bay that helps channel flow into and out of the Bay. The bottom substrate in Saginaw Bay consists primarily of limestone and dolomite bedrock and large cobble. The deeper outer portion of the bay, which mixes more completely with Lake Huron water, is more oligotrophic, clearer, and colder relative to the inner bay.

Beginning in the early 1990s, Saginaw Bay was invaded by both zebra mussels (*Dreissena polymorpha*) and quagga mussels (*Dreissena bugensis*) (Pillsbury et al., 2002; Vanderploeg et al., 2001). Both species became well established and were a fundamental component of the food web during this study period (Heath et al., 1995; Pillsbury et al., 2002). Their presence is important because these species likely promote cyanobacterial blooms by differentially consuming diatoms and other competing organisms (Vanderploeg et al., 2001). Another factor

promoting cyanobacteria abundance is excess phosphorus (P) loading. Like most lacustrine systems, P is the primary limiting nutrient in Saginaw Bay with current riverine inputs causing sufficient enrichment to favor cyanobacterial blooms (Jacoby et al., 2000). Because the system is so shallow, remineralization of P will likely reach the photic zone directly promoting cyanobacterial dominance. The feeding activity of the mussels also enhances internal remineralization of phosphorous, further increasing eutrophic conditions favorable for cyanobacterial dominance (Johengen et al., 1995; Arnott and Vanni, 1996; Gardner et al., 2001; Welch and Cooke, 1995).

Nitrogen (N) may also limit primary production in general, and cyanobacteria bloom formation in particular, in certain lakes (Xu et al., 2009). Paerl and Otten (2013) have noted that the non-nitrogen fixing cyanobacteria, *Microcystis*, is capable of producing dense blooms in areas of rapid N enrichment. This frequent co-dependence of blooms on both N and P is problematic because P is generally the only regulated nutrient allowing N build-up favoring intense non-nitrogen fixing cyanobacteria blooms. Nitrogen fixation is metabolically expensive and will only be undertaken when conditions are favorable. The tradeoff for the energy invested in N-fixation is lower net growth. When sufficient N is present, faster growing non-fixing cyanobacteria species will have the competitive advantage and dominate. This is the situation typically prevailing in the WLEB and Saginaw Bay where N is generally not limiting and the cyanobacterial assemblage is dominated by non-nitrogen fixing species in the genus *Microcystis* (Conley et al., 2009).

3.2.2. Western Lake Erie basin characteristics

The WLEB, west of Pelee Point to Sandusky Bay (Figure 3.1C), is located approximately 215 kilometers south of Saginaw Bay (Figure 3.1). It occupies the westernmost portion of the 25,740 km^2 surface area of Lake Erie and encompasses the area where cyanobacterial blooms in the region develop. The WLEB has a surface area of 3,375 km^2. It is relatively warm, shallow (mean depth of 7 m), and productive relative to the other Great Lakes. Approximately 12 million people, 1/3 of the population of the Great Lakes basin, reside within the Lake Erie watershed. In addition to supporting the largest fisheries stocks, it is the most anthropogenically-impacted portion of the Great Lakes. In the 1970s, the chlorophyll levels in the WLEB were often extremely high, exceeding the 50 $\mu g\ L^{-1}$ range (EPA, 1984). The Maumee River is the main supply of phosphorus-enriched waters into the WLEB (Stumpf et al., 2012). The Detroit River, though having a much larger discharge (~35 times), has much lower phosphorus concentrations than the Maumee River and due to high dilution rates, cyanobacteria blooms do not develop in the Detroit River Plume (Wynne and Stumpf, 2015). The predominant land use in the watershed (78%) is agricultural, primarily row crops. Nearly the entirety of the WLEB watershed was once home to the approximately 4000 km^2, Great Black Swamp, which was drained for agriculture in the mid-19^{th} century leaving the WLEB nearly devoid of wetlands (Mitsch, 2017).

The primary role the Maumee River plays in regulating cyanobacterial bloom intensity in WLEB is through P delivery (Figure 3.1). Numerous studies have confirmed this linkage (Stumpf et al., 2012; Stumpf et al., 2016; Bertani et al., 2016). Unlike Saginaw Bay, there is some evidence the WLEB can become nitrogen limited during a bloom during the time of this study period. In 2010, after a large bloom of *Microcystis* senesced, a bloom of nitrogen fixing cyanobacteria in the genus *Dolichospermum* (*formerly Anabaena*) developed (Wynne et al., 2013a). It has been suggested by Michalak et al. (2013) that low ratio of bioavailable nitrogen-to-phosphorus in the

late summer in the WLEB will provide non-nitrogen fixing species, a competitive advantage over other phytoplankton (Smith, 1983). Though no nutrient data were available from the *Dolichospermum* bloom observed by Wynne et al. (2013a), it is reasonable to hypothesize bloom succession was due to *Dolichospermum*'s ability to overcome N-limitation through fixation of atmospheric N. This switch to N-limitation, however, appears to be a somewhat anomalous event as nitrogen is generally a non-limiting nutrient in this system (Stumpf et al., 2012) and *Microcystis* dominates during most cyanobacteria bloom events.

In summary, though Saginaw Bay and the WLEB are part of similar sized watersheds, receive a majority of their nutrients from a single river of equivalent size, are eutrophic, and relatively shallow, the cyanobacterial blooms are generally reported to be less severe in Saginaw Bay (Figure 3.1, Sayers et al., 2016). In this study, a 20-year time series of satellite derived cyanobacterial bloom estimates are calculated and used to characterize the bloom phenology in spatiotemporal detail. The role of P-inputs, land use practices, water residence times, as well as other environmental factors in regulating the observed cyanobacterial bloom phenology were examined. The objective was to characterize what factors govern the variability, timing and intensity of cyanobacterial blooms in both Saginaw Bay and the WLEB and to determine if those governing dynamics were similar or different in each system.

3.3. Materials and methods

3.3.1. Satellite data

Imagery from the Moderate-resolution imaging spectroradiometer (MODIS) was acquired from NASA. The MODIS sensor is onboard two separate spacecraft: Aqua and Terra. Imagery from both satellites was used in this study. The MODIS imagery was used to detect and quantify

cyanobacteria blooms by applying the Cyanobacterial Index (CI). This algorithm was originally derived for the MEdium Resolution Imaging Spectrometer (MERIS) (Wynne et al., 2008; Wynne et al., 2010; Wynne et al., 2013b), and is described in Equation 1.

(eq. 1) $CI = (- SS(678))*1.33$

Where SS is the spectral shape (or curvature; Stumpf and Werdell, 2010) and is determined as

(eq. 2) $$SS(678) = Rho\_s(678) - Rho\_s(667) - \{Rho\_s(748) - Rho\_s(667)\} * \frac{(678-667)}{(748-667)}$$

Where *Rho_s* is the top of atmosphere reflectance corrected for Rayleigh radiance (NASA, 2019) and 1.33 in eq. 1 is a correction factor originating from Wynne et al. (2013b). *Rho_s* allows potential data retrieval in conditions where the atmospheric correction might fail, such as areas of high glint or aerosols (Gower and King, 2007). The standard cloud flagging procedure was used to mask clouds (L2 flags; NASA, 2019, Wynne et al., 2018). Wynne et al. (2013b) showed that the CI could be calculated from MODIS and that with proper corrections the MODIS CI is equivalent to the MERIS CI. A similar correction should be possible with the relatively newly launched Ocean Color Land Imager (OLCI). This will ensure data continuity to build a climatological time series of cyanobacteria blooms in the Great Lakes when MODIS, which is well beyond its mission life, fails. The CI algorithm has been used extensively in disparate water bodies, including the WLEB (Wynne et al., 2010; Wynne and Stumpf, 2015; Wynne et al., 2008), Saginaw Bay (Wynne et al., 2008); and various lakes in New England (Lunetta et al., 2015) and Ohio and Florida lakes (Mishra et al., 2019). More recently the algorithm has been applied to lakes across the continental U.S. with successful results (Clark et al., 2017; Urquhart et al., 2017; Schaeffer et al., 2015, 2018).

The red bands used in this algorithm penetrate pure water only a little over one meter due to red light being strongly absorbed by water (Pope and Fry, 1997). The addition of material into the water column will lessen the depth penetration of the algorithm to under a meter (and shallower still in a cyanobacteria bloom). The spectral shape corrects for total albedo of shallow water, however, it may detect benthic cyanobacteria ("algal mats"). Bottom effects were problematic in the very shallow waters in areas of emergent land in eastern Saginaw Bay, near the Wildfowl Bay State Wildlife Area. Whether due to actual interference or benthic cyanobacteria in this region the wildlife area was included as part of the land mask to avoid potential interference due to benthic cyanobacteria (Figure 3.1). Sediment does not typically cause false positives in the CI. Hawley et al. (2014) did an in-depth analysis on sediment resuspension in Saginaw Bay. A MODIS image with particularly high resuspension was used as an example in their manuscript. The same image showed no false positives with the algorithm employed in equation 1. The CI product has been used for years in Lake Erie without evidence of impact due to resuspended sediments (Wynne et al., 2012; Stumpf et al., 2016).

To analyze the data set, I partitioned the composites at 10-day intervals starting June 1 and extending through October 31 (Table 3.1). This follows the convention used by Stumpf et al. (2012) and Wynne and Stumpf (2015) and is based on the assumptions that the cyanobacteria are slow growing (in Michigan ~0.295 day^{-1}; Wilson et al., 2006) and that during at least one day within the 10-day window, winds will be low and atmospheric conditions will be cloud free. Low winds allow cyanobacteria to accumulate at the surface, providing a better estimate of overall cyanobacteria concentrations within the water column. Wynne et al. (2010) showed that wind speeds where stress exceeds 0.1 Pascal (generated by winds > 7.7 m s^{-1}) were enough to mix the bloom through the water column so that the majority of the bloom material was out of the detection limit of satellite

(roughly a depth of 0.5 meters in bloom conditions). Approximately 24 hours after the stress was removed cyanobacterial cells were able to redistribute to the surface of the water, where an accurate bloom biomass estimations from satellite could be made. Because cyanobacteria prefer warm water temperatures, and Saginaw Bay often freezes in the winter, the CI values were calculated only from satellite images obtained during the warmer months. For each 10-day period the maximum CI value at each pixel observed in any of the satellite images for that time were retained to form a final "*composite*" image of maximum CI values at each pixel. All subsequent references to CI will indicate a composite image containing these pixel-specific maximum CI values for each 10-day period (Stumpf et al., 2012). CI values are useful for showing the spatial distribution of maximum CI values for a given 10-day composite. Each month has three ten-day composites, so the third 10-day composite of a 31-day month encompasses 11-days. For simplicity, these 11-day composites are also referred to as "10-day" composites (see Table 3.1 for details). In any CI data comparisons between Saginaw Bay and WLEB the same 10-day periods were used.

Table 3.1: The 10-day composite numbering system used for each year in both Saginaw Bay and western Lake Erie basin.

Composite Number	Start Date	End Date
1	June 1	June 10
2	June 11	June 20
3	June 21	June 30
4	July 1	July 10
5	July 11	July 20
6	July 21	July 31

7	August 1	August 10
8	August 11	August 20
9	August 21	August 31
10	September 1	September 10
11	September 11	September 20
12	September 21	September 30
13	October 1	October 10
14	October 11	October 20
15	October 21	October 31

3.3.2. Interannual variability in bloom biomass

To address interannual variability of cyanobacteria biomass in Saginaw Bay the following steps were taken. The maximum pixel values for each available composite MODIS scene were summed to produce an "integrated CI" or maximum biomass value. This was done for all 15 composites from June 1 - October 31 (Table 3.1), for each year from 2000 to 2019, for both Saginaw Bay and the WLEB. Cyanobacterial blooms in Saginaw Bay blooms were retained within the Bay, only the pixels covering the 2,650 km^2 surface area were included in each scene. In contrast, blooms originating in the WLEB are sometimes transported into the central basin to the area near Avon Point (Figure 3.1C). To capture this transport, satellite surveillance of blooms was extended beyond WLEB proper to include the areas west of a line between Pelee Point and Avon Point. This region has a surface area of 4,983 km^2. Hereafter, bloom in "the WLEB" will refer to cyanobacterial blooms that originated in the shallow basin proper plus biomass exported

out of the basin captured in the satellite imagery. The goal was to capture all the biomass originating within WLEB proper, but to exclude any blooms developing independently in the central basin of Lake Erie.

3.3.3 Bloom maxima in Saginaw Bay and western Lake Erie Basin

Given the similarities between Saginaw Bay and WLEB, a logical question to address is whether blooms in each develop and peak at the same or different times during the summer. To address this question, statistics (mean, standard deviation, mode, and median) describing the time period where the maximum CI value occurred were then determined for the integrated CI values for each 10-day period (e.g., June 1 to June 10) over all 20 years (Table 3.1).

3.3.4 Role of total phosphorus (TP) in driving cyanobacterial blooms in Saginaw Bay and the western Lake Erie basin

Because total phosphorus (TP) is known to be a driver of cyanobacterial blooms in the WLEB, I examined the relationship between TP-inputs and the magnitude of cyanobacterial blooms in both Saginaw Bay and WLEB. This analysis required determining river discharge rates for the Saginaw and Maumee Rivers, establishing which period of discharge most impacted cyanobacterial bloom development, obtaining flow weighted mean concentrations (FWMC) and P loading during the most relevant time periods, and comparing the estimated P-load with the magnitude of blooms (integrated CI values) in both systems. The FWMC used in any given analysis represented the summed P (TP or DRP) concentrations for a river across a specified time period divided by the volumetric discharge of the river during the corresponding time period. This average FWMC times flow for a given period of months/year was used to calculate

the various time specific TP loads. Details of how these various components of the analyses were developed and utilized are provided below.

River discharges

The Saginaw River, and the Maumee River are the primary sources of P that drive cyanobacterial growth in both systems (Baker et al., 2014; Stumpf et al., 2012; Withers and Jarvie, 2008). Within the Saginaw Bay watershed, the Saginaw River is by far the largest source of water flowing into the bay contributing ~70% of the freshwater input (Stow et al., 2014) and contributing an estimated 90% of the nutrient load (Bierman et al., 1984). Likewise, the Maumee River is a key source of the nutrients entering WLEB, and along with the much smaller Cuyahoga and Sandusky Rivers contribute 50% of the P load into Lake Erie (Baker et al., 2014). Consequently, any differences in the magnitude in timing of water discharges from the Saginaw and Maumee Rivers can potentially affect timing and magnitude of cyanobacterial blooms. To document any differences in discharge patterns between the two rivers, Saginaw River flow measurements were obtained from the United States Geological Survey's (USGS) gage station 04157005 at Holland Avenue at Saginaw, MI, and those for the Maumee River from the USGS gage station 04193500 at Waterville, Ohio. The resulting data were utilized as described in the sections 2.4.2 and 2.4.3.

Estimating what period of river flow best correlated with the 10-day maximum CI value

Research on cyanobacterial blooms in the WLEB demonstrated total P-input from March - June best correlated with maximum bloom biomass later in the summer (Stumpf et al. 2012). How the timing of P inputs affected bloom formation in Saginaw Bay was unknown. To address this question, I examined three different integrated periods of river discharge ($m^3 \times 10^9$). These were:

(1) October - September, (2) March - June and (3) March - July. The October - September time period reflects the TP input starting from the termination of cyanobacterial blooms by early October of the previous year through the bloom maximum the next summer as well as the termination of the bloom in September. Outflow for these various time periods each year were compared to the corresponding highest integrated 10-day (Table 3.1) CI value that year, which was assumed to represent the maximum annual bloom biomass each summer. The comparison made it possible to estimate which input period best predicted maximum biomass development.

Additionally, a direct comparison of the average river discharge patterns in Saginaw Bay and the WLEB was also undertaken. The objective was to establish how similar or different the pattern of monthly discharge was in Saginaw Bay compared to WLEB. This was accomplished by determining the mean monthly water discharge volume for both rivers from 2000-2019. The data were analyzed from October to September which corresponds with the annual bloom progression observed in Saginaw Bay and Lake Erie.

Relationship between TP loading and maximum 10-day CI in Saginaw Bay and Western Lake Erie Basin

As a means of investigating how P-inputs drive bloom phenology between Saginaw Bay and the WLEB I determined the relationship of TP input to maximum 10-day CI. Total phosphorus is generally used to set limits for eutrophication based on it being the form most commonly and readily measured. TP inputs for the Saginaw River and the Maumee River were estimated as follows. Initially, average TP and Dissolved Reactive Phosphorus (DRP) concentrations for the Saginaw and Maumee Rivers were determined. For Saginaw Bay, the only reliable estimate of TP-loading comes from the study by Cha et al. (2010). That study utilized known phosphorus

concentrations, river flow rates, and loading estimates directly measured by Michigan Department of Environmental Quality or obtained from other sources from 1974 - 1991 and 2001 - 2005 (MDEQWB, 2010). Those data allowed development of a Bayesian model predicting the TP loads from flow rates. This model, along with flow rates from the USGS allowed continuous estimation of loading from 1968-2008, despite the lack of measured nutrient concentration data in some years. The last 9 years of this data set overlap with the first 9 years of this study. As a result, it was only possible to obtain estimates of TP concentrations for the period 2000-2008. For the WLEB, TP is routinely measured in the watershed, including the Maumee River, by Heidelberg University's National Center for Water Quality Research (NCWQR) (Heidelberg University, 2019). Those values and those from Cha et al. (2010), along with the March to June river discharges from the USGS during the 2000-2008 study period, were used to calculate the FWMC for TP in both the Saginaw and Maumee Rivers.

Cumulative TP loading for each year for the Saginaw River from 2000-2008 was then calculated using the following equation:

(eq. 3) $$M = \sum_{i=March}^{n=June\ 30} (x)\ f_i$$

Where M is the annual total mass of TP in grams by riverine transport, x is the FWMC of TP (mg L^{-1}) determined above, f is the river discharge per month for the Saginaw River calculated from sources described in section *2.4.1*, and i is month (Sigleo and Frick, 2003). The resulting estimated annual P-inputs of TP and DRP (dissolved reactive phosphorus) were converted to metric tons.

Finally, the annual March - June volumetric runoff estimates for the Saginaw and Maumee Rivers from 2000-2008 were compared to the maximal annual biomass estimate determined as

described in section *2.3*. An equivalent comparison was constructed for annual March - June TP inputs versus the maximal annual biomass (CI) values.

Historical versus current estimation of P-loading in Saginaw Bay to estimate efficacy of P abatement efforts

In the 1970s phosphate abatement regulations were put in place and eutrophication declined only to emerge again in the 1990s in the WLEB (Scavia et al., 2014). Data on the annual volumetric discharge form the Saginaw River and annual TP loading from the periods 1974 - 1991 and 2001 - 2005 were collated from different sources by the Michigan Department of Environmental Quality Water Board (MDEQWB, 2010; Figure 3.2). These data provide an estimation of the overall efficacy of TP abatement in the Saginaw River watershed and if the same trend of increased eutrophication as observed in the WLEB occurred. This analysis was done by performing a regression analysis of annual volumetric outputs from the Saginaw River versus the TP from each dataset and then comparing the slope of the regression lines. An increase in slope of the 2001 - 2005 data compared to that of the 1974 - 1991 data would indicate an actual increase in TP concentration relative to 1974-1991 and vice versa.

3.3.5. Modeled maximum, cumulative 10-day CI predicted from total phosphorus (TP) and dissolved reactive phosphorus (DRP) inputs

Another means of assessing the similarity or differences in response to P-inputs in Saginaw Bay and WLEB is to use models previously developed for western Lake Erie. Specifically, Stumpf et al. (2016) modeled the maximum, cumulative 10-day CI from both TP and DRP for the Maumee River - WLEB system. Research in the WLEB (Baker et al., 2014), however suggests DRP, not TP, is the primary driver of *Microcystis* blooms. Similarly, Tarczyńska et al. (2001) reported that

DRP, in conjunction with temperature and water retention time, were the primary factors in promoting *Microcystis* blooms in the Sulejow Reservoir in Poland. By running the Stumpf et al. (2016) model using data available from both the Saginaw Bay and WLEB from 2000-2008 it was possible to determine how closely the modeled, integrated 10-day CI values matched the actual measured 10-day integrated CI values in both systems. An equivalent ability for TP and DRP to predict actual cyanobacterial biomass in both systems would indicate P-inputs are governing bloom dynamics in both systems in a similar fashion. Comparing the TP versus DRP results also allows insight into whether DRP was a better predictor of cyanobacterial biomass in Saginaw Bay as was found previously in WLEB.

Most of the flow rate and nutrient concentration data needed to run the model were all readily available from USGS and the NCWQR database (Heidelberg University, 2019), respectively. DRP concentrations for the Saginaw River, which have not been measured, were the only exception. An indirect estimate of average DRP for the Saginaw River was obtained using the following approach. Average March-June TP and DRP concentrations in mg L^{-1} for the period from 2000-2019 were obtained for the nearby Cuyahoga, Sandusky, and Maumee Rivers (Heidelberg University, 2019; Baker et al. 2014). Agriculture, primarily corn and soybean production, constitutes 83% of the land use in the Sandusky River watershed, 78% in the Maumee River watershed, 45% in the Saginaw watershed and 22% in the Cuyahoga watershed. The Sandusky River basin covers 4,735 km^2 with 220,000 residents. The Maumee River watershed covers 21,538 km^2 and has 278,000 residents. The Cuyahoga watershed covers 2,106 square kilometers and is the most intensely urbanized. It receives runoff from the municipalities of much of metropolitan Cleveland, Akron, Kent, and Cuyahoga Falls and has a resident population of 1.8 million people. It receives substantial nutrient inputs from non-agricultural as

well as agricultural sources. The Saginaw River watershed is much larger, covering 22,261 km^2, but still contains a more dispersed population of 1.4 million residents.

The four month period from March-June was chosen because total volumetric discharge from the Saginaw River during this time, analyzed as detailed in *2.4.2*, correlated best with the highest integrated CI values each summer. The average TP and DRP concentrations for all the March-June periods between 2000-2019 ± 1 standard deviation were next determined and a regression equation fit to the data. The resulting regression equation, in conjunction with the average FWMC TP concentration for the Saginaw River obtained from the Cha et al. (2010) study for the period from 2000-2008, made it possible to estimate the FWMC for DRP in the Saginaw River. The corresponding March-June average DRP FWMC from the Maumee River were obtained from the NCWQR database as reported above (Heidelberg University, 2019). Once these data were assembled, the modeling studies were conducted as follows.

Modeling Maximum CI from Total Phosphorus

The modeled integrated CI (CI_{MERIS}) equation for TP developed by Stumpf et al. (2016) using the existing MERIS and adjusted MODIS data is:

(eq. 4) $$CI_{MERIS\ model} = B \times 10^{a \times X}$$

Where $CI_{Meris\ model}$ = modeled CI value, a = 7.48x10^{-4}, B = 0.57 and X = total phosphorus load in metric tons. As the MERIS sensor failed it was replaced by the MODIS sensor. This transition required recalibration of the MERIS algorithm from Stumpf et al. (2016) to fit the MODIS data used in this study because the MERIS composited imagery had CI_{max} values slightly lower than the MODIS CI_{max} values for overlapping scenes. This was particularly true of the 2011 bloom in

which the MODIS sensor experienced saturation of the sensor in the scum areas (Wynne et al., 2013b). The algorithm that was used to estimate the CI in the scum arrears most likely overestimated the scum CI relative to MERIS, which does not have a saturation issue (Wynne et al., 2018). Equation 4 above needed to be recalibrated to account for these differences. The CI MERIS from Stumpf et al. (2016) was plotted against with the CI_{MODIS} in this study (Figure 3.3) and the resultant equation was

(eq. 5) $$CI_{MODIS} = 0.81 \times CI_{MERIS} - 1.3$$

Combining equations 4 and 5 yields the following equation for $CI_{MODIS\ model}$

(eq. 6) $$CI_{MODIS\ model} = B_{MODIS} \times 10^{a \times X} + 1.6$$

where *a* remains = 7.48×10^{-4} , B_{MODIS} = 0.70, with X = total phosphorus load in metric tons. For Saginaw Bay and WLEB, it was possible to insert the March-June TP loading values previously determined in section *2.4.3* into eq. 6 to calculate maximal 10-day $CI_{modeled}$ values for both Saginaw Bay and WLEB from 2000 - 2008.

Modeling maximum CI from total dissolved reactive phosphorus (DRP)

Equation 6 also models the relationship between DRP inputs and resulting maximal 10-day CI values where *X*= DRP load in metric tons, $a = 3.87 \times 10^{-3}$ (Stumpf et al., 2016), and $B_{MODIS} = 0.59$ *determined* from *B*=0.48 in Stumpf et al. (2016).

The total March - June DRP inputs for the WLEB needed to predict the maximal 10-day CI values using eq. 5 were estimated using a mean DRP value for the Maumee River as described above. The corresponding March - June DRP loading for the Saginaw River was calculated using eq. 3 and the mean flow-weighted DRP value obtained as by the method described in

section *2.5.* As before, the actual 10-day integrated CI values estimated from satellite data for both systems were compared to the modeled integrated CI values.

3.3.6. Effects of other forcing functions on bloom dynamics in Saginaw Bay

Other forcing functions besides P-input can potentially modulate the intensity of blooms in the two systems. Potential factors for consideration were selected because they are likely to be associated with cyanobacteria growth or dominance. These include cloud cover, incoming shortwave irradiance (proxy for incoming photosynthetically active radiation), water temperature, and wind stress (intensity and direction). Differences in average light availability associated with latitude and cloud cover will potentially affect the growth of cyanobacteria that often prefer high light. Many cyanobacteria such as *Microcystis* vertically migrate in the water column to optimize photosynthesis. Surface temperature was chosen because cyanobacteria grow better at warmer waters associated with a stable thermocline that reduces mixing losses. Under these conditions, cyanobacteria often outcompete other co-occurring species (Paerl and Huisman, 2008). Wind stress was chosen because it can affect the vertical distribution of cells and vertical migration directly affecting CI values that only come from the top meter or so of the water column (Reynolds et al., 1987; Wynne et al., 2010).

For comparative purposes, the available June-October data listed above were downloaded as climatological monthly means from NASA's Giovanni reanalysis dataset (Giovanni, 2020) for the years 2000 to 2019. The corresponding CI scenes were binned to create monthly composites instead of the 10-day integrated CI composites used elsewhere in this study. Once the June-October monthly values were calculated they were averaged to provide an average value for each

year. Single parameter correlations were then performed between the factors listed above to identify the factors with significant correlations with the annual June-October CI values.

3.3.7 Bloom phenology in Saginaw Bay

The following analysis was performed to provide a more detailed resolution regarding the temporal and spatial distribution of Saginaw Bay cyanobacterial blooms, which have been less well investigated than those in western Lake Erie. The analysis was conducted by segregating all the scenes 2000-2019 into 15 datasets each containing the scenes for the same 10-day period each year (Table 3.1). Each of the 15 datasets was then analyzed separately. CI values from each corresponding pixel from all 20 scenes (2000-2019) was identified, averaged and plotted as a single composite image showing the average CI distribution across Saginaw Bay for that 10-day period. The resulting 15 composite plots of average CI values across Saginaw Bay for each 10-day period were then presented in chronological order to show the seasonal bloom progression from the summertime initiation to the final demise in the fall. This analysis included any bloom where the CI is above the detection limit, i.e. > 0, which is estimated to be ~10,000 - 20,000 cells mL^{-1} (Davis et al., 2018).

In addition, two frequency analyses previously used to investigate bloom severity in WLEB were performed (Wynne and Stumpf, 2015). The 2000-2019 MODIS imagery were used to illustrate the bloom phenology described above and were partitioned into the same 15 datasets containing the scenes for specific 10-day composite images from the first 17 years of the study. However, instead of using the data to calculate an average composite pixel CI value, the data for each year was examined to determine how many years during the time series the CI value for each pixel exceeded a defined threshold value. The number of years where the threshold exceeded the

prescribed threshold value was then divided by 17 and multiplied by 100 to provide a frequency estimate ranging from 0 to 100 percent. In the first frequency analysis, the threshold value was CI = 0 as defined above. The resulting 15 frequency plots for each 10-day period were plotted in chronological order to show how frequently a bloom with CI>0 was present in each section from spring to early spring. The second analysis was performed in exactly the same manner, but used a threshold value CI ≥ 0.001, equivalent to a concentration of ~10^5 cells mL^{-1} (Stumpf et al., 2012). This is the concentration recommended by the World Health Organization as the upper limit for recreational exposure to cyanobacteria (Chorus and Bartram, 1999) and represents the frequency of severe blooms throughout Saginaw Bay on average over the bloom season. By analyzing the frequency of severe blooms only, the noise in the data is reduced.

3.3.8 Spatial distribution of blooms in Saginaw Bay relative to the prevailing circulation pattern

Another understudied aspect of the cyanobacterial blooms in Saginaw Bay is their spatial distribution. The predominant flow in Saginaw Bay consists of water entering from Lake Huron along the western side of the Bay and exiting along the eastern shore. This flow is reinforced by an island located in the approximate center of the Bay that helps channel flow into and out of the Bay. To determine how this flow pattern might influence spatial difference in the bloom intensity, Saginaw Bay was divided into five different subregions. These included: (1) the area closest to the river mouth at the southern end of the Bay, (2) the inner and (3) outer regions on the eastern side of the Bay and (4) the inner and (5) outer regions along the western side. Previous studies have similarly partitioned the Bay into these same subregions as a means of documenting spatial differences in various biological measurements associated with differences in depth and circulation patterns (Bierman et al., 1984; Fishman et al., 2010). The integrated CI

for each subregion for each 10-day composite period (Table 3.1) were then determined from the MODIS data and shown as a separate time series from 2000-2017.

To further quantify interannual variability in bloom intensity among the different subregions of Saginaw Bay, an integrated CI value for each year from 2000-2019 for each subregion was determined. The annual subregional, integrated CI values were then normalized to the surface area of each corresponding subregion (integrated CI km^{-2}).

3.4 Results

3.4.1. Satellite-derived interannual variability

Every year during the 2000-2019 study period Saginaw Bay experienced a cyanobacterial bloom (Figure 3.4). The magnitude of these blooms, as indicated by the largest integrated CI value (biomass) during a 10-day period, showed relatively little interannual variation. The largest 10-day integrated biomass estimate for the entire Bay occurred from 1-10 September, 2017. The smallest bloom maximum occurred from 1-10 August, 2016. These maximum and minimum bloom biomasses indicated blooms varied by no more than 4.25-fold interannually. If the 2017 maximum biomass value is excluded, the interannual variation drops to a 1.6-fold difference. In contrast, blooms in the WLEB exhibited a much higher degree of interannual variability during the same period. Maximal 10-day biomass estimates in this system ranged from an integrated CI of 1.5 in 2005 to CI of 40 in 2011, corresponding with a 27-fold interannual difference in bloom concentrations. If 2011is excluded, the interannual variation was still 15-fold. Figure 3.4B shows the maximum integrated CI values for the same 10-day composites in Saginaw Bay superimposed over the WLEB integrated CI. Blooms in WLEB during “non-bloom years” (2000-2002; 2005-2007) were of similar magnitude to those in Saginaw Bay. Starting in 2008

the two systems diverged. While the magnitude of the cyanobacterial blooms remained relatively stable in Saginaw Bay, much larger blooms began to develop in WLEB during the years 2008-2009, 2011, 2013-2015 and 2017. This divergence corresponded to a shift from drier years (2000-2008) on average to wetter years on average (2009-20017, 2019; Figure 3.4).

3.4.2. Timing of bloom maxima in Saginaw Bay and western Lake Erie Basin

The mean, median, and mode of integrated CI values for each of the 10-day periods (Table 3.1) over the course of the times series were determined. The 10-day period having the highest mean, median, and mode values in Saginaw Bay and WLEB are shown in Table 3.2. The mean, median, and mode results all showed blooms peaked in Saginaw Bay 20 days before those in WLEB. Corresponding mean monthly water temperature estimates for 2002-2019 from the USGS discharge stations from the Maumee River and the Saginaw River indicate the warmest 10-day in both rivers occurred in the 6th composite period, corresponding to 21 July - 31 July. The maximal temperatures, however, were slightly different between the two systems. Mean monthly water temperatures from MODIS nighttime 11-micron 4 km data for WLEB were 24.0 °C in July, 24.2 °C in August and 21.6 in September, compared to 21.7 °C in July, 22.0 °C in August and 19.4 in September for Saginaw Bay.

Table 3.2: The 10-day composite periods (in parentheses) exhibiting the highest mean, median, and mode integrated CI values during the 20-year MODIS time series. Details on how values were calculated are given in section 2.3.

Statistic	western Lake Erie Basin	Saginaw Bay
Mean ± SD	9.7 ± 2.4 (Sep 1 - Sep 10)	7.75± 1.7 (Aug 11 - Aug 20)

Median	10.0	(Sep 1 - Sep 10)	7.5	(Aug 11 - Aug 20)
Mode	10.0	(Sep 1 - Sep 10)	9.0	(Aug 21 - Aug 31)

3.4.3 Flow period best corresponding to maximum 10-day CI value

The March to June and March to July volumetric output of the Saginaw River best correlated with the maximal 10-day integrated CI value later in August (Table 3.2). There was no significant difference between these two time periods with regard to their ability to predict maximal CI values (Figure 3.5). Consequently, in each of the following analyses, flow rate and associated nutrient loading were integrated over the March - June period which has produced the best correlation between river flow and the extent of blooms in WLEB (Stumpf et al., 2012). This also simplified comparisons of the mechanisms driving cyanobacterial blooms in both systems.

The average annual discharge pattern for the Saginaw and Maumee Rivers were similar with peak flow occurring in April in the Saginaw River and March in the Maumee River (Figure 3.6). Though the pattern was similar, average discharge volumes from the Maumee River in March were substantially higher than from the Saginaw River. April and May discharges from both rivers were equivalent while those in June were again substantially higher from the Maumee River. As a result, on average the overall discharge volume from the Maumee River is higher than that from the Saginaw River. Another major difference between the two rivers was the larger interannual variation relative to mean flow in the Maumee River, particularly between March and July (Figure 3.6).

Table 3.3. Correlations between the discharge volumes from Saginaw and Maumee Rivers and the annual maximum 10-day integrated CI *values.*

Water Body	Time Period	r^2
Saginaw Bay	March - June	0.15
Saginaw Bay	March - July	0.16
Saginaw Bay	Water Year	0.2
western Lake Erie Basin	March - June	0.6
western Lake Erie Basin	March - July	0.6
western Lake Erie Basin	Water Year	0.07

3.4.4 Efficacy of P-reduction effort in Saginaw River basin

The relationship of annual output from the Saginaw River versus TP loading from 1974 - 1991 had a slope of 2.7 versus 1.7 for the 2001 - 2005 period (MDEQWB, 2010) (Figure 3.2). This difference in slope indicates a 37% drop in average TP concentrations in response to efforts to reduce loading as of 2005.

3.4.5. Relationship between the estimated March-June TP loading versus subsequent maximal 10-day composite CI values

The relationship between TP loading from the Saginaw and Maumee Rivers versus resultant maximal cyanobacterial biomass was calculated as detailed in section *2.5*. The volumetric discharge of the Saginaw and Maumee Rivers during the drier period from 2000-2008, for which TP data for the Saginaw River, were similar. In contrast, the amount of cyanobacterial biomass

produced for the same amount of river discharge were not equivalent. As March - June outflow increased in the Saginaw Bay, the cyanobacterial biomass rose in a linear fashion. In contrast, as discharge exceeded about 2 x 10^9 m^3 cyanobacterial biomass in WLEB increased in a non-linear fashion with the linear increases in flow producing progressively and disproportionately more intense blooms compared to Saginaw Bay (Figure 3.7A).

The plot of March - June TP inputs versus maximal cyanobacterial biomass showed a different pattern than observed for river discharges (Figure 3.7B). TP inputs between 110 to 450 metric tons caused similar, linear increases in maximal bloom intensity in both Saginaw Bay and WLEB. TP input into Saginaw Bay for 8 of the 9 years examined fell below this cut off point. The remaining year received TP inputs of only 450 metric tons. TP inputs into WLEB exceeded 400 metric tons for 7 of the 9 years with maximal loading exceeding 1,050 metric tons. As loading levels exceeded 450 metric tons TP in the WLEB, linear increases in TP produced a non-linear response of progressively more intense cyanobacterial blooms (Figure 3.7B).

3.4.6. Modeled CI as a function of TP and DRP

The modeled cyanobacterial biomass based in March - June TP input fell along a 1:1 line for both Saginaw Bay and WLEB (Figure 3.8A). This is consistent with the model having been developed for WLEB, which takes into account the non-linear response with increased TP loading. Because the Saginaw Bay loading values were low, they fell in the more linear portion of the model consistent with the observations in Figure 3.8B. The tight clustering of points in Saginaw Bay are also consistent with the low interannual variation in bloom intensity compared to the much larger dynamic range for WLEB. When interpreting these data, it should be noted that the Maumee River Basin entered a wet phase in 2008 (Figure 3.4) and that is the only wet

year included in this analysis. Even greater TP loading for 2009 - 2019 would be anticipated if the requisite TP concentration in the Saginaw River had been available to estimate the corresponding loading (Stumpf et al., 2016).

CI modeled on DRP from the Maumee River again fell along the 1:1 line with slightly more scatter than was observed for TP. This scatter indicates that in the lower flow years from 2000-2008, TP inputs did outperform DRP estimates in predicting cyanobacterial bloom biomass (Figure 3.8B). The CI values based on the lower DRP input from the Saginaw River deviated from the expected 1:1 line. These values again clustered together at the low end of the P-input to cyanobacterial output curve, but exhibited a much higher slope than expected based on the estimated DRP value used in the model (Figure 3.9). This higher slope is likely due to the actual DRP concentrations in the Saginaw River being even lower than estimated.

3.4.7. Additional forcing functions effects on bloom dynamics in Saginaw Bay

The single regression analyses of cloud cover, incoming shortwave irradiance, mean water and wind stress (intensity and direction) versus CI were conducted. Results revealed that no input parameter had an $r^2 > 0.05$.

3.4.8. Bloom phenology and intensity in Saginaw Bay

The average CI patterns from each 10-day composite for the entire 20-year time series is shown in Figure 3.10 for Saginaw Bay. The blooms peak in August, and subside relatively quickly in early September. This differs from the WLEB, where a similar analysis showed peak concentrations in mid-September (Wynne and Stumpf, 2015). Blooms are primarily distributed along the shoreline every year forming a halo that does not fully extend into the center of the bay. Nguyen et al. (2014) showed the prevailing current field in Saginaw Bay has strong

divergent currents in the center portion of the bay that move water away from the center of the bay towards the shore, which prevents the cyanobacterial cells from accumulating there. These currents are particularly strong in July and August, when the blooms are at their peak. The frequency of all blooms (CI > 0) per 10-day composite are shown in Figure 3.11A, and the severe blooms (CI > 0.001) are shown in Figure 11B. These analyses also show the same pattern as observed in Figure 3.10 with nearshore areas clearly experiencing more blooms on average. In combination these results show blooms reliably initiating in July, reaching peak in mid-August, fully dissipated by October and disproportionately impacting areas adjacent to shore.

3.4.9. Quantifying magnitude of cyanobacterial blooms in subsections of Saginaw Bay

To examine differences in bloom intensity along various segments of the shoreline in Saginaw Bay, the integrated CI values were calculated for 5 different subregions of Saginaw Bay for the entire 20-year time series (Figure 3.12). The time series again revealed the same relatively invariant pattern of annual blooms across the entire study period (Figure 3.12A). The subsection where the Saginaw River enters Saginaw Bay exhibited the highest composite CI values and the inner Bay had generally higher CI values than the outer Bay. There was also an across Bay gradient in CI values with Regions 2 (inner Bay) and 4 (outer Bay) along the western shore exhibiting lower CI values than the corresponding subregions 3 (inner) and 5 (outer) along the eastern shore (Figure 3.12C). This general pattern in cyanobacterial bloom intensity is again corresponds with inflowing oligotrophic waters from Lake Huron preferentially diluting the cyanobacteria bloom along the western shore and outflowing currents differentially transporting bloom populations from near the mouth of the Saginaw River along the eastern shore. A minor portion of the observed CI differences may also be partially due to regions on the western side of the Bay having a lower percentage of coastal adjacent pixels relative to the two regions on the

eastern part of the bay. Pixels immediately along the shoreline can sometimes have bottom reflectance or other adjacency issues that cause overestimated CI values.

3.5 Discussion

3.5.1 Factors governing severity and variability of cyanobacterial blooms in Saginaw Bay and the western Lake Erie Basin (WLEB).

The interannual differences in the variability and intensity of cyanobacterial blooms observed in the WLEB relative to Saginaw Bay were extreme given both watersheds are similarly sized and have a close geographic proximity. Saginaw Bay experienced relatively moderate, similarly sized, cyanobacterial blooms each year from 2000-2019. In contrast, blooms in the WLEB ranged from the intensities observed in Saginaw Bay to an order of magnitude higher (Figure 3.4). Many of the larger WLEB blooms caused significant adverse impacts (Michalak et al., 2013; Stumpf et al. 2016). The differences in bloom intensity were largely driven by two factors: the greater flow weighted mean concentrations (FWMC) of P in the Maumee River and the higher and more variable volumetric discharge from the Maumee River (Figure 3.6). The impact of the differences in FWMC of TP on cyanobacterial bloom formation was evident in comparing the influence of discharge and TP on the maximal summertime biomasses in Saginaw Bay and the WLEB (Figure 3.7). During this relatively dry 9-year period, the range in annual discharge volumes was equivalent for these two similarly sized watersheds. Yet the same volumetric discharge from the Maumee River produced more intense cyanobacterial blooms than equivalent discharges by the Saginaw River (Figure 3.7A). In contrast, when maximal biomasses in Saginaw Bay and the WLEB were plotted versus the total March-June TP loading for both the Saginaw and Maumee Rivers, comparable loading produced equivalent cyanobacterial biomass

in both systems (Figures 3.6 and 3.7). Blooms in Saginaw Bay clustered at the low end of the TP input range and were tightly grouped reflecting the small interannual variation in TP inputs and resulting blooms. The largest variation in cyanobacterial biomass occurred in the WLEB during the wetter period from 2009-2019, and was again driven by much greater variations in May-June phosphorus loads from the P-enriched Maumee River compared to the less enriched Saginaw River (Figure 3.4; Stumpf et al. 2016).

The higher nutrient load in the Maumee River is due to approximately 78% of the land use being devoted to agriculture compared to 45% in the Saginaw Bay watershed (Ohio EPA, 2008). Most of the agriculture in both watersheds is devoted to cultivation of row crops of corn and soybeans. The soil types in both basins require drainage to make them agriculturally productive. As fertilizers became commonly utilized, excess P was released into streams and rivers connected to these drainage systems. Historically, efforts were undertaken in the 1970s and 1980s to reduce the total load of TP into Great Lakes watersheds as a means of reducing the intensity of cyanobacterial blooms. Significant progress was made toward meeting this goal during this period (Baker et al., 2014). Then, in the 1990s a major shift in agricultural practices occurred in the Maumee and Saginaw River watersheds with the widespread adoption of no-till farming with fertilizer being directly applied to the soil surface (Smith et al., 2015a; Jarvie et al., 2017). A major goal achieved using this approach was to stabilize or reduce export of particulate P to streams and lakes (Jarvie et al. 2017). Adoption of the no-till farming practices required large-scale installation of tile drainage systems in the Saginaw and Maumee watersheds as a way to maintain more optimal soil moisture levels. A major unintended consequence documented the Maumee River was a doubling in DRP load from the 1990s to 2000s while particulate phosphorus (PP) remained relatively constant (Baker et al., 2014; King et al., 2015a; Smith et al.,

2015a; Williams et al., 2016; Baker et al. 2017; Jarvie et al. 2017). Approximately 65% of the DRP load increase after 2002 was attributable to increased delivery of excess DRP (increased FWMC; Baker et al., 2014), with higher runoff volumes accounting for the remaining 35% (Jarvie, 2017). The DRP export from tile drainage systems accounted for >90% of all measured concentrations exceeding recommended levels for minimizing cyanobacterial blooms King et al. (2015b). This increased DRP input, which is immediately utilizable by phytoplankton for growth, more than any other factor resulted in a re-eutrophication of the WLEB and contributed greatly to increased cyanobacterial biomass in the WLEB (Young et al., 1985; Kane et al., 2014; Smith et al., 2015b; Verhamme et al., 2016).

In contrast, measured TP levels in the Saginaw River Basin where forests and wetlands account for 22% and 16% of land cover, respectively, remain relatively low (Figure 3.7). Maintenance of relatively low P concentrations over time in the Saginaw River is further supported by the 37% drop in TP observed from the 1974-1991 period versus the 2001-2005 period (MDEQWB, 2010; Figure 3.2). While DRP was not measured directly in the Saginaw River, the modeling work done in this study indicates DRP concentrations for the Saginaw River are low in comparison to those in the Maumee River, consistent with the lower TP levels (Figure 3.7). The higher proportion of wetlands and forest also help buffer the flow from the Saginaw River. The combination of lower FWMC of P and less variable flow caused cyanobacterial blooms in Saginaw Bay to be more consistent from year to year. Though reduced, there is still sufficient P input to cause Saginaw Bay to be classified as eutrophic with blooms comparable to years with low loading in the WLEB (Figure 3.4).

Another difference between the two systems is the extent of remaining wetland along their shorelines. Saginaw Bay is bordered by 18,000 acres of wetlands (~73 km^2), the largest coastal

freshwater wetlands system in the USA (USFWS, 2019). An important component of this wetlands network is the wide swath of the three-square bulrush, *Schoenoplectus pungens*. This species is known to act as a nutrient sink preventing large pulses of phosphorus from reaching the open waters of the bay (Kohler et al., 2004). A review of 203 North American and European wetlands reported median removal rates of 93 g m^{-2} $year^{-1}$ for total nitrogen and 1.2 g m^{-2} $year^{-1}$ of total phosphorus (Land et al., 2016). Assuming the median total phosphorus removal rates reported by Land et al. (2016), Saginaw Bay's surrounding wetlands should remove 88 metric tons (29%) of total phosphorus per year, compared to the average spring input of 300 metric tons (IJC, 2019). This is sufficiently high to have a further ameliorating impact on reducing the severity of cyanobacterial blooms in Saginaw Bay. Approximately 5,100 acres (20.6 km^2) of Lake Erie's original wetlands remain in the WLEB. Using the same uptake assumptions, these marshes could remove 25 metric tons P which is a small amount (~2%) compared to the average 1,126 metric tons discharged between March and June into the WLEB (Stumpf et al., 2016).

3.5.2 Nonlinear response to phosphorus loading in western Lake Erie

A critical feature of the response of TP loading in the WLEB that warrants consideration from a management perspective is the non-linear response of cyanobacterial bloom intensity versus TP input over 500 metric tons (Stumpf et al., 2012; Obenour et al. 2014; Bertani et al. 2016; Stumpf et al., 2016; Verhamme et al., 2016; Ho et al. 2017). At TP loads less than 500 metric tons, Saginaw Bay and the WLEB experience similar sized blooms (Figures 3.4B; 3.7). In addition at these lower TP loading levels there is a linear response of bloom size to the amount of TP input (Figure 3.7B). This raises the question of why TP loading exceeding 500 metric tons causes maximal summertime cyanobacterial biomass to rise in a steep non-linear fashion (Figure 3.7B). The mechanism accounting for the non-linear response, however, has not been identified. A

logical hypothesis is that there is an internal cycling mechanism that causes the recent P inputs to be utilized more effectively as loading increases (Gächter and Mares, 1985). A likely possibility is that blooms of diatoms and other phytoplankton occurring in early summer are capable of effectively sequestering incoming nutrients even in high flow years (Stoermer and Theriot, 1985; Butts and Carrick, 2017; Reavie et al. 2018; O'Donnell et al., 2019). As water temperatures increase in these shallow systems, the water column stabilizes, nutrients taken up by the initial blooms can be remineralized directly via grazing or bacterial degradation as blooms senesce later in the season (Kreusad et al., 2015; Bartoli et al. 2018; Depew et al. 2018; Null et al., 2020). In essence, early blooms may provide a time release mechanism for initially capturing, then supplying, highly utilizable DRP to support more intense cyanobacterial blooms later in the season. This hypothesis is consistent with the cyanobacterial biomass pattern observed in WLEB for the wetter years in 2011, 2013, 2015, 2017, and 2019 (Figure 3.4B).

3.5.3 Management implications for controlling cyanobacterial blooms in the WLEB

From a management perspective, the Saginaw Bay watershed provides a realistic model for further cyanobacterial abatement efforts in the WLEB. The results show that TP inputs into the WLEB would have to drop below 500 metric tons to regularly produce cyanobacterial blooms with comparable intensity to those observed in Saginaw Bay. Particular attention should be paid to reducing TP and DRP inputs as reflected in the Great Lakes Water Quality Agreement Nutrients Annex (GLWQANAS, 2019). These TP and DRP reductions may have to be even more drastic than the 40% recommended in the GLWQANAS to achieve the desired reduction in bloom intensity (Scavia et al. 2014, 2016; 2017; Iho et al., 2017; Smith et al. 2018; Wilson et al., 2018; Baker et al., 2019). Numerous approaches for reducing P- inputs have been proposed, but are beyond the scope of this manuscript (e.g. Baker et al., 2017; King et al., 2018). The non-

linear response observed with loading in the WLEB means that initial reductions in the highest P-loading rates will have the greatest benefit in terms of reducing bloom biomass (Figure 3.7B). The largest loading observed in Saginaw Bay is just below the threshold where nonlinear intensification of blooms would be expected to begin (Figure 3.7B). Accordingly, increases in agricultural land use or continued loss of wetlands in the Saginaw Bay watershed or surrounding the Bay will significantly increase potential for severe cyanobacterial blooms (Mitsch and Wang, 2000; USFWS, 2019).

3.5.4. Secondary influences on bloom intensity, retention time and water temperature

Cyanobacteria blooms are caused by a combination of factors. The best documented of these are temperature (Paerl and Huisman, 2009), residence (retention) times (Romo et al., 2013) and eutrophication (Paerl, 1998). Michalak et al. (2013) showed that the large bloom present in the WLEB in the summer of 2011 was partially a result of longer than usual residence times. Summer mean residence time in the WLEB is reported to be 51 days (Millie et al., 2009). This is a little less than half of the average summer residence time in Saginaw Bay, which is estimated to be about 115 days (Nguyen et al., 2014). Therefore, residence times would indicate that Saginaw Bay should have larger blooms relative to WLEB if all other factors were equal. This reinforces the importance of the relatively low TP and estimated DRP concentrations in producing consistently moderate annual blooms in Saginaw Bay where advective losses are lower. It also argues that any future increases in nutrient loading will cause a more rapid and intense eutrophication of Saginaw Bay than occurs in the WLEB.

Temperatures in the two systems are similar to one another throughout the year and show little interannual variability (Sayers et al., 2016). Regression analysis failed to show a correlation

between temperature and maximum CI concentrations. Similarly, other climatic drivers such as wind stresses and light availability were not correlated with maximum CI values. Temperature may, however, have affected the timing of the bloom which peaks 20 days earlier in Saginaw Bay (Aug 11 - Aug 20) compared to the WLEB (Sep 1 - Sep 10) (Table 3.2). The average July temperatures for Saginaw Bay and the WLEB are 24.0 °C and 21.7 °C, respectively. These temperatures are high enough to support maximal growth rates of *Microcystis aeruginosa* in the WLEB (~0.69 d^{-1}) and near optimal rates in Saginaw Bay (~0.60 d^{-1}) (You et al., 2018). In August the temperatures in the WLEB were 24.2 °C and 22.0 °C in Saginaw Bay, corresponding to maximal growth rates of ~0.69 d^{-1} and ~0.63 d^{-1}, respectively. In September temperature declined to 21.7 °C in the WLEB and 19.4 °C in Saginaw Bay, supporting maximum growth rates of ~0.62 d^{-1} and ~0.5 d^{-1}, respectively. The continued warm temperatures in the WLEB support growth into September, explaining why blooms peak later in WLEB compared to Saginaw Bay.

3.5.5 Temporal and geographic variation in bloom intensity in Saginaw Bay

On average the cyanobacterial bloom initiates during June and begins intensifying along the southern and eastern shore in early July (Figure 3.12). The bloom fully develops mid-July though the end of August, begins to dissipate in early September and is gone by mid to late October. The prevailing currents cause the bloom to be most intense along the shoreline with the middle of the Bay relatively free of cyanobacteria. During the blooms, cyanobacterial concentrations are highest along the southern shore adjacent to where the Saginaw River enters the bay (Figure 3.12C). Concentrations along the eastern shore are also higher than those along the western shore, consistent with the prevailing currents.

3.6 Conclusions

The more intense and variable blooms in the WLEB relative to Saginaw Bay are driven by higher and more variable P-inputs from the Maumee relative to the Saginaw River. On a per metric ton of P input both systems produce equivalently intense blooms. The main difference observed between the two systems is the WLEB has loads above 500 metric tons. Above this loading level cyanobacterial blooms in the WLEB increase rapidly in a non-linear fashion (Figure 3.7B). TP inputs into Saginaw Bay ranged from ~120-500 metric tons and overlapped levels observed in the WLEB in lower input years. Over this range equivalent phosphorus loads produce equivalent biomass blooms.

From a management perspective, these results demonstrate that reductions in TP loading, particularly the DRP component, below the current maximal loading values in the WLEB will disproportionately reduce boom intensity (Figure 3.7B). If loading into the WLEB were reduced to approximately 500 metric tons, blooms would be expected to be equivalent to those observed in Saginaw Bay. Conversely, if P-inputs in Saginaw Bay are increased due to a shift toward more intense agricultural land use, or if destruction of wetlands is allowed to continue, the blooms are likely to intensify significantly. The highest P-inputs into Saginaw Bay are already at the 500 metric tons P threshold and it is reasonable to predict loads above this threshold will begin to produce non-linear intensification of cyanobacterial blooms.

3.7 Acknowledgements

I would like to acknowledge Wayne Litaker, Rick Stumpf, and Raleigh Hood for many contributions to this chapter. This work was partially supported by the U.S. EPA Great Lakes

Research Initiative. Andrew Meredith maintains the image processing system. I would like to thank Bryan Eder for assistance in making the map in Figure 3.1.

3.8 Figures

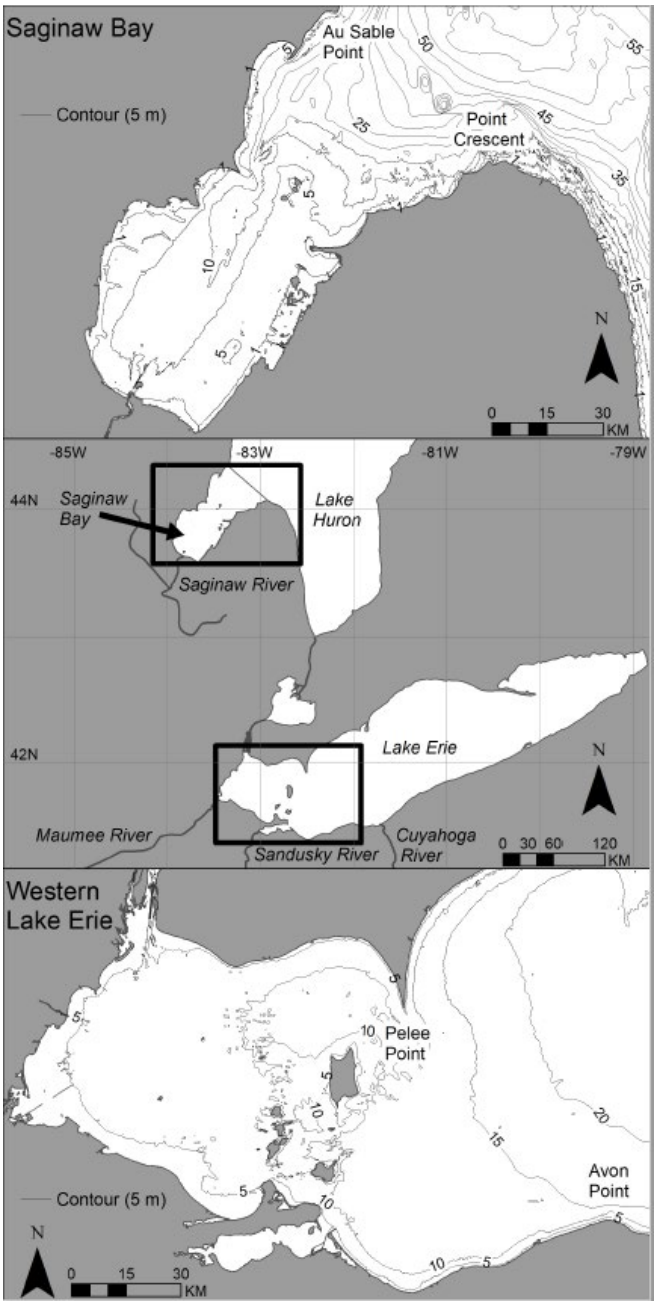

Figure 3.1 (A) Map showing the bathymetry and other relevant features of Saginaw Bay. (B) Map showing the geographic location of Saginaw Bay and the WLEB relative to one another. The Saginaw River, which supplies a majority of the nutrients to Saginaw Bay, and the Maumee River, which similarly supplies a majority of nutrients to the WLEB are also shown. (C) Map showing the bathymetry and other relevant features of the WLEB.

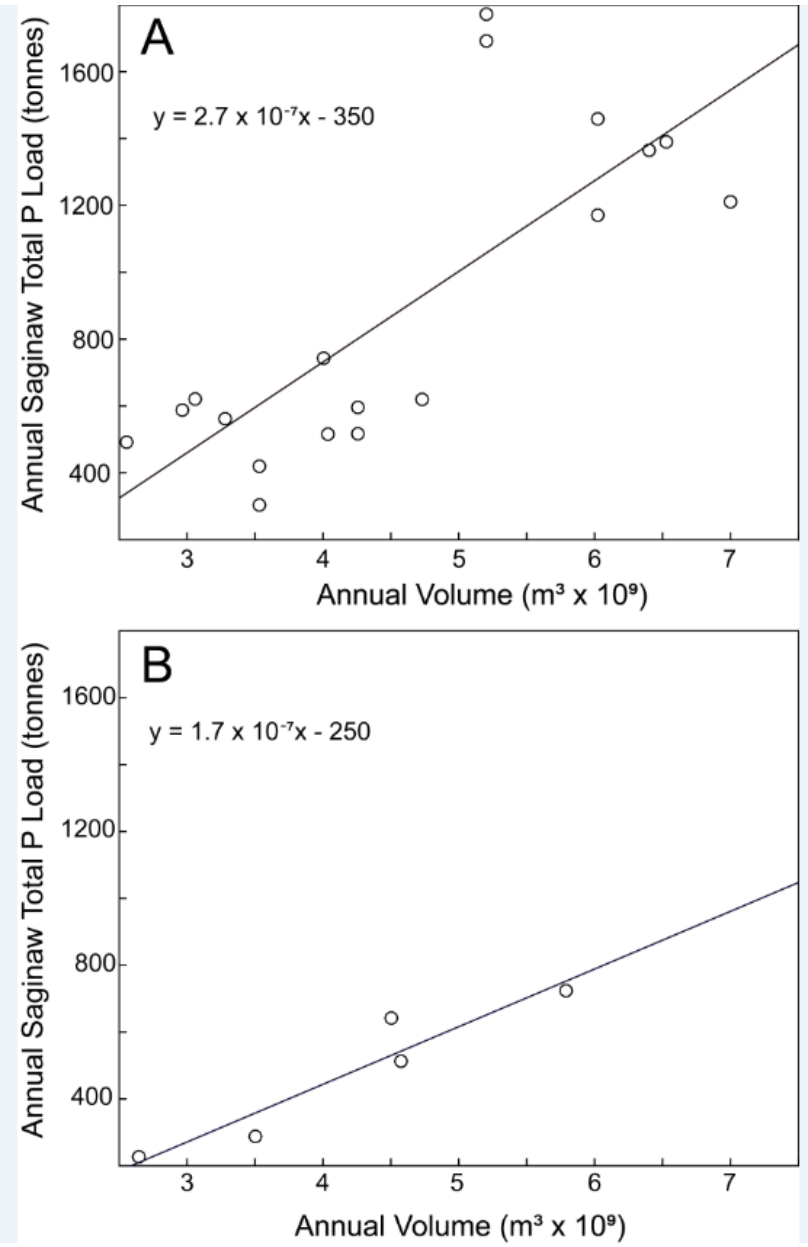

Figure 3.2. (A) Regression analysis of the relationship between annual volume of water from the Saginaw River and total annual phosphorus load from the 1974- 1991 (MDEQWB, 2010) (B) Same as for (A) except for the 2001-2005 time period (MDEQWB, 2010). The slope of the regression line in (A) compared to that in (B) is consistent with phosphorus abatement strategies begun in the 1970s having successfully reduced TP loading into Saginaw Bay from the Saginaw River.

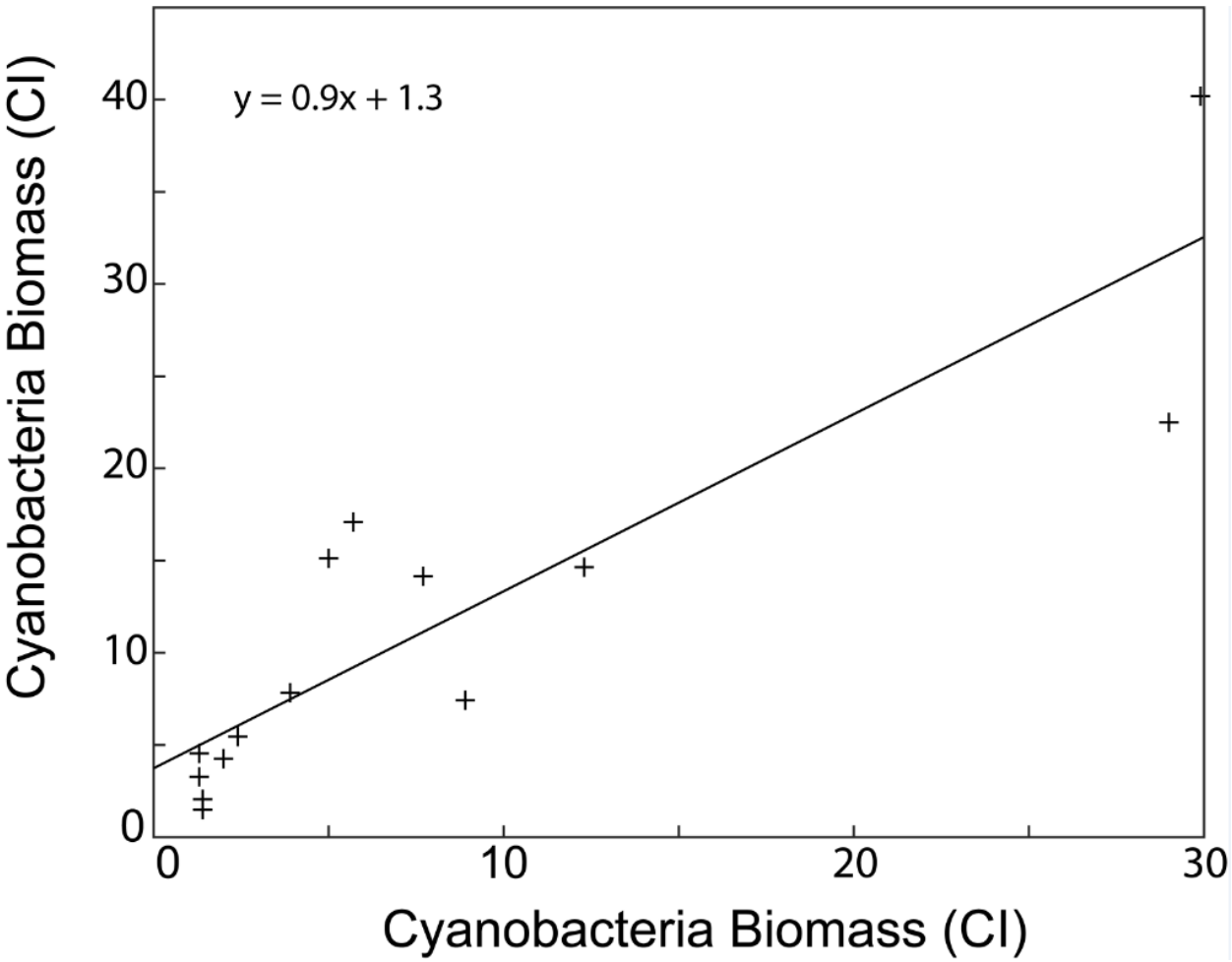

Figure 3.3. Regression analysis of the CI from the Stumpf et al. (2016) model on western Lake Erie against the CI from the MODIS data used in the current study. The slope (m) and the slope intercept (b) of the relationship shown here was used to adjust equation 6.

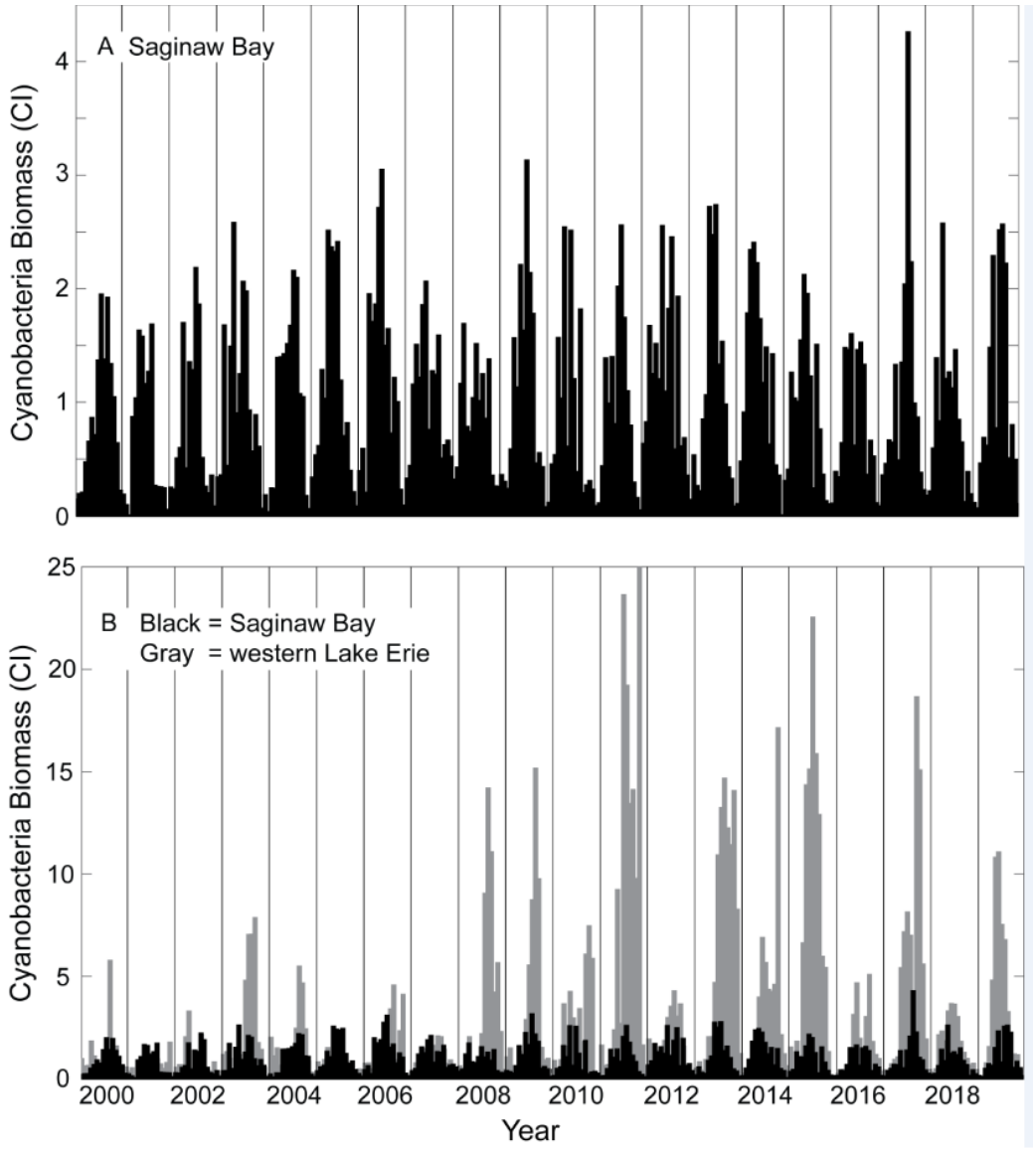

Figure 3.4. (A)The maximal cumulative cyanobacterial index (CI) values from every 10-day composite (see Table 3.1) available for Saginaw Bay for 2000-2019. (B) The maximal commutative CI values for the WLEB (light bars) and Saginaw Bay (dark bars) allowing comparison of relative differences in the biomass of the cyanobacterial blooms in the two systems. The vertical black lines delimit the bloom season for each year, which starts on June 1 – June 10 and ends October 20-October 31 (See Table 3.1). Each bloom year was divided into the same 15, 10-day composite periods.

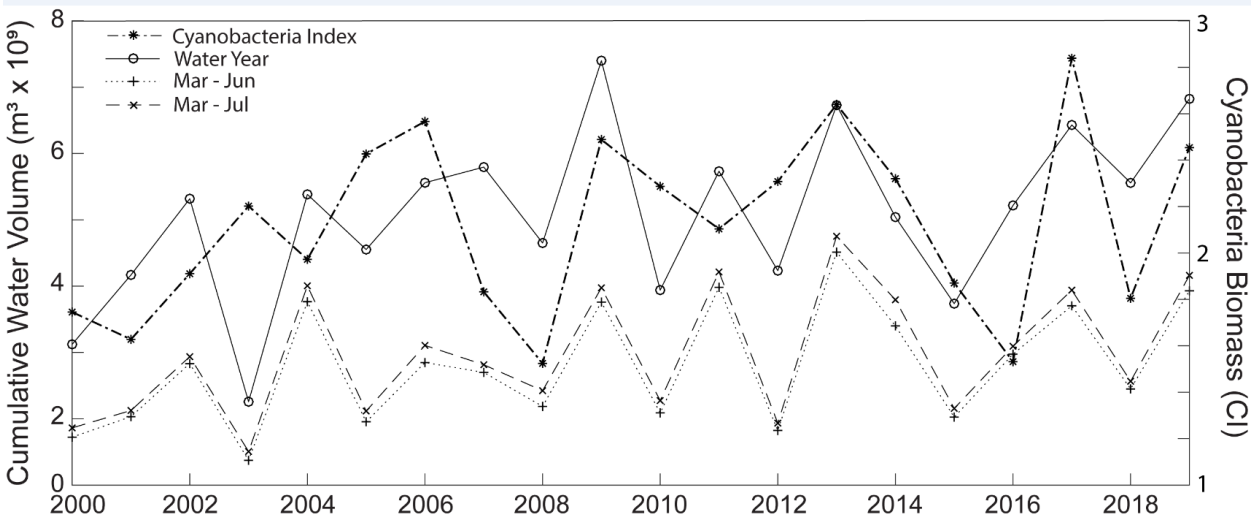

Figure 3.5. Relationship between the maximal annual CI value (*) and the total volume of water discharged from the Saginaw River per water year (October previous year to September of the current year - o; corresponds to period from demise bloom previous September to start of bloom decline in the current year), March – June (+) current year and March – July (x) current year.

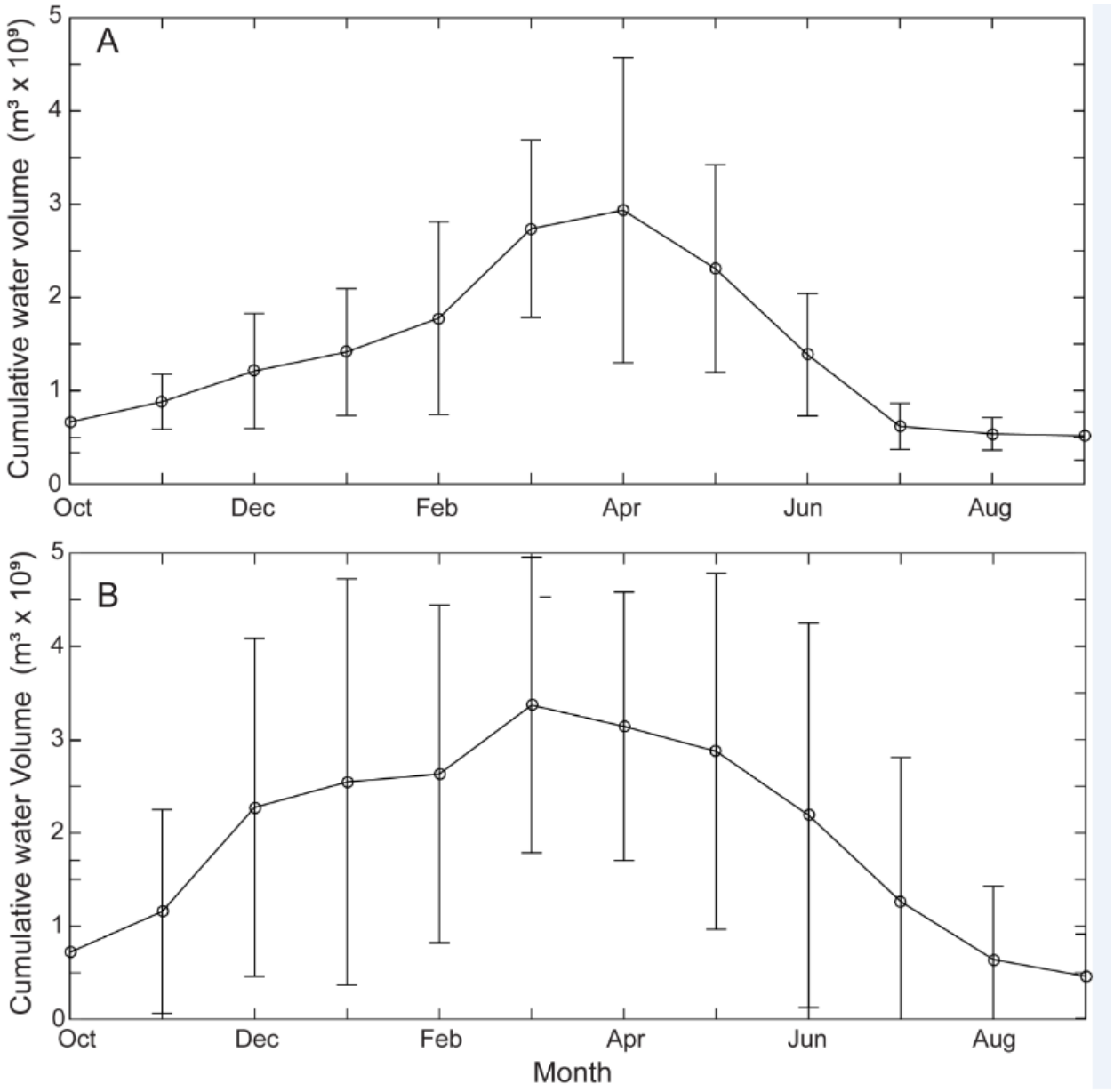

Figure 3.6. (A) March - June discharge from the Saginaw and Maumee Rivers versus the corresponding maximal 10-day Cyanobacterial Index in Saginaw Bay (*) and the WLEB (o) respectively. (B) March - June total phosphate loading from the Saginaw and Maumee Rivers versus the corresponding maximal 10-day Cyanobacterial Index in Saginaw Bay (*) and the WLEB (o) respectively.

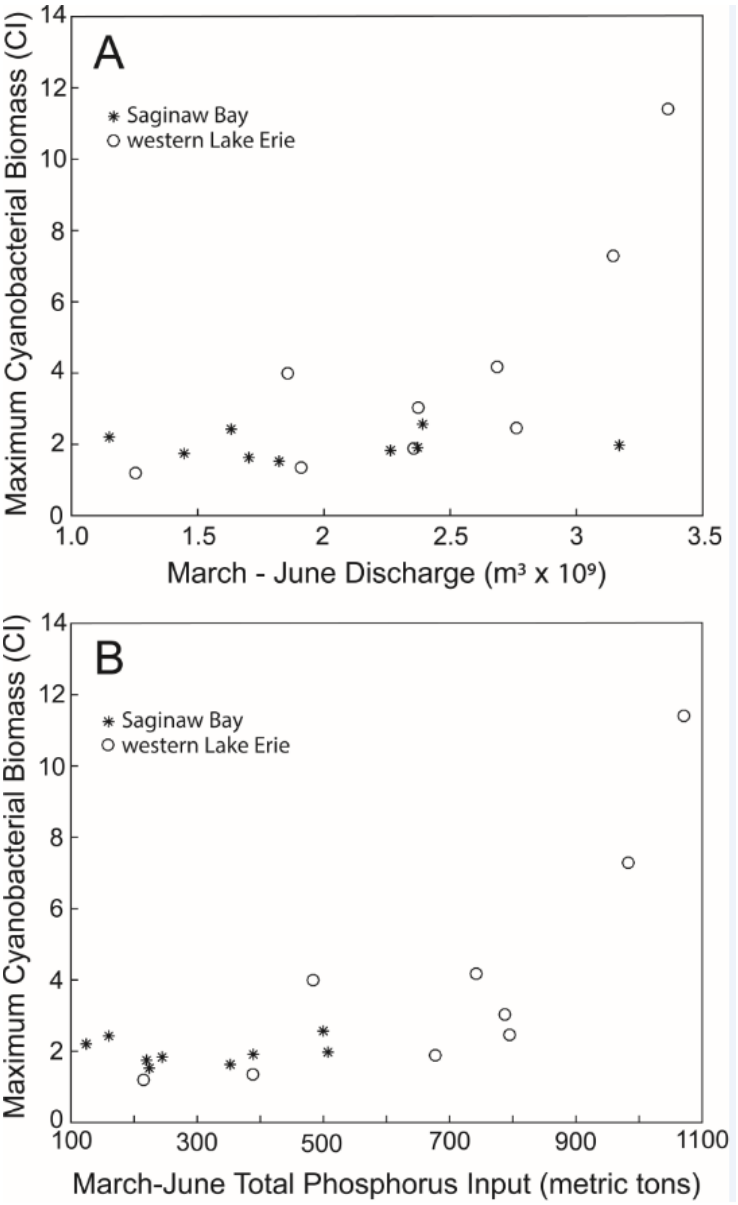

Figure 3.7. (A) Observed annual maximum 10-day, Cyanobacterial Index (CI) value vs modeled maximal CI based on total phosphorus (TP) input from the Maumee (o) and Saginaw (*) Rivers. (B) Observed annual maximum CI value vs modeled maximal CI value based on dissolved reactive phosphorus (DRP) input from the Maumee (o) and the Saginaw (*) Rivers. The models used for predicting CI from TP and DRP input were originally developed using data available for the WLEB (Stumpf et al. 2016).

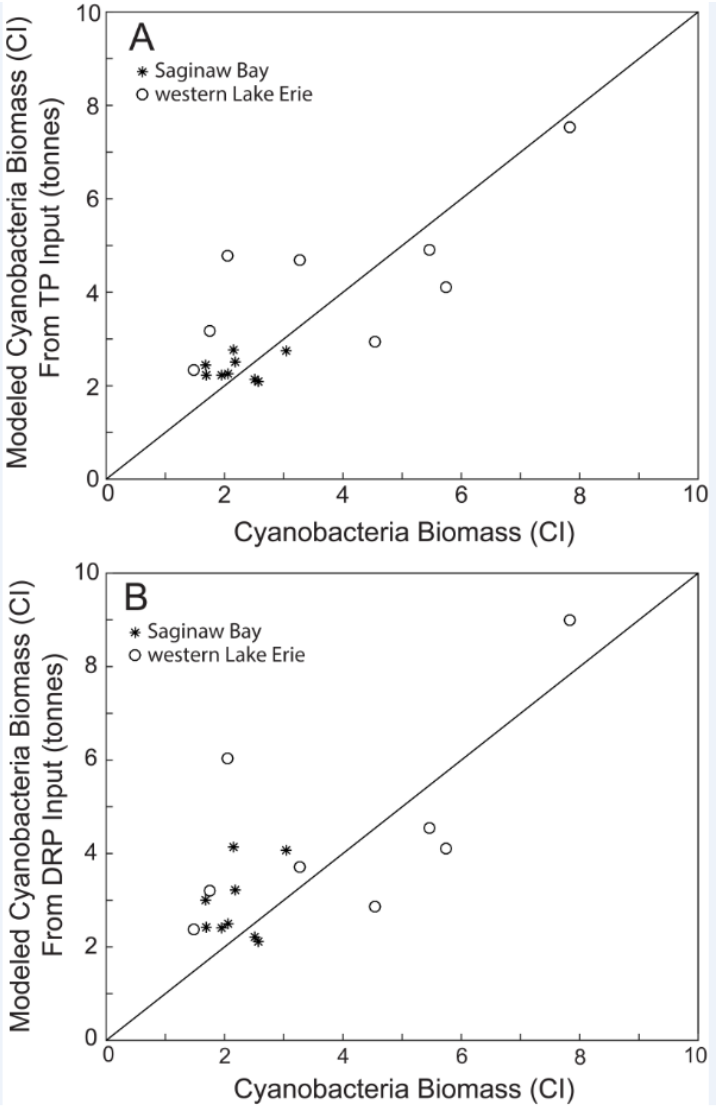

Figure 3.8. (A) Observed annual maximum 10-day, Cyanobacterial Index (CI) value vs modeled maximal CI based on total phosphorus (TP) input from the Maumee (o) and Saginaw (*) Rivers. (B) Observed annual maximum CI value vs modeled maximal CI value based on dissolved reactive phosphorus (DRP) input from the Maumee (o) and the Saginaw (*) Rivers. The models used for predicting CI from TP and DRP input were originally developed using data available for the WLEB (Stumpf et al. 2016).

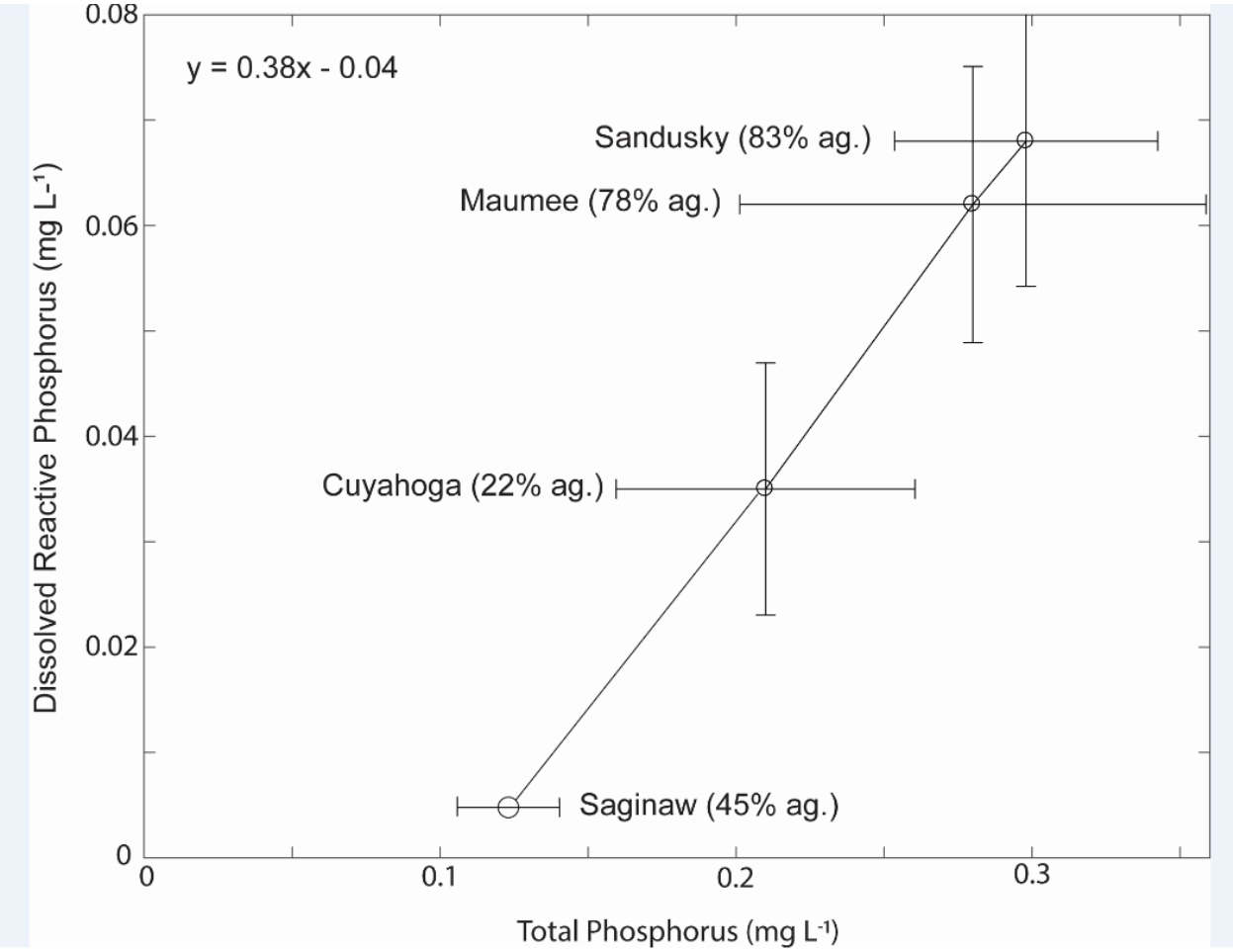

Figure 3.9. Relationship between the flow weighted mean concentrations of total phosphorus (TP) and dissolved reactive phosphorus (DRP) from the *in situ* dataset from the National Center for Water Quality Research for the Maumee, Sandusky, and Cuyahoga Rivers. The Saginaw River TP data was from the Cha et al (2010) dataset. These data were graphed and the linear equation was used to convert the TP values available from the Saginaw River into an estimated average flow weighted DRP concentration.

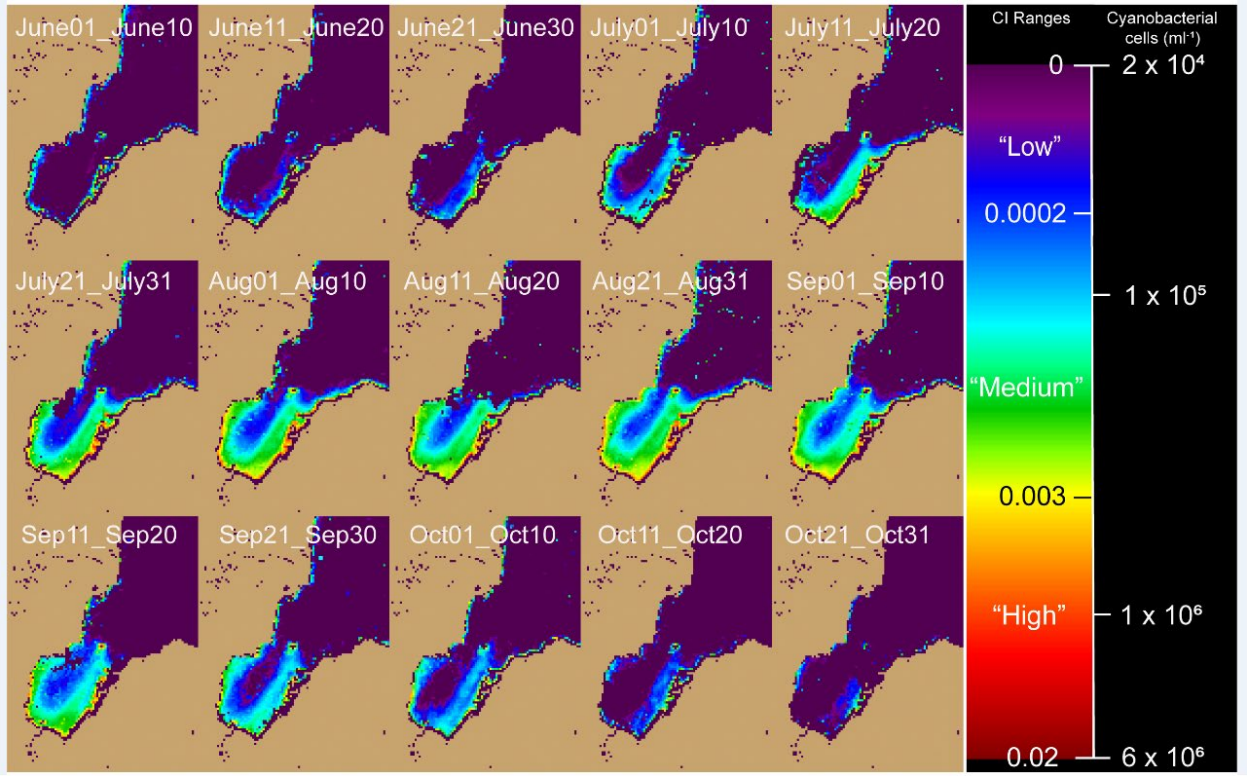

Figure 3.10. Time series showing maximal CI values for every pixel in Saginaw Bay for each of the 15, 10-day periods. The composited images for each 10-day period were arranged in chronological order to show development and decline of the bloom. Data for each image were determined by extracting the maximal CI values for the same pixel in every corresponding 10-day period from all 20 years and then averaging those data to provide an average pixel value for a given 10-day period. The center of the bay has lower concentrations relative to the shoreward areas, due to prevailing circulation within the bay. The inner bay has higher concentration relative to the outer bay. Warmer colors indicate higher levels of cyanobacteria, while cooler colors indicate lower levels.

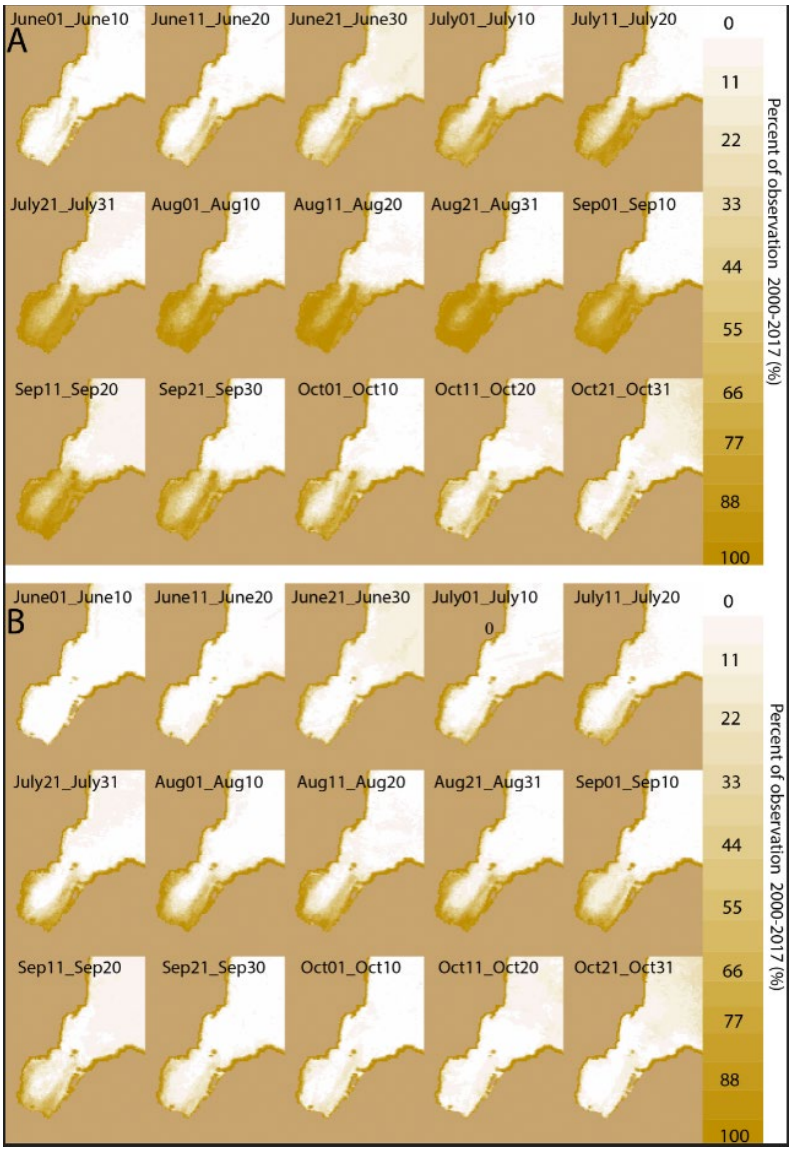

Figure 3.11. (A) The percent of time a pixel exceeds a Cyanobacterial Index (CI) exceeded 0 in each of the 15 10-day periods between 2000 and 2017 in Saginaw Bay. (A) CI=0 is estimated to be ~20,000 cells mL^{-1} (Stumpf et al., 2012). This provides a probability estimate of a cyanobacterial bloom being present in a given location in each of the 15 of the 10-day periods (Table 3.1) from June 1 to October 31. (B) Same as A except it is percent of time the CI value of a ≥ 0.001, which is equivalent to a concentration of 10^5 cells mL^{-1}.

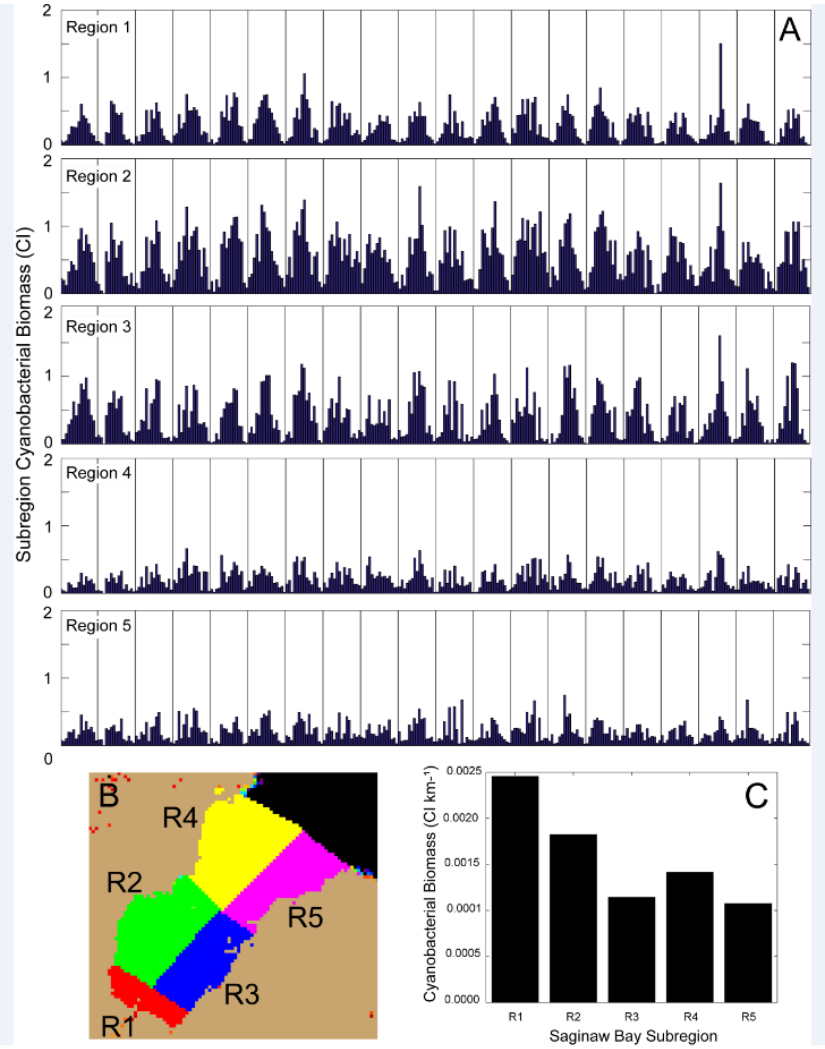

Figure 3.12. (A) Saginaw Bay was subdivided into 5 regions to examine geographic variation in bloom intensity. The cumulative maximal CI values for each 10-day composites from each of these five regions was then plotted as time series from 2000 to 2019. (B) Map showing the different subregions of the Bay. (C) The average of the cumulative maximal CI values for each subregion over all 20 years of the study normalized to surface area. Region 1, closest to the primary nutrient source, the Saginaw River, had the highest CI value. The inner bay (R2, R3), had a higher CI value than the outer bay subregions (R4, R5). Values for the eastern shore subregions (R3, R5) were higher than the corresponding ones on the eastern shore (R2, R4).

Cyanobacterial Bloom Phenology in Green Bay using MERIS Satellite Data and Comparisons with western Lake Erie and Saginaw Bay

4.1 Abstract

Cyanobacteria blooms have been reported to be increasing worldwide. In addition to potentially causing major economic and ecological damage, these blooms can present a potential hazard to human health. Furthermore, these blooms can be exacerbated by a warming climate. One approach to monitor and model cyanobacterial biomass is to use processed satellite imagery to obtain the long-term data sets. In this paper, an existing algorithm developed for MERIS for cyanobacterial biomass (cell counts and chlorophyll concentration) is validated for cyanobacterial biovolume estimates in Green Bay. The satellite data set is then used to determine the bloom phenology of the cyanobacterial biomass in Green Bay and adjoining Lake Winnebago from 2002-2011. The linkages between the bloom phenology from Lake Winnebago and Green Bay were noted and no evidence that the size or timing of the cyanobacteria blooms found in Green Bay could be explained by the bloom in Lake Winnebago. Heat flux, wind speed, backscatter, and absorption data from the NASA Giovanni dataset was used to separate the upper 50% of bloom years and lower 50% of bloom years in Green Bay. The Giovanni dataset was then used to compare cyanobacterial blooms from two other cyanobacterial bloom hotspots in the Laurentian Great Lakes: western Lake Erie and Saginaw Bay. These data showed that separation was possible using as few as three variables (water temperature, river discharge, and water absorption) from ancillary datasets.

4.2. Introduction

Green Bay, the world's largest freshwater estuary (Wisconsin DNR, 2017), is a long (190 km), narrow (15-30 km) sub catchment of Lake Michigan that is bound by the Door Peninsula on the east and mainland Wisconsin on the west (Figure 4.1). The Bay constitutes 7% of the surface area and 1.4% of the volume of Lake Michigan (Klump et al., 2009). It has been estimated that approximately one third of the total nutrient input into Lake Michigan originates in Green Bay (Ditton and Goodale, 1973). The Green Bay watershed drains 48,468 km^2, which is about 1/3 the total drainage of Lake Michigan (Harris et al., 2018).

There is a long history water quality degradation, low oxygen levels and eutrophication (Harris et al., 2018) in Green Bay and much of this degradation is attributable to nutrient pollution via the northward flowing Fox River. The Fox River is the largest tributary into Lake Michigan and the third largest tributary into the Great Lakes, draining 16,000 km^2 (Kraft, 2006). The lower Fox River extends a length of 66 km from the hyper eutrophic Lake Winnebago in the south to the southwestern portion of Green Bay in the north. The watershed is home to some 750,000 people, and 100,000 people rely on Green Bay surface waters for their drinking water (Kraft, 2006). The Fox River has been heavily engineered since the 19^{th} century. The river has a 51-meter elevation change between the head and the mouth, which is navigable through a system of 17 locks traversing 12 dams. The river has an average current velocity of 0.43 km/hour so it would take ~ 6.4 days for the water to travel between Lake Winnebago and Green Bay. The Fox River has an annual discharge of 3.69×10^9 m^3. Fox River provides 60% of the phosphorus (P) load into Green Bay and 30% of the P load into Lake Michigan (Dolan and Chopra, 2012). This is a similar situation to the Great Lakes other two major eutrophic catchments, Saginaw Bay and

western Lake Erie, where a substantial amount of the new nutrients are input by single river sources, the Saginaw River in the former and Maumee River in the latter. The Fox River has also experienced extensive industrial use. In the 1920s there were 34 paper mills on the River. By the 1990s there were still 13 mills, at that time the largest concentration of mills in the world (Kraft 2006).

The eutrophic Fox River water entering the south and the oligotrophic Lake Michigan water entering from the north sets up a remarkable nutrient gradient. The northern portion Green Bay is influenced by the oligotrophic waters of Lake Michigan, and the southern portion of Green Bay is influenced by the eutrophic Fox River, which supplies large amounts of nutrients into the system. Secchi depths range from less than 1 meter near the mouth of the Fox River to 10 meters near Lake Michigan. The residence time of Green Bay is ~ 6 years, which is influenced by the large mouth of the Bay allowing for substantial exchange with the Lake Michigan (Gons et al., 2008). The average total P concentration in Green Bay was relatively constant from 1980 – 2012 reported to range from 0.140 - 0.146 mg L^{-1}. However the total P from the1970s was ~35% higher and reported to be 0.206 mg L^{-1} (Harris, 2018). Mean annual total P loading in the lower Fox River Basin is estimated to be 250 metric tons $year^{-1}$. Lake Winnebago is estimated to contribute another 660 metric tons $year^{-1}$. 67% of the annual P load from the Lower Fox River tributaries occurs in 14 days of loading (Grayczyk et al., 2012).

Cyanobacterial blooms are a common visible sign of eutrophication in freshwater systems, and Green Bay is no exception (Sayers et al., 2016). The majority of the cyanobacteria blooms occur in the southernmost portion of Green Bay, which is most heavily influenced by the Fox River. As well as nutrients, it has been shown that Green Bay receives large amounts of algae and

cyanobacteria exported from hypereutrophic Lake Winnebago resulting in hypereutrophic to eutrophic conditions in the inner portion of Green Bay (Gons et al., 2008), where satellite derived chlorophyll concentrations exceeding 126 mg m^{-3} at the Fox River mouth have been observed (Gons et al., 2008). Phosphorus is typically the limiting nutrient in Green Bay. The reported reductions in TSS concentrations may have helped to lower phosphorus concentration in Green Bay as P is a highly reactive nutrient that tends to attach to particulates (Lin et al., 2016).

Like the rest of the Laurentian Great Lakes, invasive mussels of the genus, *Dreissena*, colonized Green Bay, with the first reported colonization happening in 1992-1993 (Harris, 2018; DeStasio et al., 2014). These mussels have dramatically affected the water quality and plankton communities in Green Bay. There is evidence that Dreissenid mussels have an ability to change the nutrient cycling in basins they have colonized, making biologically available nitrogen more available (Arnott and Vanni, 1996; Conroy et al., 2005), which could give a competitive advantage to cyanobacteria, such as *Microcystis*, that do not rely on the metabolically expensive process of nitrogen fixation. The average water column chlorophyll concentrations in southern Green Bay did not exceed 50 µg L^{-1} prior to mussel invasion (before 1997); however, since then the invasion, average chlorophyll concentrations have often approached 100 µg L^{-1}. Likewise, peak chlorophyll concentrations were below 100 µg L^{-1} prior to invasion but now can exceed 250 µg L^{-1} after invasion (DeStasio et al., 2014). One of the main causes of the increased chlorophyll concentrations was the proliferation of cyanobacteria. The cyanobacteria was estimated to be less than 30% of the total pre-invasion phytoplankton community, and greater than 50% post invasion, with *Microcystis* sp. making up the majority of the cyanobacteria but with *Aphanizomenon* sp. and *Anabaena* sp. also present in abundances up to 15,000 cells mL^{-1} (DeStasio et al., 2014).

Green Bay (Figure 4.1) is one of the three major hotspots for cyanobacterial blooms in the Laurentian Great Lakes (Sayers et al., 2016) and is identified as one of the International Joint Commission's 43 Areas of Concern (AOCs) in the Laurentian Great Lakes (IJC, 2012). Cyanobacteria, which can produce a hepatotoxin, microcystin, potentially present a host of public health threats (Carmichael, 1992; Chorus and Bartram, 1999). The public impacts are the health risk to people through recreational exposure and the impact on treatment of public water supplies to avoid toxin contamination (such as what happened in Toledo, Ohio in the summer of 2014 (Steffen et al., 2017)). The city of Marinette, WI (Figure 4.1) is the only municipality that withdraws municipal water supplies from Green Bay (Qualls, et al., 2013), and as such is the only location where this is a concern. Recreational human exposure to the hepatotoxins can cause skin irritation and accidental ingestion can cause gastrointestinal stress (Chorus and Bartram, 1999). Cyanobacteria hepatotoxin also presents a risk to wild and domestic animals (Backer 2002). Finally, pervasive cyanobacteria blooms cause the public to perceive the water as "polluted" and can lower property values in affected areas (Dodds et al., 2009).

High temporal resolution ocean color satellite imagery has been shown effective in monitoring cyanobacteria blooms (Vincent et al., 2004; Wynne et al., 2010; Sayers et al., 2016). This study utilizes remotely sensed imagery from the MEdium Resolution Imaging Spectrometer (MERIS) to quantify blooms of cyanobacteria in Green Bay. Specifically, these data are used to quantify the interannual variability of the cyanobacteria blooms, and determine if there is a significant relationship between the cyanobacteria blooms and the discharge from the Fox River. The phenology of the blooms in Green Bay are quantified by determining the annual start day of the

bloom, the variability in the start date, where the blooms are most likely to start and the progression of the blooms within the inner Bay, and the export of bloom material to the outer Bay. Relationships between the blooms in Lake Winnebago and Green Bay are also examined focusing specifically on differences in the timing of the blooms and the potential for Lake Winnebago to provide seed populations of cyanobacteria to Green Bay. The paper concludes with a comparison of the phenology and causes of the cyanobacteria blooms in Green Bay with those in Saginaw Bay (Lake Huron) and the western Basin of Lake Erie.

4.3. Methods:

4.3.1. Satellite Imagery:

Satellite imagery has long been shown useful for monitoring and describing the abundance of cyanobacteria blooms and is a key component of the data presented in this manuscript. The algorithm used in this study to estimate the cyanobacterial biomass is a derivation of the Cyanobacterial Index (CI), initially developed by Wynne et al. (2008, 2010) for use with MERIS imagery. Cyanobacteria have the majority of their chlorophyll in non-fluorescing photosystem I, whereas most phytoplankton have the majority of their chlorophyll in fluorescing photosystem II (Seppala et al., 2007). If there is chlorophyll present but fluorescence is low (or absent), the CI will be positive. However, it is possible to have low fluorescence and high chlorophyll concentrations with no cyanobacteria present, which can occur with very small phytoplankton, such as chlorophytes. The CI is calculated following Equation 1.

Equation (1)

$$CI = \left[\rho_s(681) - \rho_s(665) - \{\rho_s(709) - \rho_s(665)\}\frac{(681-665)}{(709-665)}\right] \times (-1)$$

Where CI is the dimensionless Cyanobacterial Index, the parenthetical is the MERIS wavelength expressed in nanometers, and where ρ_s is Rayleigh corrected bi-directional reflectance.

This algorithm showed several areas with blooms where no bloom was reported. Many of these unreported blooms were considered false positives when applied to the Green Bay- Lake Winnebago system. Small celled phytoplankton, such as chlorophytes, will scatter more light than is fluoresced, thereby producing a positive CI value (Wynne et al., 2010). In an attempt to negate these false positives the CI was further investigated, and it was concluded that Green Bay often had a mixed bloom. A mixed bloom occurs when the plankton community has multiple functional plankton types (e.g., diatoms, green algae, cyanobacteria, and others). This is in contrast to western Lake Erie, where monospecific blooms of *Microcystis,* make up the vast majority of the phytoplankton community when in bloom condition.

Lunetta et al. (2015) investigated separating the CI into two component parts; The CI due to the cyanobacteria population (CI_{cyano}) and the CI due to the biomass that is not comprised of cyanobacteria ($CI_{noncyano}$). This separation was based on the second derivative around the 665 nm band according to equation 3.

Equation 2:

$$S_{2d}(665) = \rho_s(665) - \rho_s(620) - \{\rho_s(681) - \rho_s(620)\}\frac{(665-620)}{(681-620)}$$

If the quantity of $S_{2d}(665)$ is positive, the CI from Equation 1 was used and the planktonic concentration of the representative satellite pixel was assumed to be cyanobacteria. When the quantity of $S_{2d}(665)$ was negative, the CI from Equation 1 was assumed to be zero, as the plankton in the representative satellite pixel was assumed to be dominated by a planktonic functional group other than cyanobacteria. The basis behind using $S_{2d}(665)$ is based on the 620 nm band being near the absorption peak of phycocyanin, which is a key photosynthetic pigment unique to cyanobacteria (Simis et al., 2005). If there are high concentrations of phycocyanin the S_{2d} will be positive, which would be indicative of cyanobacteria. If the S_{2d} is negative that would indicate a population of low fluorescing non-cyanobacteria plankton. Matthews and Odermatt (2015) used the same algorithm for cyanobacteria discrimination in their biomass algorithm. It should be noted that the separation using $S_{2d}(665)$ is not possible using ocean color sensors that lack the band at 620nm (such as MODIS or SeaWiFS). An example of this separation is seen in Figure 4.2.

Clouds were masked and 10-day composites were made for each year during the bloom period using the maximum value of the CI_{cyano} at each pixel. The CI algorithm was then used to create 15 separate 10-day composites from the bloom season (Stumpf et al., 2012; Wynne and Stumpf, 2015), which is defined here as the time period between June 1 and October 31. Each month has three 10-day composites, with the final composite of a 31-day month being an 11-day composite. When a metric of annual bloom intensity is needed the average of the maximum 3 sequential 10-day composites was taken (Stumpf et al., 2012) and will be given as the "annual CI". There are

several advantages to utilizing maximum value 10-day composites. The first advantage is that the composite reduces cloud interference, and therefore, reduces the data to a systematic set of generally cloud-free images (Stumpf et al., 2012). The second key advantage is that the composites facilitate estimation of areal biomass. When winds are strong (>7.7 m s^{-1}, or stress of 0.1 Pa), the bloom is mixed through the water column, diluting the surface concentration (Wynne et al., 2010; Hunter et al., 2008). Under calm winds, however, *Microcystis* floats upward forming dense accumulations visible on the surface of the lake (Aparicio et al., 2013). The surface concentration (CI) estimated from satellite during calm conditions therefore represents the *Microcystis* that is present in the water column (Wynne et al., 2008), whereas the concentration detected during high winds underestimates the true biomass. Typically, during any 10-day period in the summer, there is a period of calm clear weather (Wynne et al., 2013b), which allows an estimate of total *Microcystis* biomass. The cells return to the surface within 24–48 hours after a wind event. The bands used for the algorithm quantify concentration within one meter of the surface in the clearest water (Pope and Fry, 1997), and less as turbidity increases (usually because of the bloom), therefore any material less than the optical depth will not be visible by satellite. Finally, using a 10-day composite makes biological sense, as the doubling time for *Microcystis* can be as low as 10 days in the Great Lakes region (Fahnenstiel et al., 2008). Wilson et al. (2006) reported growth rates of 0.13 to 0.46 day^{-1}.

Table 4.1: Shown here is the 10-day composite numbering system used for each year.

Composite Number	Start Date	End Date	Mean Date

1	June 1	June 10	June 5
2	June 11	June 20	June 15
3	June 21	June 30	June 20
4	July 1	July 10	July 5
5	July 11	July 20	July 15
6	July 21	July 31	July 25
7	August 1	August 10	August 5
8	August 11	August 20	August 15
9	August 21	August 31	August 25
10	September 1	September 10	September 5
11	September 11	September 20	September 15
12	September 21	September 30	September 25
13	October 1	October 10	October 5
14	October 11	October 20	October

			15
15	October 21	October 31	October 25

In the seemingly similar cyanobacterial rich waters of Saginaw Bay and western Lake Erie these false positives were not an issue. Figure 4.3 shows the relationship between the CI and the CI_{cyano} for western Lake Erie, Saginaw Bay, and Green Bay derived from the 10 year MERIS timeseries of ten-day composites. Figure 4.3A shows that the relationship from western Lake Erie has the tightest fit, indicating that CI and CI_{cyano} are very similar and that when cyanobacteria blooms, it typically dominates the biomass. Figure 4.3B shows that the relationship from Saginaw Bay is somewhat weaker, indicating that there are likely other planktonic functional groups present in the water column when the cyanobacteria bloom. Figure 4.3C shows the relationship in Green Bay. There are a number of points (circled) where the CI varies independently of the $CI_{cyano,}$ indicating that these are mixed blooms. The CI to CI_{cyano} separation is not possible with the MODIS sensor, as it lacks the spectral resolution needed (i.e., there is no 620 nm band). The results show that unlike in Saginaw Bay or western Lake Erie, MODIS cannot be used effectively to estimate the cyanobacteria biomass in Green Bay.

4.3.2 Field Data:

Biovolume enumeration:

Green Bay was sampled during the summers of 2004, 2005, 2006, 2007, 2010 and 2011 at five locations established during previous studies along the trophic gradient from the mouth of the Fox River to just south of Sturgeon Bay (Figure 4.1; De Stasio et al. 2018). Phytoplankton Samples were collected approximately biweekly each year from June through August. Duplicate integrated samples were collected from the top 4 m of the water column using a submersible pump (or to just above the bottom at sites shallower than 4 m). Samples were transported in opaque bottles kept on ice in the dark until returned to the laboratory later the same day, and then preserved in 1% Lugol's solution. In the laboratory replicate subsamples (15 – 50 mL, depending on sample concentration) for phytoplankton identification and enumeration were examined using settling chambers viewed on an inverted microscope or on permanent slides made by filtering subsamples onto membrane filters (0.45 μm pore size) under low vacuum. Filters were cleared with immersion oil, sealed with Permount and enumerated at 100 – 500 X magnification. Cell linear dimensions were determined with an ocular micrometer and used to estimate cell biovolume based on published relationships between linear dimensions and volume (Wetzel and Likens, 1991). Biovolume data were obtained for three classes of algae: Diatoms, green algae, and cyanobacteria, as well as the sum of the three classes, the total biovolume. The data were used to validate the algorithm described in section 2.1. The summer phytoplankton assemblage in Green Bay is different relative to western Lake Erie and Saginaw Bay as the cyanobacteria populations can covary with other classes of phytoplankton. The CIcyano algorithm would be a preferred detection technique relative to more traditional chlorophyll algorithms, which will be unable to discriminate one functional algal group from another.

Quantifying cyanobacterial chlorophyll with other functional groups

The biovolume data was matched with satellite data that occurred +/- one day from the data of biovolume data acquisition. A 3x3 satellite pixel box around the biovolume sample point was extracted. The median of this 3x3 box was then calculated as long as $n \geq 1$. Overall there were 69 different samples that met this criteria. Of the 69 samples, 36 had a positive CI_{cyano} relationship. Least squares regression was done with the samples that had a positive CI_{cyano} against the cyanobacteria biovolume.

4.3.3 Climatology

A climatology was built using the 10-day composites over the 10-years of satellite data from both Green Bay and Lake Winnebago. The mean of the 10-years of the available CI_{cyano} product were extracted from the 10-day composites to form a cyanobacterial climatological product and graphed into a timeseries. The bloom start date will be assumed when the cumulative CI_{cyano} is above a cumulative CI of 0.5. The mean, median, and standard deviations of the annual maximum value of the CI_{cyano} will be calculated and reported. By using the 10-day composite numbers in Table 4.1, different years may be compared to one another. Furthermore different regions, such as Saginaw Bay and wester Lake Erie could be compared with Green Bay and Lake Winnebago.

4.3.4 Interactions with Lake Winnebago

It has been suggested that Green Bay receives large amounts cyanobacteria exported from hypereutrophic Lake Winnebago resulting in hypereutrophic to eutrophic conditions in the inner

portion of Green Bay , which is supported that Lake Winnebago has both higher cyanobacteria biomass and high chlorophyll concentrations (Gons et al., 2008). The potential connection between cyanobacteria blooms in Lake Winnebago and Green Bay was examined first by plotting a timeseries of the extracted 10-day CI_{cyano} composites from Green Bay and Lake Winnebago to see if any obvious connection exists. A second analysis was done using the ten-day composites with various temporal lags to test the hypothesis that the cyanobacteria (or the needed nutrients and micronutrients) flow from Lake Winnebago to Green Bay. As was previously mentioned it takes slightly over 6 days for water to travel from the head of the Lower Fox River in Lake Winnebago to the mouth of the Lower Fox River in Green Bay, which makes the 10-day composites a reasonable time step for this analysis. For this analysis, Lake Winnebago was divided into equally-sized quadrants, as it is hypothesized that the north western quadrant of Lake Winnebago may correlate better than any of the other quadrants (or the whole of the lake) with Green Bay, as that is the location of the head of the Lower Fox River. The data from the 10-day composites for both Lake Winnebago (and the 4-different quadrants) and Green Bay were extracted and used for the correlation analysis. The extracted data from the five different scenarios (each of the quadrants as well as the whole lake) were then correlated against the extracted data from Green Bay. These correlations were run at lags of 0 days, 10-days, 20-days, and 30-days.

4.3.5 Model Building

Building empirical models that can predict cyanobacterial blooms in the Laurentian Great Lakes can have a number of positive benefits, which include the reduction of the detrimental economic and environmental impacts of the blooms. Furthermore, modeling the blooms can provide insight

into the factors that give rise to them and thus provide guidance on how to undertaken measures to reduce the severity of future bloom. Hence, an attempt is undertaken to build a model to predict the annual severity of cyanobacterial blooms using a dataset from NASA's Giovanni program as well as river discharge data available from the USGS.

River Discharge

River discharge has been shown to correlate with P concentrations (Dolan et al., 1981; Baker et al., 2014) and P is the limiting nutrient in most lacustrine systems, including Green Bay. Sager and Wiersma (1975) reported that the Fox River was the main source of P for Green Bay and estimated the loading to be 2.2 million kg $year^{-1}$ between 1970-1971. This situation, with a single eutrophic river delivering the majority of the P load into a basin, is similar to the conditions in western Lake Erie and Saginaw Bay, so it may be expected that all three of these systems behave similarly in terms of bloom response to P loading variability. It is therefore hypothesized that the Fox River discharge will correlate strongly with cyanobacterial biomass in Green Bay. The river discharge for the Fox River was obtained from the United States Geological Survey (USGS) station 04084445 at Appleton, Wisconsin. The monthly option for the discharge statistics was selected and mean monthly flow rates calculated. Stumpf et al. (2012) found that mean monthly discharge rates from March-June from the Maumee River gave the best fit to annual CI concentrations in western Lake Erie. All plausible monthly combinations are examined for correlation between of annual CI concentrations and mean monthly flow rates. The annual CI concentration is the average of the three highest sequential 10-day composites in a given year.

Ancillary Data from NASA Giovanni

Additional potential forcing factors will be considered to determine if a model can be formulated to predict the cyanobacterial biomass in Green Bay. Temperature has been proposed as a driver for cyanobacteria blooms (Paerl and Huisman, 2008). Wind stress and surface pressure can be used as a proxy for vertical mixing and turbulence. Vertical mixing and turbulence has been shown to have negative impacts of cyanobacteria bloom abundance and that blooms are more prevalent under low turbulence (Huisman et al., 2004; Paerl and Huisman, 2008; Paerl and Huisman, 2009). Both the northward wind stress component and the eastward wind stress component were therefore used as a proxy for wind mixing/turbulence. However, increased turbulence and wind stress is not necessarily detrimental to the formation of cyanobacteria blooms. In fact, it has been suggested that an increase in turbulence may actually promote cyanobacteria blooms (Liu et al., 2019). This is due to the fact that under turbulent conditions *Microcystis* may form larger colonies which can counteract some of the turbulence effects on buoyancy. Furthermore it has been suggested that under high turbulence that *Microcystis* can produce an increase in toxin production which can negatively affect other algae thereby giving cyanobacteria a competitive advantage (Neilan et al., 2013). Precipitation data can be a proxy for atmospheric pressure, as well as a proxy for surface runoff, and river discharge, which can in turn be a proxy for P inputs. Latent Heat flux can be defined as the flux of heat from the surface of the Earth into the atmosphere that is associated with the evaporation of surface water and its subsequent condensation in the atmosphere (Giovanni, 2020). Sensible Heat flux is the process which causes heat to be transferred from the surface of the Earth into the atmosphere by convection and conduction. Three optical properties, the absorption of gelbstoff at 443 nm, absorption due to phytoplankton at 443 nm, and the particulate backscattering at 443 nm are also used in the effort to formulate an empirical model for predicting cyanobacteria blooms. These

three properties together describe the apparent optical properties of a body of water (Lee et al., 1996). Albedo can be used as a proxy for the amount of light that is transferred over the atmosphere-water interface.

These data were downloaded from the NASA Giovanni project (NASA, 2019) as an area averaged product calculated over the time span of one month. The Giovanni data corresponding to the bloom year (defined here as June – October) were considered. The three absorption optical properties (gelbstoff absorption, particle absorption, and phytoplankton absorption) were only available in a 10-day data product and were averaged to create a monthly product. To create a direct temporal comparison with the CI_{cyano} values the average of the three 10-day CI_{cyano} composites from each month was used to represent monthly cyanobacterial biomass. In cases where only two 10-day composites were available for a given month the average was taken of the two 10-day composites that were available. The NASA Giovanni variables are summarized in Table 4.2. The monthly Giovanni data were correlated with the monthly CI_{cyano} data product. The annual data were used in a Principal Components Analysis (PCA) in an effort to determine the factors that may lead to bloom formation.

Table 4.2: shown here is the data downloaded by NASA's Giovanni dataset that will be used for model development

Parameter	Giovanni Name	Unit	Model Name
Surface pressure [NLDAS Model]	pressfc	Pa	NLDAS NOAH

Absorption of gelbstoff at 443 nm	adg_443	m^{-1}	MODIS IOP
Absorption of phytoplankton at 443 nm	aph_443	m^{-1}	MODIS IOP
Particulate backscattering coefficient at 443 nm	bbp_443	m^{-1}	MODIS IOP
Diffuse attenuation coefficient for downwelling irradiance at 490 nm	KD	m^{-1}	MODIS KD
Near surface wind speed [FLDAS model]	wind_f	$m\ s^{-1}$	FLDAS NOAH
Meridional wind speed 10 meters above surface [NLDS model]	vgrd10m	$m\ s^{-1}$	NLDS FORA
Zonal wind speed 10	ugrd10m	$m\ s^{-1}$	NLDS FORA

meters above surface [NLDS model]			
Albedo [NLDAS model]	albdosfc	%	NLDS NOAH
Sea Surface Temperature 11 μ night	nsst	Degrees C	MODIS SST
Sensible heat flux [NLDAS model]	shtflsfc	W m^{-2}	NLDS NOAH
Latent heat flux [NLDAS model]	lhtflsfc	W m^{-2}	NLDS NOAH
Precipitation total [NLDAS model]	apcpsfc	Kg m^{-2}	NLDS FORA [NLDAS model]
Net Downward Shortwave Radiation	Swnet	W m^{-2}	FLDAS NOAH

4.3.6 Differences in Green Bay relative to western Lake Erie and Saginaw Bay

The CI versus CI_{cyano} plot in Figure 4.3 suggests that there are mixed blooms of phytoplankton in Green Bay, whereas in Saginaw Bay and western Lake Erie when cyanobacteria bloom it is generally a more monospecific bloom of *Microcystis*. This further suggests that there is

something fundamentally different in the physical and/or biogeochemical environment in Green Bay relative to western Lake Erie and Saginaw Bay. In an effort to examine and quantify potential differences in these environments a Principal Components Analysis (PCA) was performed using the ggplot2 package in R. The input variables in the PCA are those listed in Table 4.2 along with the river discharge from the USGS gage stations at the Maumee (USGS station 04193500), Saginaw (USGS station 04157005), and Fox (USGS station 04084445) Rivers. The Maumee River is the main source of P to the western basin of Lake Erie (Baker et al., 2014), while the Saginaw River is the main source of P to Saginaw Bay (Stow et al., 2014). Various means from the river discharge out of the Fox River were calculated, including: the mean from March – June, the mean from March – July, and the mean for the water year.

4.3.7 Maximum CI Years vs Minimum CI Years

Further PCAs will be run to determine if maximum CI years (bloom years) can be separated from minimum CI years (non-bloom years). The input data into the PCA was the river discharge and all the Giovanni parameters in Table 4.2. Two separate bloom scenarios were considered. The first one was achieved by considering two classes: bloom and non-bloom. The 5 years with the highest annual CI_{cyano} values were considered bloom years, and the 5 years with the lowest CI_{cyano} values were considered non-bloom years. These analysis will be run for Green Bay and then for comparison purposes they will be run for western Lake Erie and Saginaw Bay.

4.4 Results:

4.4.1 Satellite Imagery

All available satellite data from the MERIS Reduced Resolution timeseries was processed and used in this manuscript.

4.4.2 Field Data Validation

Separating cyanobacteria from the non-cyanobacteria

All 69 samples with available satellite data are graphed along with the three different planktonic functional groups, as well as the total phytoplankton biovolume in Figure 4.4A. The median percent of the total biovolume from cyanobacterial origins was 31% for all the samples. A subset of Figure 4.4A showing just the 36 samples that had a positive CI_{cyano} are shown in Figure 4.4B. The median percent of the biovolume from cyanobacterial origins increased to 48% when just samples with a positive CI_{cyano} was used, indicating that the CI_{cyano} is detecting elevated cyanobacteria concentrations.

Comparisons with Chlorophyll Algorithms

Figure 4.5 shows the correlation between the cyanobacteria biovolume and the CI_{cyano}. The error bars are 30% error, which is the error estimated by Hawkins et al. (2005) on measuring cyanobacterial biovolume with Lugol's solution.

4.4.3 Climatological Analysis

Lake Winnebago reaches its maximum CI_{cyano} value earlier than does Green Bay, with its maximum value occurring during composite number 6 (July 21- July 31) (Figure 4.6). Green Bay reaches its maximum value some 20 days later, occurring during composite number 8 (August 11-August 20). Lake Winnebago has less interannual variation relative to Green Bay, but does

have higher CI_{cyano} levels (Figure 4.7). 2009 and 2010 both showed very little signal from the CI_{cyano} algorithm. The CI_{cyano} is higher in every year in Lake Winnebago relative to Green Bay. The statistics on the maximum 10-day composite of the CI_{cyano} from Green Bay are shown in Table 4.3.

Table 4.3: The 10-day composite periods (dates in parentheses) exhibiting the highest mean, median, and mode integrated CI values during the 10-year MERIS time series. Details on how values were calculated are given in section 2.3.

Year	Green Bay	Saginaw Bay	Western Lake Erie
Mean ± SD	6.8 ± 2.9 (Jul. 21 – Jul. 31)	8.4 ± 2.1 (Aug. 11 – Aug. 20)	10.3 ± 1.6 (Sep. 1 – Sep. 10)
Median	7 (Aug. 1 – Aug. 10)	9 (Aug. 21 – Aug. 31)	10 (Sep. 1 – Sep. 10)
Mode	3 (Jun. 21 –Jun. 30)	9 (Aug. 21 – Aug 31)	10 (Sep. 1 – Sep. 10)

So generally blooms peak in late July to Early August in Green Bay. The blooms in Green Bay achieve peak biomass ~20 days before blooms in Saginaw Bay and ~30 days before peak bloom formation in western Lake Erie. The blooms in Green Bay also exhibit more variability relative to Saginaw Bay and western Lake Erie.

4.4.4 Interactions between Green Bay and Lake Winnebago

No noticeable trends indicating that the cyanobacteria blooms start first in Lake Winnebago are apparent in Figure 4.7. As described in section 2.4, all data was extracted from the four

quadrants from Lake Winnebago and correlated against the extracted data from Green Bay. The entirety of Lake Winnebago produced a better correlation with the CI_{cyano} in Green Bay than any single quadrant did. Therefore, in further analysis the sum of the four quadrants was used as a total for all of Lake Winnebago. Correlations between Green Bay (GB) and Lake Winnebago (LW) were run using a lag of 0 days (same ten day composite numbers), 10 days (GB against LW + 10 days), 20 days (GB against LW + 20 days), and 30 days (GB against LW + 30 days). The correlations with the various temporal lags are summarized in Table 4.4.

Table 4.4: Shows the correlation statistics between the average CI_{cyano} between Green Bay and Lake Winnebago. Four scenarios were considered, a lag of 0 days, 10days, 20 days and 30 days. The correlation decreased with each lag period indicating that the blooms from Green Bay co-occur with blooms in Lake Winnebago as opposed to the blooms in Green Bay being transported from Lake Winnebago.

Lag (number of days)	r^2
0	0.34
10	0.28
20	0.12
30	0.03

The results of this analysis indicate that the blooms co-occur in Green Bay and Lake Winnebago and there is no discernable temporal lag using these methods. If the blooms started in Lake

Winnebago and the bloom material was transported into Green Bay the correlations should be tighter with a 10, 20, or 30 day lag or Lake Winnebago blooms should systematically start earlier than those in Green Bay. Lake Winnebago had an earlier maximum CI_{cyano} concentration 6 out of the 10 years considered here, and Green Bay had the earlier CI_{cyano} maximum concentration 4 out of the 10 years. While Lake Winnebago may supply nutrients and some cyanobacterial biomass into Green Bay, these analyses do not indicate that Lake Winnebago is seeding the blooms in Green Bay. Rather, these analyses indicate that the blooms co-occur.

4.4.5 Model Building

There were two main challenges in the model building that hampered the formation of a predictive model. The first is a relative size of the bloom severity. The proportional range of the cyanobacteria blooms in Green Bay were high as two of the years, 2009 and 2010, had virtually no bloom at all. The other eight years in the MERIS timeseries recorded blooms in Green Bay that were small relative to the blooms found in small bloom or non-bloom years in western Lake Erie and Saginaw Bay. In some years shown here, cyanobacteria blooms in Green Bay are only slightly above what may be considered to be background levels in the other basins. The second factor that hampered a development of a robust predictive model was a lack of data, with the MERIS mission providing only 10 years of cyanobacterial estimates.

The monthly area averaged NASA Giovanni data was correlated to the average monthly CI_{cyano} product. The best relationships were made with the gelbstoff absorption and sensible heat flux, which (both had an r^2 =0.6) yielded the best relationship. Unfortunately, these two parameters are no easier to predict than the cyanobacterial blooms making the development of a predictive model challenging. The sensible heat flux is expected to increase with a changing climate

(Myhre et al., 2018), which may in turn lead to an increase in cyanobacterial blooms in Green Bay.

The maximum CI_{cyano} never occurred in June or October during the 10-year timeseries considered here. Rerunning the correlations with those two months taken out of the Giovanni dataset, so the only remaining months were July, August, and September, yielded no better results with the average monthly CI_{cyano} for the entire bloom season (June- October).

4.4.6 Comparisons with western Lake Erie and Saginaw Bay

To compare the three different basins a PCA was run, the seasonal (March – June) averages were calculated using all the Giovanni parameters listed in Table 4.2 and were entered into a Principal Components Analysis (PCA), in hope of being able to separate Saginaw Bay, western Lake Erie, and Green Bay based on these data. One additional variable that was considered was the sum of the gelbstoff absorption (adg) and the phytoplankton absorption (aph) which is called adg + aph. The first and second principal components accounted for 47% and 18.2% of the variance with all of the parameters (data not shown). The PCA was rerun reducing the number of variables to just what was needed to maintain reasonable separation between the three regions. It was determined that good separation was given using just three variables: river discharge, NSST, and, adg + aph. The first principal component was 52.4% of the explained variance, and the second principal component explained 29.9% of the explained variance (See Figure 4.8A). The river discharge explains much of the interannual variability of the western Lake Erie cyanobacterial bloom (Stumpf et al., 2012; Stumpf et al., 2016). However removing the river discharge are rerunning the PCA still resulted in satisfactory separation for the three different geographic areas, with a PCA just based on temperature and absorption (Figure 4.8B). The temperature is easily

explained by latitude, with Lake Erie being the warmest and the most southerly and Green Bay the coldest and the most northerly, and Saginaw Bay filling an intermediate role. The absorption is a bit more difficult to explain.

The absorption of water is based on three main physical components: the absorption of: gelbstoff, phytoplankton and water itself. The absorption of water is known and increases with increasing wavelength (Pope and Fry, 1997). The absorption of gelbstoff and phytoplankton for the bloom season are presented in Figure 4.9. Green Bay generally has higher absorption in both of these constituents throughout the timeseries relative to Saginaw Bay and western Lake Erie, which have relatively similar absorption patterns. Saginaw Bay has slightly higher gelbstoff absorption relative to western Lake Erie (Figure 4.9A) and western Lake Erie has slightly higher phytoplankton absorption relative to Saginaw Bay (Figure 4.9B). Lower adg and aph would make the water in Green Bay less turbid relative to the water in western Lake Erie or Saginaw Bay, thus making it easy to differentiate Green Bay based on the absorption.

4.4.7 Separating Bloom Years from Non-Bloom years

An additional set of PCAs were run to illustrate the differences between the bloom years and non-bloom years in Green Bay and then the analysis will be repeated for comparison sake for western Lake Erie. Saginaw Bay was also considered but no combination of parameters led to a separation between bloom years and non-bloom years using the definition set here (5 largest CI is classified a bloom, and the lowest CI is classified as a non-bloom year). This is largely of a result of Saginaw Bay having very low variability in the annual cyanobacteria bloom. A PCA is

an effective tool in data reduction. As such the data were reduced as much as possible for this analysis, while still giving some measure of separation between the bloom years and the non-bloom years. Two separate models were developed using 5 parameters or less that showed the best separation for Green Bay and another for western Lake Erie. The best model for Green Bay was then run in western Lake Erie for comparison purposes, and likewise the best model in Green Bay was also run in western Lake Erie. Figure 4.10A shows the best separation between the bloom and non-bloom classes for Green Bay with the first two components explaining 75% of the explained variance and Figure 4.10B shows the same model for western Lake Erie with the first two components responsible for 70.5% of the explained variability. Figure 4.11 shows the results of the best PCA separation between the bloom class and the non-bloom class for western Lake Erie (Panel A), with the first two components explaining 93.9% of the variability. Figure 4.11B shows the same four parameters applied for separation in Green Bay, with the first two components explaining 86.7% of the explained variance.

The best western Lake Erie model uses just three parameters: river discharge, latent heat flux, and sensible heat flux. The best Green Bay model uses the wind speed, the latent heat flux, the sensible heat flux, the gelbstoff absorption, particulate backscatter, and the meridional wind component in the five parameter model used. Two thirds of the parameters that were used in the chosen western Lake Erie PCA were used in the Green Bay PCA, yet the overall results are drastically different. Suggesting that different physical properties govern bloom and non-bloom years between the two systems.

The PCA was used in an attempt to answer why there were no blooms in Green Bay for 2009 and 2010. Essentially this is just repeating the experiment above but selecting the bloom class as

being 2002-2008 and 2011, and the non-bloom class being just 2009 and 2010. The initial PCA just used the parameters that were previously used in the final PCA plots already used in the PCAs represented in Figures 4.8, 4.9, 4.10, and 4.11: river discharge, sensible heat flux, latent heat flux, meridional wind component, NSST, adg, bbp, and adg + aph. The PCA with all eight previously used parameters is shown in Figure 4.12A. The number of parameters that were needed to separate the two non-bloom years from the bloom years was two: NSST and adg, shown in Figure 4.12B. It appears clear water with relatively low gelbstoff absorption and low water temperature produce essentially no bloom in Green Bay.

One further analysis focusing on the interannual variability between Green Bay, Lake Winnebago, Saginaw By, and western Lake Erie was done to look at variability within each system. The maximum annual CI for each of the four regions was divided by the minimum annual CI from each of the regions to determine the interannual variability. The results from this analysis are shown in Table 4.5:

Table 4.5: Shows the results of the Maximum annual CI and the Minimum annual CI between Green Bay, Lake Winnebago, western Lake Erie and Saginaw Bay.

Region	Max annual CI	year	Min annual CI	year	Variability (Max annual CI / Min annual CI)

Green Bay	5.4	2004	0.2	2010	27
Lake Winnebago	7.9	2008	2.5	2010	3.2
Western Lake Erie	25.6	2011	2.7	2002	9.5
Saginaw Bay	7.2	2006	3.2	2008	2.3

The interannual variability for Green Bay is much higher than for the other regions using these metrics. This is largely the result of the lack of bloom in 2009 and 2010. If the minimum annual CI from 2009 (annual CI = 0.4) is removed the variability drops significantly, to 12.9, which is on the order of the variability recorded in western Lake Erie. Neither 2009 nor 2010 should be classified as having a bloom and cyanobacteria concentrations are near the detection limit of the algorithm. The maximum 10-day cyanobacterial index from Green Bay, Lake Winnebago, western Lake Erie, and Saginaw Bay derived from the RR MERIS timeseries is seen in Figure 4.13. Green Bay had a higher CI than western Lake Erie in 2 out of the first four years of the timeseries, after which the Green Bay cyanobacteria blooms diminished while the western Lake Erie blooms grew much larger. 2003 was the only year that Green Bay had a higher cyanobacteria biomass than did Saginaw Bay. The Green Bay bloom followed the same trends that Lake Winnebago did, but the CI_{cyano} was much smaller, with Green Bay never eclipsing that of Lake Winnebago during the MERIS timeseries shown in Figure 4.13.

4.5 Discussion

I have shown here that while the cyanobacteria blooms in Green Bay are relatively small in biomass, they show a high degree of interannual variability. However, there was considerable difficulty determining a useable model to predict annual cyanobacteria biomass from the suite of environmental parameters considered here. The three main issues preventing such a statistical model were: 1.) a lack of annual data as the MERIS sensor only provided a 10-year dataset, 2.) relatively small cyanobacterial biomasses, 3.) that cyanobacteria can co-occur with other phytoplankton functional groups.

I have shown that Green Bay has lower cyanobacteria concentrations than does Saginaw Bay, which in turn has lower cyanobacteria concentrations than western Lake Erie. In spite of the very high variability of cyanobacterial blooms shown in Table 4.5, it has been noted that there is little interannual variability in respiration and gross primary productivity in Green Bay (LaBuhn and Klump, 2016). The average gross primary production of Green Bay is 288 mmol O^2 m^{-2} day^{-1} (LaBuhn and Klump, 2019). This is a factor of five higher than the gross primary production in Saginaw Bay of 40.6 – 65.1 reported by Fahnenstiel et al., (1995). While Saginaw Bay has higher cyanobacteria biomass relative to Green Bay, the primary production is higher in Green Bay further indicating the confounding issues of mixed phytoplankton assemblages present in Green Bay. Much of this variability in the cyanobacterial bloom is a result of having essentially no bloom at all in 2010 and particularly in 2009. Despite a lower standing stock of chlorophyll it is still possible that the primary production is similar rates in 2009 and 2010 than it is for the remaining years as the production was most likely based on increased concentrations of diatoms and green algae which are grazed more heavily than cyanobacteria (Davis et al., 2012). I hypothesize that the PCA shown in Figure 4.12B indicates that cooler and clearer invoked an ecological switch giving a competitive advantage to other functional types of phytoplankton over

cyanobacteria, and that the lower absorption was due to lower standing stock of phytoplankton and higher grazing rates.

The cyanobacterial biomass is much lower in Green Bay relative to Saginaw Bay and western Lake Erie, despite all three basins being similarly sized (Figure 4.1). Cyanobacteria often co-occurs with other classes of algae in Green Bay whereas cyanobacteria generally form monospecific blooms in western Lake Erie and Saginaw Bay. The biovolume data from Green Bay presented in Figure 4.4 show that cyanobacteria can co-occur with diatoms and green algae. Figure 4.3 shows that the CI often flags blooms of non-cyanobacteria in Green Bay whereas it does not in Saginaw Bay and western Lake Erie, further indicating that Saginaw Bay and western Lake Erie generally have monospecific blooms of cyanobacteria while Green Bay does not.

Why there are mixed assemblages of phytoplankton when cyanobacteria is blooming in Green Bay and not in Saginaw Bay and western Lake Erie is an interesting question. The PCA analysis in Figure 4.8 shows that there are consistently higher temperatures in western Lake Erie and Saginaw Bay than there are in Green Bay. It has been well documented that cyanobacteria have an affinity for warm water. Downing et al. (2001) uses primarily just sea surface temperature to predict cyanobacterial dominance in lakes. The increased SST in western Lake Erie and Saginaw Bay relative to Green Bay is most likely a key contributor to the ability of other planktonic groups to successfully compete against cyanobacteria. Figure 4.14 shows the timeseries of the SST, Latent Heat Flux, and sensible heat flux from Green Bay, Saginaw Bay, and western Lake Erie from the monthly Giovanni dataset. Kahru et al. (1993) noted that the cyanobacteria blooms can warm the water surface up to 1.5^{o} C, which may be resulting in a positive feedback in

Saginaw Bay and particularly in western Lake Erie giving cyanobacteria blooms a competitive advantage over other phytoplankton.

The PCA analysis shows that Green Bay has a higher gelbstoff + phytoplankton absorption than do the other two basins, leading to higher light attenuation. Green Bay has higher gelbstoff absorption relative to western Lake Erie and Saginaw Bay and differences in phytoplankton community composition can be attributed to gelbstoff absorption (Houser, 2006). As cyanobacteria have an affinity for high light environments this may lead to an increase in competition with other phytoplankton functional groups. Furthermore it has been suggested (Bowling, 1990; Houser, 2006) that colored lakes have a relatively low heat content, which means that clearer lakes (such as Saginaw Bay and western Lake Erie) should have a higher heat content, further providing warmer conditions for the proliferation of cyanobacteria blooms.

The meridional wind is also higher in Green Bay than in the other catchments. The meridional wind was a significant contributor in Green Bay, which makes sense as the Bay is mostly oriented in a north-south direction. Increased wind speeds add turbulence and turbulence is generally beneficial to diatoms and a hindrance to the formation of cyanobacteria blooms (Margalef, 1978; Margalef et al., 1979). Alternately western Lake Erie generally has a higher surface atmospheric pressure which is indicative of more stable atmospheric conditions and less atmospheric induced water mixing leading to dominance of cyanobacteria blooms.

4.6 Summary

The cyanobacterial bloom dynamics in Green Bay are much different than they are in Saginaw Bay and western Lake Erie, which both behave similarly. The cyanobacterial dynamics in Green

Bay are heavily impacted by the absorption of gelbstoff and phytoplankton (adg + aph). When the adg + aph are low, I hypothesize that other functional groups of phytoplankton outcompete cyanobacteria. The standing stock of phytoplankton in 2009 and 2010 correspond to the lowest seasonal adg + aph (Figure 4.9). I hypothesize that the primary production was the same throughout the study (LaBuhn and Klump, 2016) and that diatoms and/or green algae classes outcompeted cyanobacteria in 2009 and 2010 and that grazing reduced the standing stock of chlorophyll. Phytoplankton and gelbstoff absorption are not key drivers in the blooms in western Lake Erie or Saginaw Bay (Figure 4.8). Western Lake Erie is heavily influenced by the discharge of the Maumee River (Figure 4.11A), and its associated phosphorus loads (Stumpf et al., 2012; Stumpf et al., 2016). Saginaw Bay is also somewhat driven by the discharge of the Saginaw River but to a much lesser extent (Wynne et al., Chapter 2). The fact that the Saginaw Bay watershed is the more pristine, with more wetlands to take up excess nutrients and that its watershed is less agrarian leads to less soluble reactive phosphorus loads corresponds to Saginaw Bay having very low interannual variability in cyanobacteria blooms.

4.7 Acknowledgements

I would like to thank, Rick Stumpf, Bart DeStasio, Victoria Coles, and Raleigh Hood for valuable input into this chapter. I would like to thank Bryan Eder for assistance in making the map in Figure 4.1.

4.8 Figures

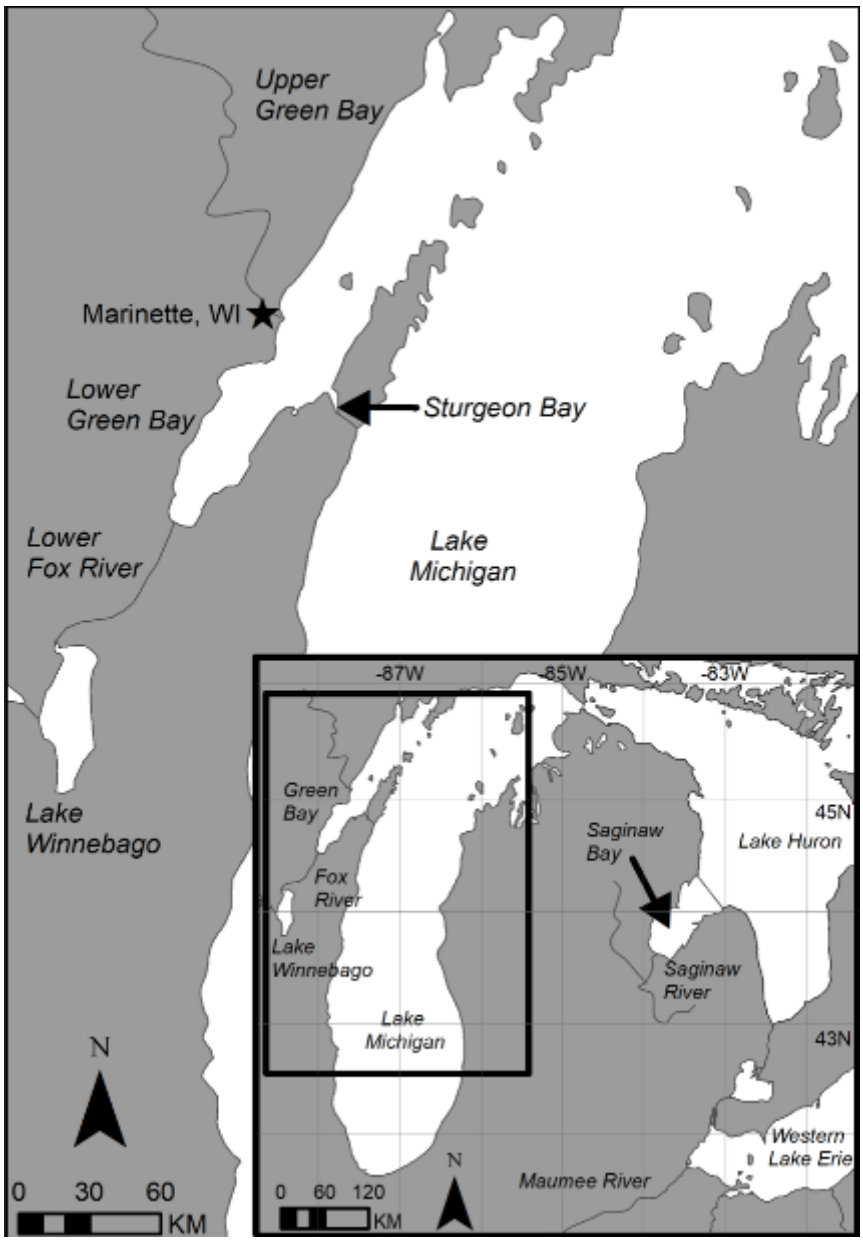

Figure 4.1. Map of the Study area showing locations mentioned in Chapter 4.

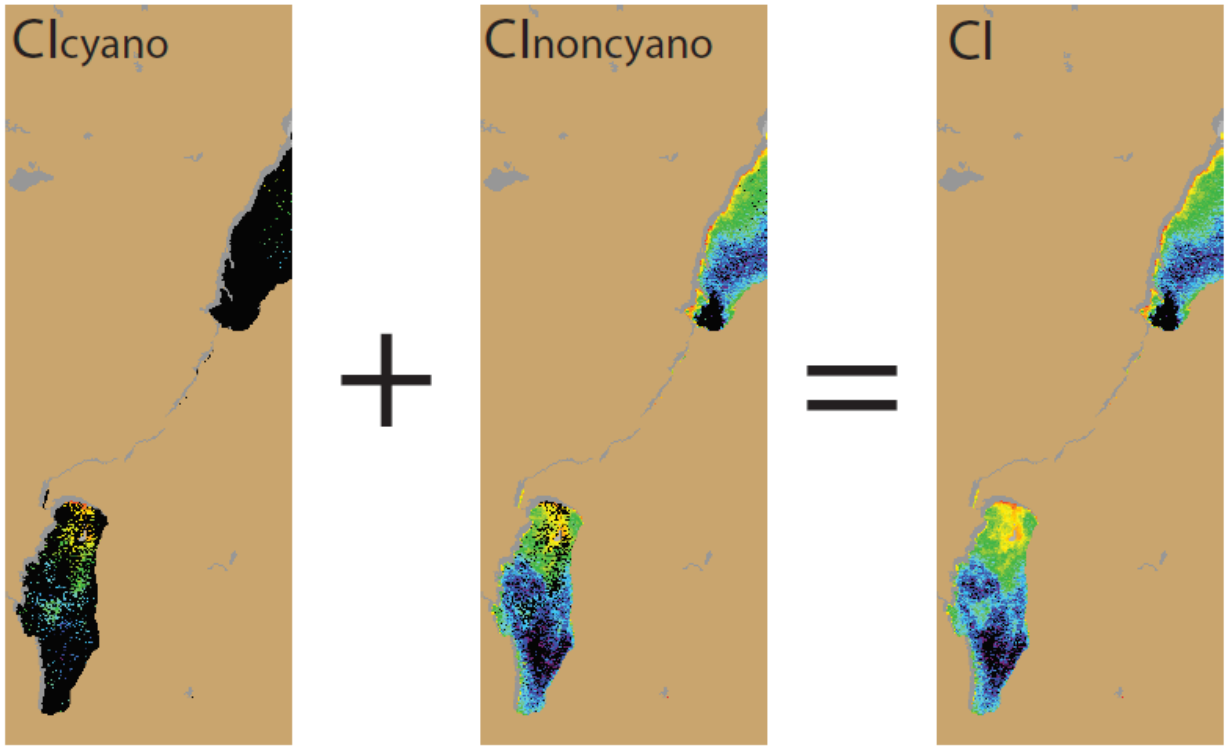

Figure 4.2. Illustration of how the CI is parsed out into two separate quantities based on Equation 3 in the text. The CI is equal to the sum of the CI_{cyano} and the $CI_{noncyano}$.

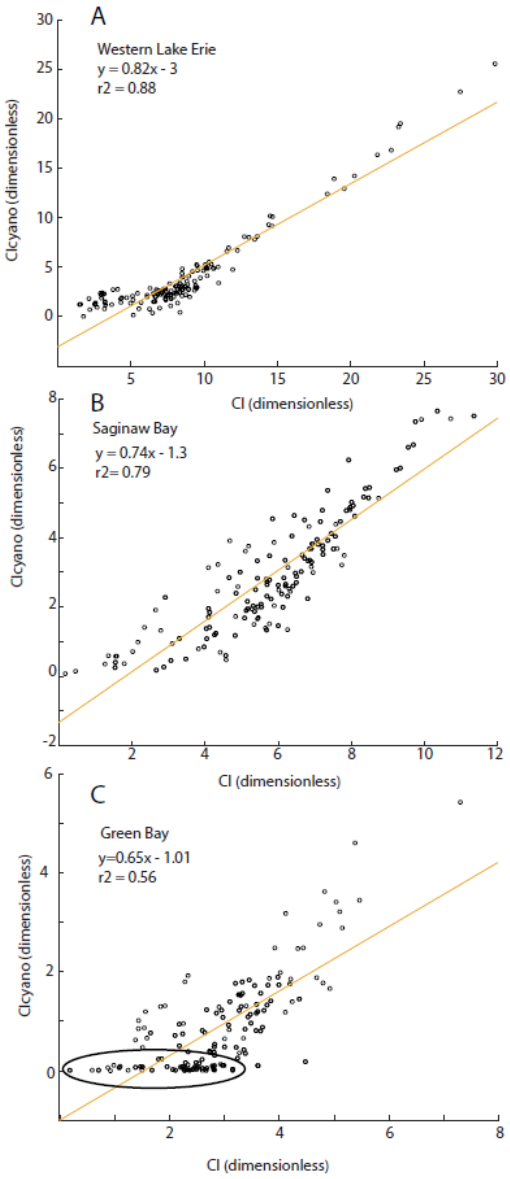

Figure 4.3. Shows the relationship between the CI and the CI_{cyano}. Each point is the integrated CI value from a 10-day period during the bloom season (June – October) from 2002-2011. Panel A shows the relationship in western Lake Erie. Panel B shows the relationship in Saginaw Bay and Panel C shows the relationship in Green Bay. The point circled show where the CI indicated that there should be a bloom but the CI_{cyano} determined that there was no bloom present.

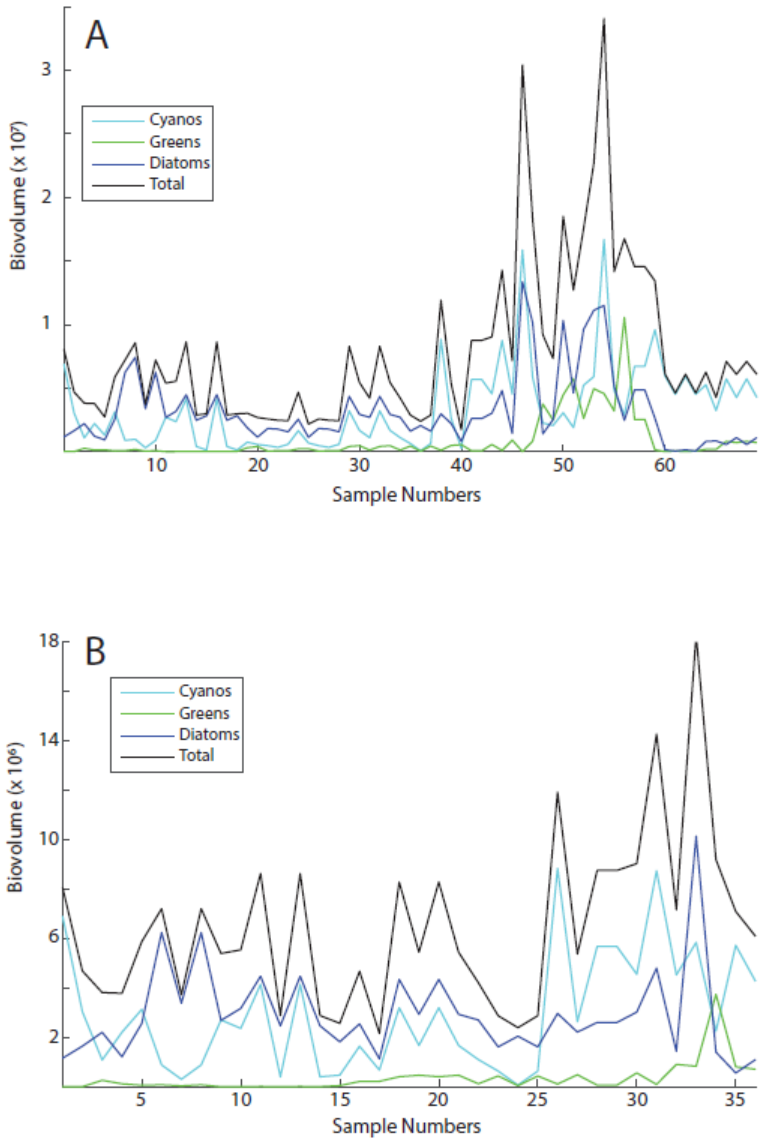

Figure 4.4. Panel A shows all 69 samples where there was at least one pixel in a 9x9 box around the sampling point. The median of the 9x9 block pixels was taken. Panel B shows the subset of Panel A where the CI_{cyano} is positive.

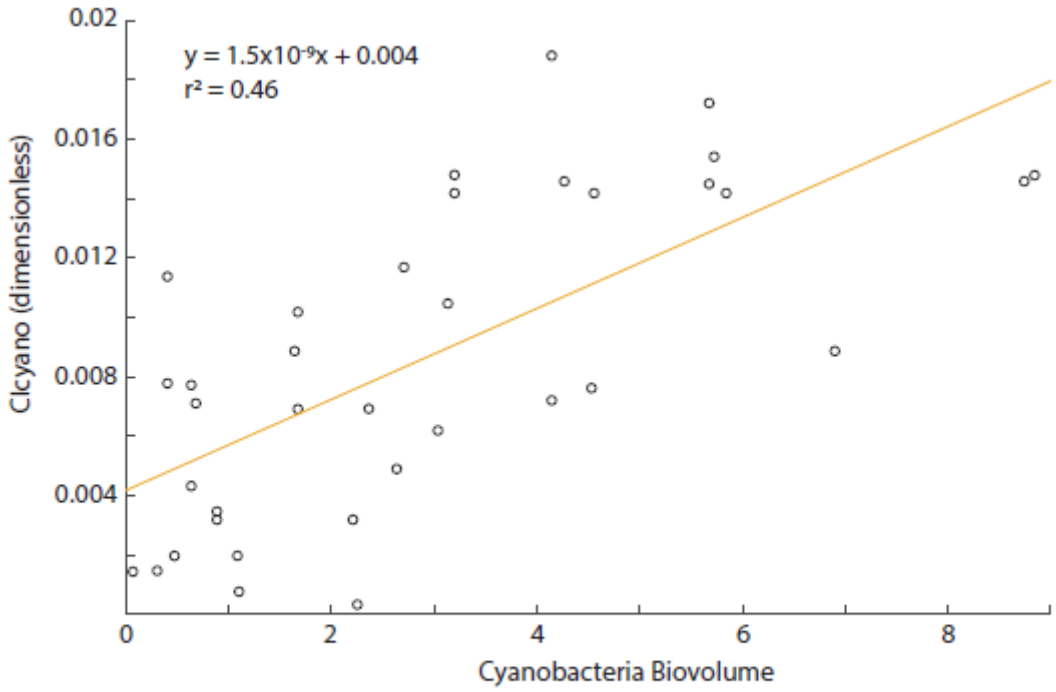

Figure 4.5. Shows the linear regression between the cyanobacterial biovolume and the CI_{cyano}.

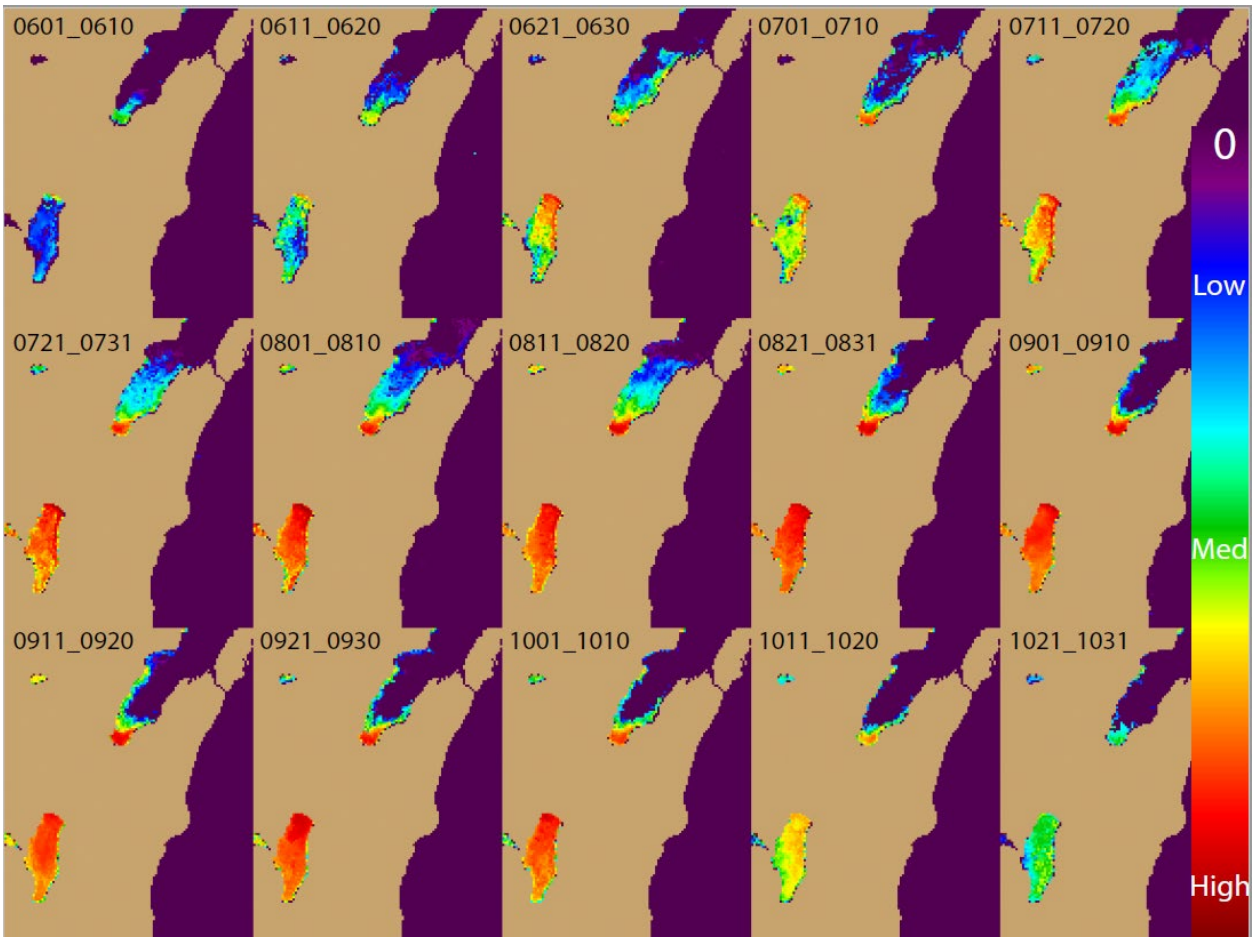

Figure 4.6. Shown here is the climatology of the CI_{cyano}. Each 10 day composite is the mean of the 10 of the MERIS data (2002-2011).

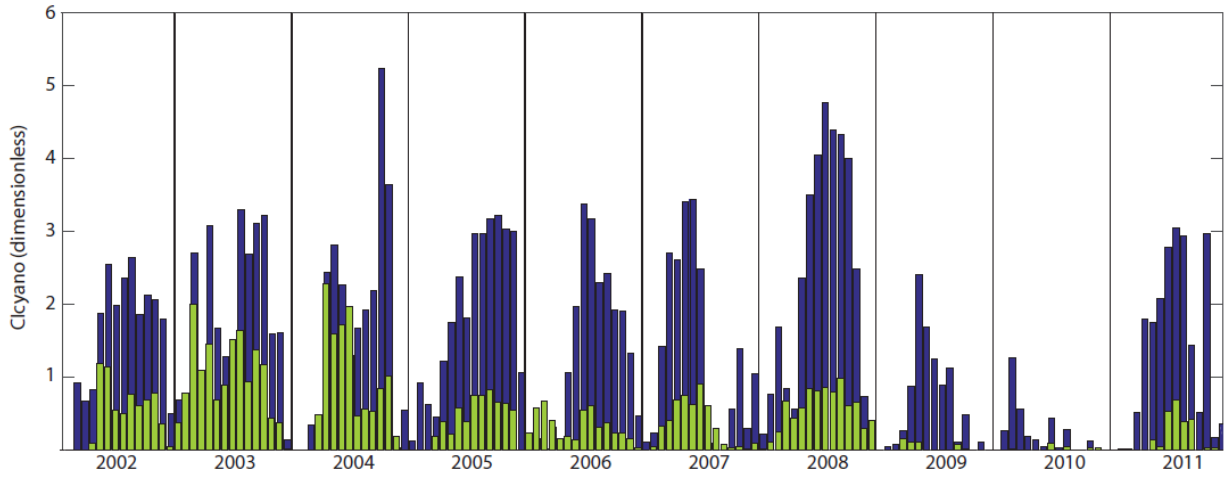

Figure 4.7. Shows the timeseries over the 10 years of the study for both Lake Winnebago (shown in blue) and Green Bay (shown in Green). There exists a high degree of interannual variability. The CI_{cyano} values in Lake Winnebago nearly always exceeds Green Bay.

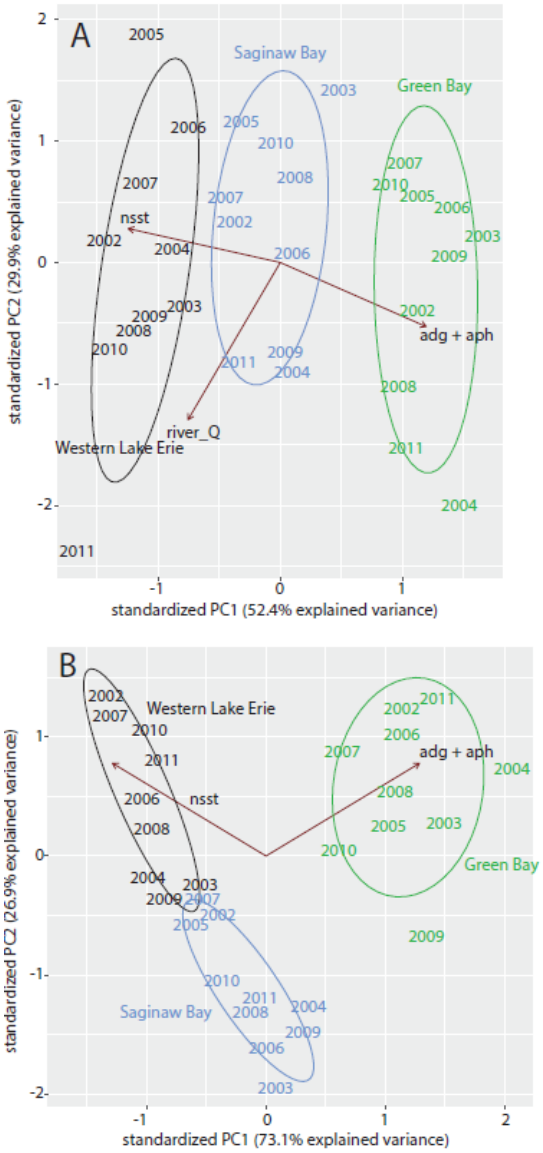

Figure 4.8. Panel A shows the results from the Principal Components Analysis (PCA) in using three parameters to discern Green Bay, western Lake Erie, and Saginaw Bay. The parameters used were the night sea surface temperature (nsst), the river discharge (river_Q) from three respective rivers (Maumee River, Saginaw River, and Fox River), and the combine gelbstoff absorption and phytoplankton absorption (adg + aph). Panel B shows the separation using just nsst and adg + aph.

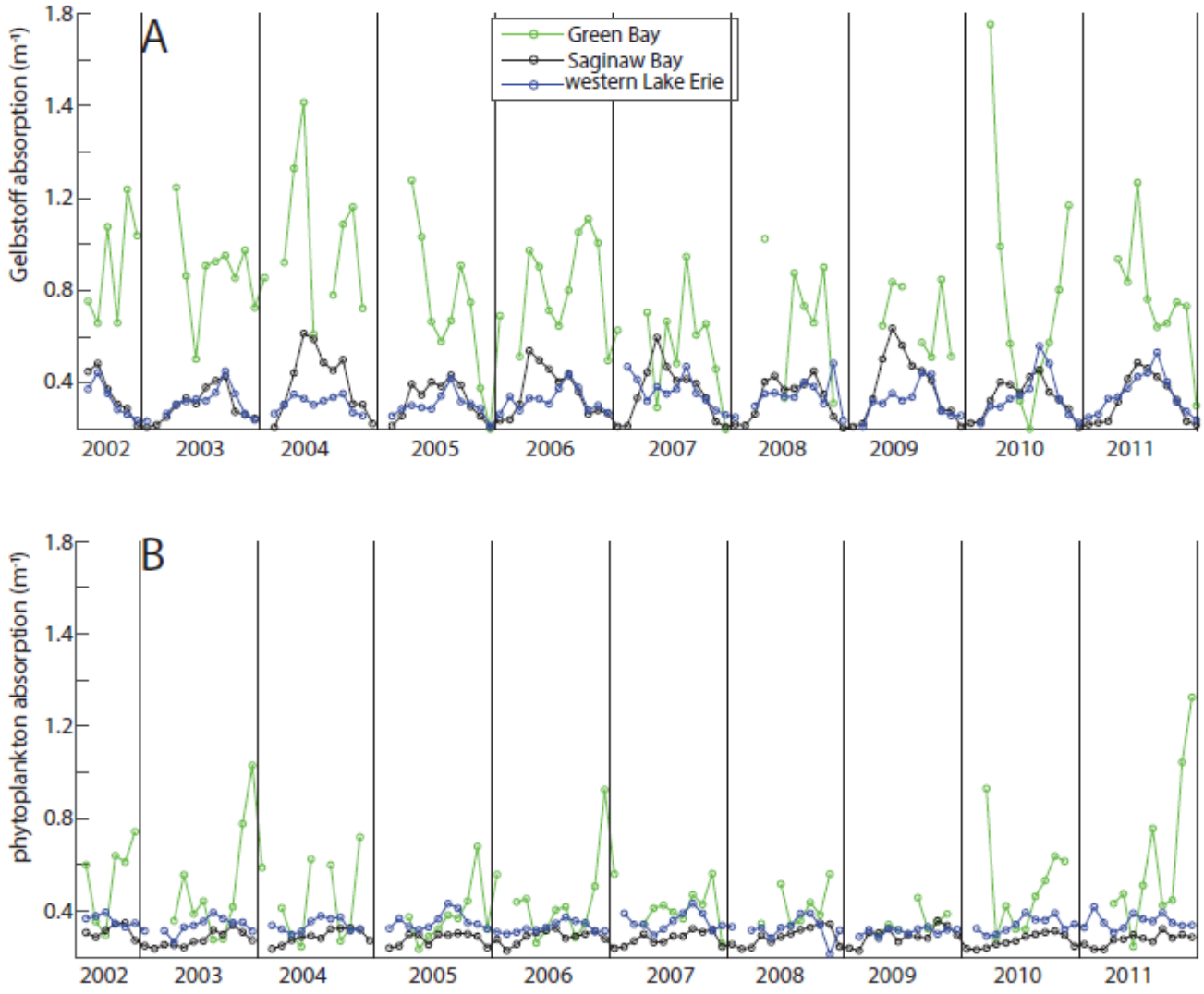

Figure 4.9. Shows the monthly timeseries of the gelbstoff absorption (Panel A) for Green Bay (Green line), Saginaw Bay (Black line) and western Lake Erie (blue line). Each point represents a month. Panel B shows the phytoplankton absorption for the same regions over the same timeseries.

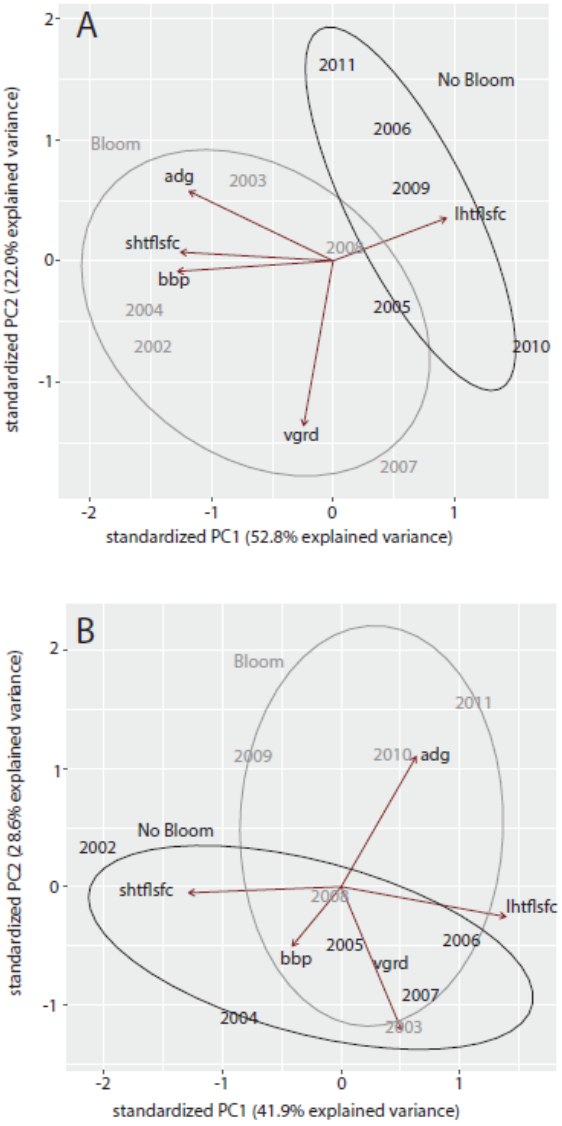

Figure 4.10. Panel A shows the separation between bloom years (gray) and non-bloom years (black) for Green Bay using a PCA. The five input parameters were particulate backscatter (bbp), gelbstoff absorption (adg), the meridional wind speed (vgrd), sensible heat flux (shtflsfc), and latent heat flux (lhtflsfc). Panel B shows the unsatisfactory separation of the bloom years form non-bloom years in western Lake Erie using the same five parameter PCA presented in Panel A.

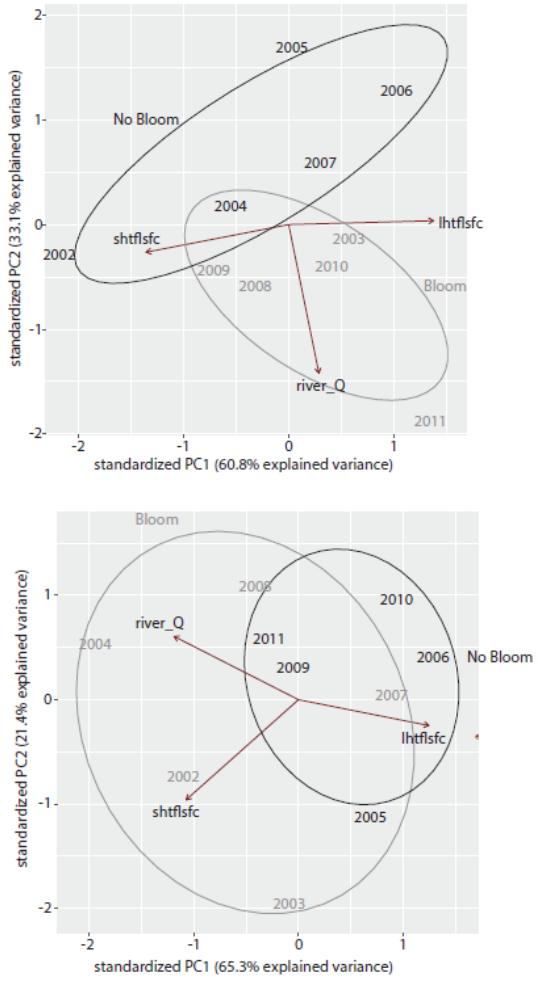

Figure 4.11. Panel A shows the separation between bloom years (gray) and non-bloom years (black) for western Lake Erie using a PCA. The three input parameters were river discharge (river_Q), sensible heat flux (shtflsfc), and latent heat flux (lhtflsfc). 2004 had the sixth highest CI out of the timeseries and was classified as a bloom in earlier work (Stumpf et al., 2012). It was not in this context as operationally the top 5 CI years were classified as a bloom and the bloom 5 CI values were classified as non-bloom. Panel B shows the unsatisfactory separation of the bloom years form non-bloom years in Green Bay using the same three parameter PCA presented in Panel A.

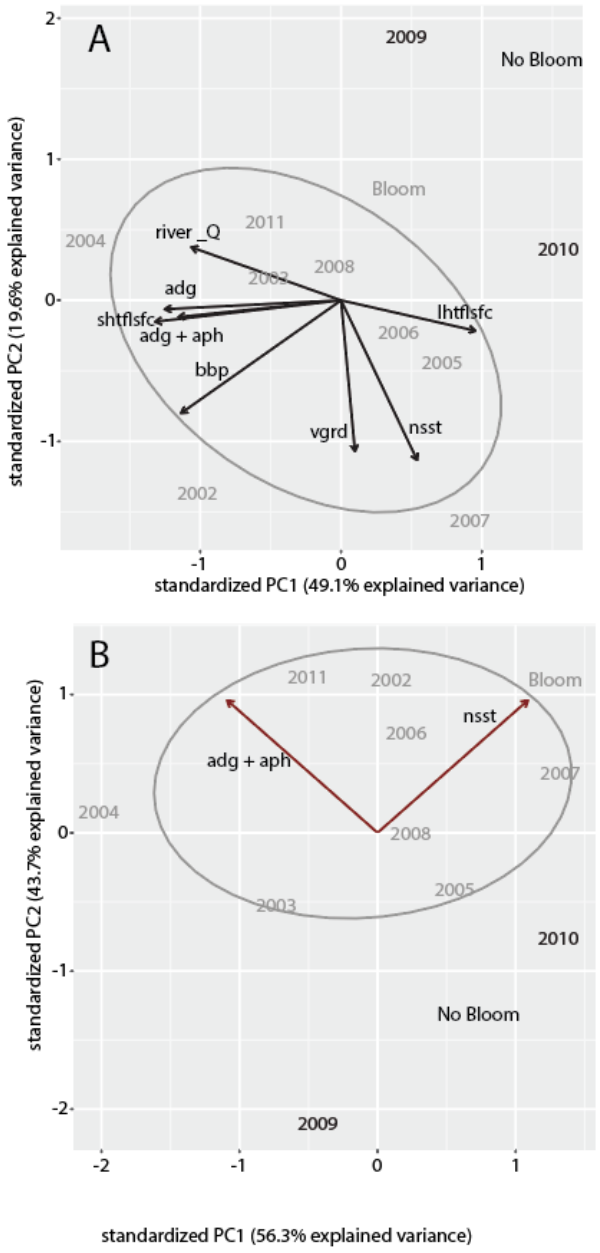

Figure 4.12. Panel A uses the eight parameters used in other PCAs (Figures 4.9, 4.11, and 4.12) to separate 2009 and 2010 from the other years in Green Bay. 2009 and 2010 had virtually no bloom at all in Green Bay. Panel B shows the PCA when only two parameters are used. Acceptable separation is still achieved, and this illustrates that the adg + aph and temperature are the driving factors in determining when no bloom forms.

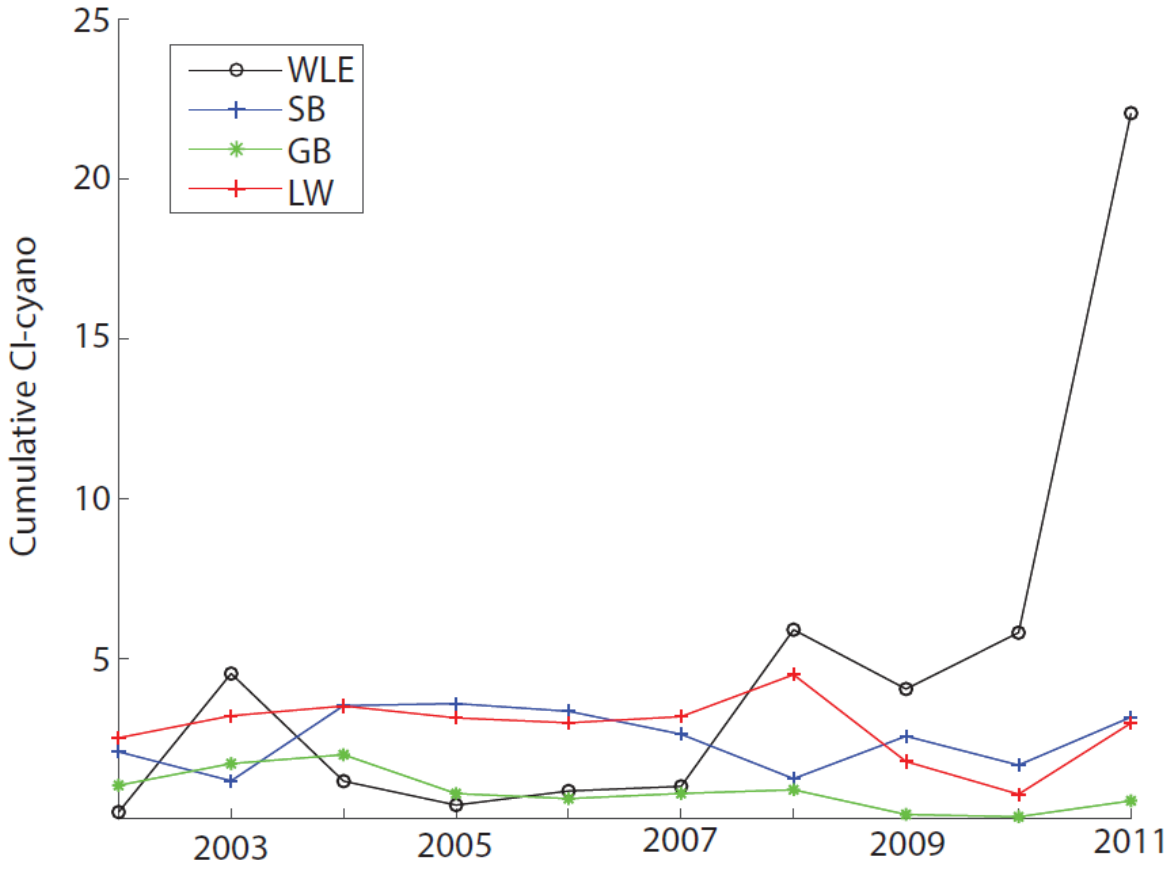

Figure 4.13. Shows the annual CI_{cyano} from western Lake Erie, (WLE), Saginaw Bay (SB), Green Bay (GB), and Lake Winnebago (LW). The annual CI_{cyano} was calculated by taking the mean of the highest three sequential 10 day composites of the CI_{cyano}.

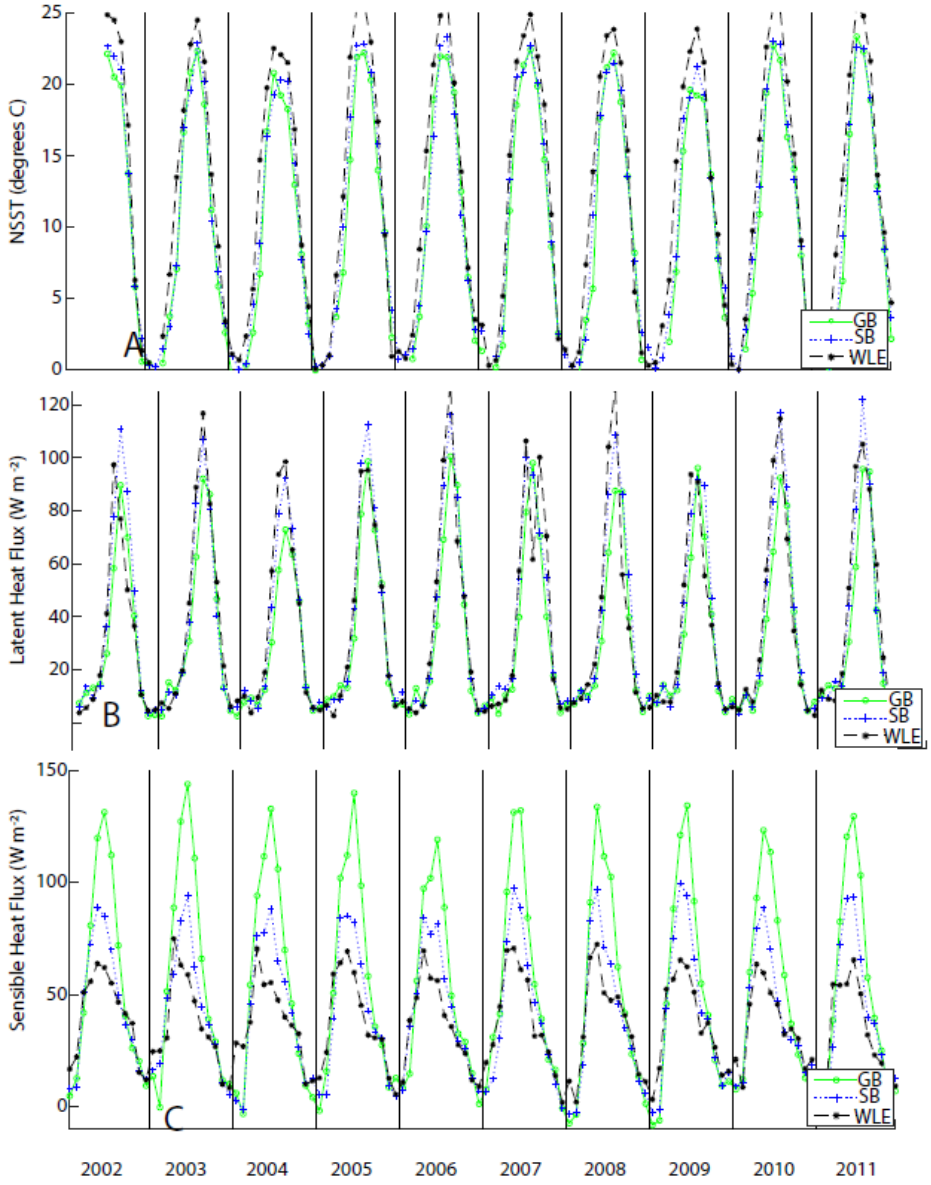

Figure 4.14. Panel A shows the night time sea surface temperature from the monthly NASA Giovanni Data from Green Bay (Green o), Saginaw Bay (blue +), and western Lake Erie (black *). Panel B shows the Latent Heat Flux from the monthly NASA Giovanni Data from Green Bay (Green o), Saginaw Bay (blue +), and western Lake Erie (black *). Panel C shows the Sensible Heat Flux from the monthly NASA Giovanni Data from Green Bay (Green o), Saginaw Bay (blue +), and western Lake Erie (black *).

Concluding Remarks

In this dissertation I examined cyanobacterial blooms in three basins in the Laurentian Great Lakes. Each basin is unique in some ways, yet all share some commonalities as well. Each basin is an enclosed, warm, shallow section of its respective lake, yet each has a unique cyanobacterial bloom phenology. Examining the bloom phenology of the disparate waters in the Laurentian Great Lakes is important because these are economically and ecologically important waters and insights gained can help with management and restoration efforts.

The five lakes of the Laurentian Great Lakes together comprise over 20% of the fresh surface water on the planet. These are also impaired waters, which have been effected to a large degree by anthropogenic processes. Including eutrophication and re-eutrophication, as well as the introduction of invasive species. Prior to the 1970s there were spectacular blooms of cyanobacteria in Lake Erie due, primarily, as a result of eutrophication. This period of eutrophication, pollution, and environmental degradation reached a peak on June 22, 1969 when the Cuyahoga River caught on fire. This led to the passage of the Clean Water Act in 1972 and the related Great Lakes Water Quality Agreement (GLWQA) that same year. From this point forwards the Great Lakes entered a period of restoration. The most critical action from the GLWQA pertaining to cyanobacterial blooms was the adoption of wide scale phosphorus abatement strategies. One of the most important adaptations pertaining to cyanobacterial bloom dynamics to come out of the GLWQA was the adaptation of target loads of total phosphorus, as each basin and lake of interest gained a target threshold to reach (e.g. Saginaw Bay was set to not exceed 440 tonnes of total phosphorus per year). Despite failing to meet these thresholds, the phosphorus abatement strategies were very successful in reducing and, ultimately, eliminating

cyanobacterial blooms in the Great Lakes. However, in the mid-1990s the Great Lakes went through a process of re-eutrophication (Scavia et al., 2014). What caused this period of re-eutrophication most likely was a combination of the colonization of invasive mussels of the genus *Dreissena* (Vanderploeg et al., 2011) and increasing concentrations of soluble reactive phosphorus (SRP) in river and runoff effluent (Baker et al., 2014). These cyanobacterial blooms started to reach massive proportions in western Lake Erie in 2008, when the lake went from a relatively dry climatological phase to a wet one.

I have used remotely sensed imagery here from both the MODIS and MERIS sensors to estimate cyanobacterial biomass over seasonal and decadal time scales to derive bloom phenologies for western Lake Erie, Saginaw Bay, and Green Bay. Satellite remote sensing provides a synoptic view providing basin wide data on cyanobacteria blooms over a number of years. Furthermore, results from these three regions can be compared as the methods are transferable. The detection method used is the cyanobacteria index (CI) developed by Wynne et al. (2008). These methods have been widely used in the Great Lakes as well as other regions (Lunetta et al., 2015; Schaeffer et al., 2018).

Each basin in this dissertation (western Lake Erie, Saginaw Bay, and Green Bay) has a significant source of nutrients that is delivered from a single river, yet the responses of the basins were are different. The Fox River provides 70% of the annual total load of Phosphorus into Green Bay (Klump et al., 1997) and the Saginaw River provides 90% of the nutrient load into Saginaw Bay (Bierman et al., 1984). In contrast, while the Maumee River is a key source of the

nutrients entering western Lake Erie it does not make up the majority of incoming phosphorus. The Maumee along with the much smaller Cuyahoga and Sandusky Rivers contribute 50% of the P load into Lake Erie (Baker et al., 2014). Despite the fact that the Maumee River supplies less than ½ of the nutrients into its basin and the other two river supply over half to their respective basins, the Maumee River has the highest correlation between its seasonal discharge and the cyanobacterial biomass as measured from the remotely sensed Cyanobacterial Index. Green Bay had no significant correlation between the river discharge and the CI product. And Saginaw Bay is weakly correlated, with the annual discharge correlating just as well as the spring discharge. These relationships most likely have to do with the type of phosphorus being delivered. The Maumee River effluent has been increasing in Soluble Reactive Phosphorus (SRP), while the Total Phosphorus (TP) concentrations have been decreasing. SRP generally originates from fertilized row crops (Baker et al., 2014) and the Maumee River watershed has far more of these crops than the Fox or Saginaw River watersheds.

The cyanobacterial blooms in western Lake Erie and Saginaw Bay are comprised of nearly monospecific blooms of *Microcystis*, but this is not the case in Green Bay. Instead cyanobacteria blooms in Green Bay can co-occur with diatoms and green algae. I have shown evidence in chapter 3 of this dissertation that this is related to the inherent optical properties of the water. The phytoplankton absorption (a_{ph}) and gelbstoff absorption (a_{dg}) are both higher relative to western Lake Erie or in Saginaw Bay, which seems to give competitive advantages to the other classes of phytoplankton in Green Bay. This is likely due to a combination of factors. The first factor is that *Microcystis* have very high light requirements and with increased a_{ph} and a_{dg} it may be more difficult to meet these light requirements. Additionally Green Bay seems to have higher wind

stress relative to Saginaw Bay and western Lake Erie, which will cause caused increased mixing, that may reduce the average light levels experienced by *Microcystis*. Furthermore, well mixed water typically leads to diatoms having competitive advantages over other classes of phytoplankton (Margalef, 1978; Margalef et al., 1979).

In conclusion, it appears that cyanobacteria blooms in the Great Lakes are in a state of flux. While these three basins are the primary "hot spots" for blooms they are not the only basins that have blooms. There have been a number of blooms in the central basin of Lake Erie (Scavia et al., 2014) and there have also been blooms in Lake St. Claire (Davis et al., 2014). Furthermore there are blooms in several smaller embayments throughout the Great Lakes. With careful remote monitoring and analysis, as carried out here for western Lake Erie, Saginaw Bay, and Green Bay, the unique phenology of these blooms can be characterized and the potential causes identified. These insights can then be used to guide management and restoration efforts.

REFERENCES

Anderson, C.R., M.R.P. Sapiano, M.B.K. Prasad, W. Long, P.J. Tango, C.W. Brown, and R. Murtugudde. 2010. Predicting potentially toxigenic *Pseudo-nitzchia* blooms in Chesapeake Bay. *Journal of Marine Systems*. 83:127-140.

Aparicio Medrano E., R.E. Uitenbogard, L.M. Dionisio Pires, B.J.H. van de Wiel, and H.J.H. Clercx. 2013. Coupling hydrodynamics and buoyancy regulation in *Microcystis aeruginosa* for its vertical distribution in lakes. *Ecological Modeling*. 248: 41-56.

Arnott, D.L., and M.J. Vanni. 1996. Nitrogen and phosphorus recycling by the zebra mussel (*Dreissena polymopha*) in the western basin of Lake Erie. *Canadian Journal of Fisheries and Aquatic Science*. 53: 646-659.

Backer, L.C., 2002. Cyanobacterial harmful algal blooms (CyanoHABs): developing a public health response. *Lake and Reservoir Management*. 18: 20-31.

Baker, D.B., R. Confesor, D.E. Ewing, L.T. Johnson, J.W. Kramer, and B.J. Merryfield. 2014. Phosphorus loading to Lake Erie from the Maumee, Sandusky, and Cuyahoga Rivers: The importance of bioavailability. *Journal of Great Lakes Research*. 40: 5502-517.

Baker, D.B., L.T. Johnson, R.B. Confessor, and J.P. Crumrine, 2017. Vertical stratification of soil phosphorus as a concern for dissolved phosphorus runoff in the Lake Erie Basin. *Journal of Environmental Quality*. 46: 1287–1295.

Baker, D.B., LT. Johnson, R.B. Confesor, J.P. Crumrine, T. Guo, and N.F. Manning. 2019. Early-term adjustments for Lake Erie phosphorus target loads to address western basin cyanobacterial blooms. *Journal of Great Lakes Research.* 45: 203-211.

Banack, S.A., J.S. Metcalf, L. Jiang, D. Craighead, L.L. Ilag, and P.A.Cox. 2012. Cyanobacteria Produce N-(*2*-Aminoethyl)Glycine, a Backbone for Peptide Nucleic Acids Which May Have Been the First Genetic Molecules for Life on Earth. *PLOS One*. 7:e49043

Beirman, V.J., D.M. Dolan, R. Kasprzyk, and J.L. Clark. 1984. Retrospective analysis of the response of Saginaw Bay, Lake Huron to reductions in phosphorus loadings. *Environmental Science and Technology*. 18: 23-31.

Behrenfeld, M.J., R.T. O'Malley, D.A. Siegel, C.R. McClain, J.L. Sarmiento, G.C. Feldman, A.J. Milligan, P.G. Falkowski, R.M. Letelier, and E.S. Boss. 2006. Climate Driven trends in contemporary ocean productivity. *Nature*. 444: 752-755.

Bertani, I., D.R. Obenour, C.E. Stegar, C.A. Stow, A.D. Gronewold, and D. Scavia. 2016. Probabilistically assessing the role of nutrient loading in harmful algal bloom formation in western Lake Erie. *Journal of Great Lakes Research*. 42: 1184-1192.

Binding, C.E., T.A. Greenberg, and R.P. Bukata. 2013. The MERIS Maximum Chlorophyll Index; its merits and limitations for inland water algal bloom monitoring. *Journal of Great Lakes Research*. 39: 100-107.

Bowling, L.C. 1990. Heat contents, thermal stabilities and Birgean wind work in dystrophic Tasmanian lakes and reservoirs. *Australian Journal of Marine and Freshwater Research*. 41: 429-441.

Bridgeman, T.B., J.D. Chaffin, and J.E. Filburn. 2013. A novel method for tracking western Lake Erie Microcystis blooms, 2002-2011. *Journal of Great Lakes Research*. 39:83-89.

Brooks, B.W., J.M. Lazorchak, M.D.A. Howard, M.V. Johnson, S.L Morton, D.A.K. Perkins, E.D. Reavie, G.I. Scott, S.A. Smith, and J.A. Stevens. 2016. Are harmful algal blooms becoming the greatest inland water quality threat to public health and aquatic ecosystems? *Environmental Toxicology and Chemistry*. 35: 6-13.

Budd, J.W., T.D. Drummer, T.F. Nalepa, and G.L. Fahnenstiel. 2001. Remote sensing of biotic effects: Zebra mussels (*Dreissena polymorpha*) influence on water clarity in Saginaw Bay, Lake Huron. *Limnology and Oceanography*. 46: 213-223.

Budd, J.W.; Beeton, A.M.; Stumpf, R.P.; Culver, D.A.; Kerfoot, W.C. 2002. Satellite observations of *Microcystis* blooms in Western Lake Erie. *Internationale Vereinigung fuer Theoretische und Angewandte Limnologie Verhandlungen* 27: 787–3793.

Carmichael, W. W. 1992. *A status report on planktonic cyanobacteria (blue green algae) and their toxins*. Environmental Monitoring Systems Laboratory, Office of Research and Development. US Environmental Protection Agency, Cincinnati, OH.

Cha, Y., C.A. Stow, K.H. Reckhow, C. DeMarchi, and T.H. Johnengen. 2010. Phosphorus load estimation in the Saginaw River, MI using a Bayesian hierarchical/multilevel model. *Water Research.* 44: 3270-3282.

Chorus, I. and J. Bartram. 1999. *Toxic Cyanobacteria in Water: A Guide to Their Public Health Consequences, Monitoring and Management*; World Health Organization: London, UK. ISBN 0-419-23930-8

Clark, J.M., B.A. Schaeffer, J.A. Darling, E.A. Urquhart, J.M. Johnson, A.R. Ignatius, M.H. Myer, K.A. Loftin, J.P. Werdell, and R.P. Stumpf. 2017. Satellite monitoring of cyanobacterial harmful algal bloom frequency in recreational waters and drinking water sources. *Ecological Indicators*. 80: 84-95.

Conley, D.J., H.W. Paerl, R.W. Howarth, D.F. Boesch, S.B. Seitzinger, K.E. Havens, C. Lancelot, and G.E. Likens. 2009. Controlling eutrophication: nitrogen and phosphorus. *Science*. 323: 1014-1015.

Conroy, J.D., W.J. Edwards, R.A. Pontius, D.D. Kane, H.Y. Zhang, J.F. Shea, J.N. Richey, and D.A. Culver. 2005. Soluble nitrogen and phosphorus excretion of exotic freshwater mussels (*Dreissena* spp.): Potential impacts for nutrient remineralization in western Lake Erie. *Freshwater Biology*. 50: 1146-1162.

Daloglu, I. K., H. Cho, and D. Scavia. 2012. Evaluating causes of trends in long-term dissolved reactive phosphorus loads to Lake Erie. *Environmental Science and Technology*. 46: 10660-10666.

Davenport, T. and W. Drake. 2011. Grand Lake St. Marys, Ohio—The case for source water protection: nutrients and algae blooms, EPA Commentary. *Lakeline*. Fall 2011. p. 41-46.

Davis, T.W., F. Koch, M.A. Marcoval, S.W. Wilhelm, and C.J. Gobler. 2012. Mesozooplankton and microzooplankton grazing during cyanobacterial blooms in the western basin of Lake Erie. *Harmful Algae*. 15: 26-35.

Davis, T.W., S.B. Watson, M.J. Rozmarynowycz, J.J.H. Ciborowski, R.M. McCay, and G.S. Bullerjahn. 2014. Phylogenies of microcystin-producing cyanobacteria in the lower Laurentian Great Lakes suggest extensive genetic connectivity. *PLOS One*. 9: e106093.

De Stasio, B.T., M.B. Schrimpf, and B.H. Cornwell. 2014. Phytoplankton communities in Green Bay, Lake Michigan after invasion by Dressenid mussels: Increased dominance of cyanobacteria. *Diversity*. 6:681-704.

Dierkes, C. 2012. Fact-checking the forecast. *Twineline*. 34: 12 pp.

Ditton, R.B., and T.L. Goodale. 1973. Water quality perception and the recreational uses of Green Bay, Lake Michigan. Water *Resources Bulletin*. 9:569-579.

Dodds, W.W., J.L. Bouska, T.J. Eitzmann, K.L. Pilger, A.J. Pitts, J.T. Riley, D.J. Schloesser, and D.J. Thornbrugh. 2009. Eutrophication of U.S. Freshwaters: Analysis of potential economic damages. *Environmental Science and Technology*. 43: 12-19.

Dolan, D.M., A.K. Yui, and R.D. Geist. 1981. Evaluation of river load estimation methods for total phosphorus. *Journal of Great Lakes Research*. 7: 207-214.

Downing, J.A., S.B. Watson, and E. McCauley. 2001. Predicting cyanobacteria dominance in lakes. *Canadian Journal of Fisheries and Aquatic Science*. 58: 1905-1908.

Dumouchelle, D.H., and E.A. Stelzer, 2014. Chemical and biological quality of water in Grand Lake St. Marys, Ohio, 2011–12, with emphasis on cyanobacteria: U.S. Geological Survey Scientific Investigations Report 2014–5210, 51 p., http://dx.doi.org/10.3133/sir20145210.

EPA. 2020. Summary of cyanotoxins treatment in drinking water. Accessed on line at https://www.epa.gov/ground-water-and-drinking-water/summary-cyanotoxins-treatment-drinking-water. Accessed online March 30, 2020.

Fahnenstiel, G.L., D.F. Millie, J. Dyble, R.W. Litaker, P.A. Tester, J. McCormick, R. Rediske, and D. Klarer. 2008. Factors affecting microcystin concentration and cell quota in Saginaw Bay, Lake Huron. *Aquatic Ecosystem Health Management*. 11: 190–195.

Fahnenstiel, G.L., M.J. Sayers, R.A. Shuchman, F. Yousef, and S.A. Pothoven. 2016. Lake-wide phytoplankton production and abundance in the Upper Great Lakes: 2010–2013. *Journal of Great Lakes Research.* 42: 619–629.

Fitzsimmons, E.G. Tap Water Ban for Toledo Residents. *New York Times*, 3 August 2014. Accessed online March 15, 2015 http://www.nytimes.com/2014/08/04/us/toledo-faces-second-day-of-water-ban.html?_r=0

Fishman, D.B., S.A. Adlerstein, H.A. Vanderploeg, G.L. Fahnenstiel, and D. Scavia. 2010. Phytoplankton community composition of Saginaw Bay, Lake Huron, during the zebra mussel (*Dreissena polymorpha*) invasion: A multivariate analysis. *Journal of Great Lakes Research*. 36: 9-19.

Flombauma, P., J.L. Gallegosa , R.A. Gordilloa , J. Rincóna , L.L. Zabalab , N. Jiaoc , D.M. Karl, W.K.W. Lie, M.W. Lomasf , D. Venezianog , C.S. Verab , J.A. Vrugta,, and A.C. Martiny. 2013. Present and future distributions of the marine cyanobacteria Prochlorococcus and Synechococcus. *Proceedings of the Academy of Natural Sciences. 110: 9824-9829.*

Franz, B.A., P.J. Werdell, G. Meister, E.J. Kwiatkowska, S.W. Bailey, Z. Ahmad and C.R. McClain. 2006. MODIS land bands for ocean color remote sensing applications*, Proceedings of Ocean Optics XVIII*. Montreal, Canada, 9-13 October 2006.

Freeman, K.S. 2011. Forecasts Aid HABs Response. *Environmental Health Perspectives*. 119:A510.

Gächter, R., Mares, A., 1985. Does settling seston release-soluble reactive phosphorus in the hypolimnion of lakes? *Limnology and Oceanography*. 30: 364-371.

Gardner, W.S., L. Yang, J.B. Cotner, T.H. Johengen, and P.J. Lavrentyev. 2001. Nitrogen dynamics in sandy freshwater sediments (Saginaw Bay, Lake Huron). *Journal of Great Lakes Research*. 27: 84-97.

Ger, K.A., L. A. Hansson, and M. Lurling. 2014. Understand cyanobacteria-zooplankton interactions in a more eutrophic world. *Freshwater Biology*. 59: 1783-1798.

Gons, H.J., M.T. Auer, and S.W. Effler. 2008. MERIS satellite chlorophyll mapping of oligotrophic and eutrophic waters in the Laurentian Great Lakes. *Remote Sensing of Environment*. 112: 4098-4106.

Gower, J. and S. King, 2007. Validation of chlorophyll fluorescence derived from MERIS on the west coast of Canada. *International Journal of Remote Sensing*. 28: 625-635.

Graham J.L., K.A. Loftin, and N. Kammon. 2009. Monitoring Recreational Freshwaters. *Lakeline.* Summer 2009, 18-24

Great Lakes Water Quality Agreement (GLWQA): Annex 4, 2012. https://www.canada.ca/en/environment-cligiovanni.gsfc.nasa.govmate-change/services/great-lakes-protection/2012-water-quality-agreement/annex-4.html. Last accessed 5/20/2020.

Great Lakes Water Quality Agreement Nutrients Annex Subcommittee (GLWQANAS). 2019. Lake Erie Binational Phosphorous Reduction Strategy. https://binational.net/wp-content/uploads/2019/06/19-148_Lake_Erie_Strategy_E_accessible.pdf. Last accessed 4/25/2020.

Gronewold, A.D., V. Fortin, B. Lofgren, A. Clites, C.A. Stow, and F. Quinn. 2013. Coasts, water levels, and climate change: A Great Lakes perspective. *Climatic Change*. 120:697-711.

Giovanni. 2020. https://disc.gsfc.nasa.gov/information/glossary?title=Giovanni%20Parameter%20Definitions. Accessed June 19, 2020.

Hallegraeff, G.M., 1993. A review of harmful algal blooms and their apparent global increase. *Phycologia*. 32: 79-99.

Harris, H.J., R.B. Wenger, P.E. Sager, and J.V. Klump. 2018. The Green Bay saga: Environmental change, scientific investigation, and watershed management. *Journal of Great Lakes Research*. 44: 829-836.

Hawkins, P.R., J. Holliday, A. Kathuria, and L. Bowling. 2005. Change in cyanobacterial biovolume due to preservation by Lugol's Iodine. Harmful Algae. 4: 1033-1044.

Hawley, N. T. Redder, R. Beletsky, E. Verhamme, D. Beletsky, and J. V. DePinto. 2014. Sediment resuspension in Saginaw Bay**.** *Journal of Great Lakes Researc*h. 40:18-27.

Heath, R.T., G.L. Fahnenstiel, W.S. Gardner, J.F. Cavaletto, and S. Hwang. 1995. Ecosystem-level effects of zebra mussels (*Dreissena polymorpha*) and enclosure experiment in Saginaw Bay, Lake Huron. *Journal of Great Lakes Researc*h. 21: 501-516.

Heidelberg University. 2019. https://ncwqr.org/monitoring/data/ Accessed December 17, 2019.

Henry, T. 2013. Carrol Township's scare with toxin a 'wake-up call'. *Toledo Blade*. September 15, 2013.

Hilborn, E.D., and V.R. Beasley. 2015. One health and cyanobacteria in freshwater systems: Animal illnesses and deaths are sentinel events for human health risks. *Toxins*. 7, 1374-1395.

Ho, J.C., and A.M. Michalak. 2017. Phytoplankton blooms in Lake Erie impacted by both long-term and springtime phosphorus loading. *Journal of Great Lakes Researc*h. 43: 221–228.

Ho, J.C., R.P. Stumpf, T.B. Bridgeman, and A.M. Michalak, 2017b. Using Landsat to extend the historical record of lacustrine phytoplankton blooms: a Lake Erie case study. *Remote Sensing of Environment*. 191: 273–285.

Houser, J.N. 2006. Water color affects the stratification, surface temperature, heat content, and mean epilimnetic irradiance of small lakes. *Canadian Journal of Aquatic Sciences*. 63: 2447-2455.

Hudnell, H.K. 2008. Cyanobacterial Harmful Algal Blooms: State of the Science and Research Needs. *Advances in Experimental Medicine and Biology.* Volume 619. Springer.

Hunter, P. D., A. N. Tyler, N. J. Willby, and D. J. Gilvear. 2008. The spatial dynamics of vertical migration by *Microcystis aeruginosa* in a eutrophic shallow lake: A case study using high spatial resolution time-series airborne remote sensing. *Limnology and Oceanography*. 53:2391-2406.

Hu, C. 2009. A novel ocean color index to detect floating algae in the global oceans. *Remote Sensing of Environnent*. 113 : 2118-2129.

Huisman, J., J. Sharples, J. Stroom, P.M. Visser, W.E.A. Kardinaal, J.M.H. Verspagen, and B. Sommeijer. 2004. Changes in turbulent mixing shift competition for light between phytoplankton species. *Ecology*. 85: 2960-2970.

Hunt, S. Ottawa County residents told drinking water might contain toxic algae. *The Columbus Dispatch*. Saturday September 7, 2013. Accessed on line Aug 29, 2016. http://www.dispatch.com/content/stories/local/2013/09/07/dont-drink-the-water-residents-told.html

Hunter, P.D., A.N. Tyler, N.J. Willby, and D.J. Gilvear. 2008. The spatial dynamics of vertical migration by Microcystis aeruginosa in a eutrophic shallow lake: A case study using high spatial resolution time-series airborne remote sensing. *Limnology and Oceanography*. 53: 2391–2406.

Ibelings, B.W., M. Vonk, H.F.J. Los, and D.T. Van der Molen, and W.M. Mooij. 2003. Fuzzy modeling of cyanobacterial surface waterblooms: Validation with NOAA-AVHRR satellite images. *Ecological Applications*. 13: 1456-1472.

Iho, A., L. Ahlvik, P. Ekhyolm, J. Lehtoranta, and P. Kortelainen. 2017. Optimal phosphorus abatement redefined: insights from coupled element cycles. *Ecological Economics*. 137: 13–19.

International Joint Commission (IJC). 1978. Great Lakes Water Quality Agreement of 1978 with Annexes and terms of reference between the United States and Canada. Signed at Ottawa, November 22, 1978. International Joint Commission, Windsor, Ont., Canada. Last accessed 5/20/2020.

International Joint Commission (IJC). 2012. 16th Biennial Report on Great Lakes Water Quality: Assessment of Progress Made Towards Restoring and Maintaining Great Lakes Water Quality Since 1987. www.ijc.org/en_/Great_Lakes_Quality

International Joint Commission (IJC). 2019. The coastal wetlands of Lake Erie: Have we lost our Swiss Army knife? Water Matters Newsletter. https://www.ijc.org/en/coastal-wetlands-western-lake-erie-have-we-lost-our-swiss-army-knife. Last accessed 5/20/2020.

IPCC. 2014. Climate Change 2014: Synthesis Report. Contribution of working groups I, II, and III to the fifth assessment report of the intergovernmental panel on climate change [Core writing team. R.K. Pachauri and L.A. Meyer (eds.)]. IPPCC, Geneva, Switzerland, 151 pp.

Jacoby, J.M., D.C. Collier, E.B. Welch, F.J. Hardy, and M. Crayton. 2000. Environmental factors associated with a toxic bloom of *Microcystis aeruginosa. Canadian Journal of Fisheries and Aquatic Sciences*. 57: 231-240.

Jeppesen, E., M. Søndergaard, M. Meerhoff, T.L. Lauridsen, and J.P. Jensen. 2007. Shallow lake restoration by nutrient loading reduction - some recent findings and challenges ahead. *Hydrobiologia*, 584: 239-252.

Jetoo, S., V.I. Grover, and G. Krantzberg. 2015. The Toledo drinking water advisory: Suggested application of the water safety planning approach. *Sustainability*. 7: 9787-9808.

Johengen, T.H., T.F. Nalepa, G.L. Fahnenstiel, and G. Goudy. 1995. Nutrient changes in Saginaw Bay, Lake Huron, after the establishment of the zebra mussel (*Dreissena polymorpha*). *Journal of Great Lakes Research*. 21: 449-464.

Juhel, G., J. Davenport, J. O'Halloran, S. Culloty, R. Ramsey, K. James, A. Furey, and O. Allis. 2006. Pseudodiarrhoea in zebra mussels *Dreissena polymorpha* (Pallas) exposed to microcystins. *The Journal of Experimental Biology*. 209: 810-816.

Kahru, M. 1997. Using satellites to monitor large-scale environmental change in the Baltic Sea, p. 43–61. *In* M. Kahru and C. W. Brown [ed.], *Monitoring algal blooms: New techniques for detecting large-scale environmental change*. Springer-Verlag.

Kane, D.D., J.D. Conroy, R.P. Richards, D.B. Baker, and D.A. Culver. 2014. Re-eutrophication of Lake Erie: correlations between tributary nutrient loads and phytoplankton biomass. *Journal of Great Lakes Research*. 40: 496–501.

King, K.W., M.R. Williams, M.L. Macrae, N.R. Fausey, J. Frankenberger, D.R Smith, P.J. Kleinman, and L.C. Brown. 2015a. Phosphorus transport in agricultural subsurface drainage: a review. *Journal of Environmental Quality*. 44: 467–485.

King, K.W., M.R. Williams, and N.R. Fausey. 2015b. Contributions of systematic tile drainage to watershed scale phosphorus transport. *Journal of Environmental Quality*. 44: 486–494.

King, K.W., M.R. Williams, L.T. Johnson, D.R. Smith, and G.A. LaBarge. 2017. Phosphorus availability in Western Lake Erie Basin drainage waters: legacy evidence across spatial scales. *Journal of Environmental Quality*. 46: 466–469.

King, K.W., M.R. Williams, G.A. LaBarge, D.R. Smith, J.M. Reutter, E.W. Duncan, and L.A. Pease. 2018. Addressing agricultural phosphorus loss in artificially drained landscapes with 4R nutrient management practices. *Journal of Soil and Water Conservation.* 73: 35–47.

Klaiber, L.B., S.R. Kramer, and E.O. Young. 2020. Impacts of tile drainage on phosphorus losses from edge-of-field plots in the Lake Champlain basin of New York. *Water*. 12: 328.

Klump, J.V., D.N. Edington, P.E. Sager, and D.M. Robertson. 1997. Sedimentary phosphorus cycling and a phosphorus mass balance for the Green Bay (Lake Michigan) ecosystem. *Canadian Journal of Fisheries and Aquatic Sciences*. 54: 10-26.

Klump, J.V., S.A. Fitzgerald, and S.A. Walpes. 2009. Benthic biogeochemical cycling, nutrient stoichiometry and carbon and nitrogen mass balances in a eutrophic freshwater bay. *Limnology and Oceanography*. 54: 692-712.

Klump, J.V., J. Bratton, K. Fermanich, P. Forsythe, H.J. Harris, R.W. Howe, and J.L. Kaster. 2018. Green Bay, Lake Michigan: A proving ground for Great Lakes restoration. *Journal of Great Lakes Research*. 44: 825-828.

Klump, J.V., S.L. Brunner, B.K. Grunert, J.L. Kaster, K. Weckerly, E.M. Houghton, J.A. Kennedy, and T.J. Valenta. 2018. Evidence of persistent, recurring summertime hypoxia in Green Bay, Lake Michigan. Journal of Great Lakes Research. 44: 841-850.

Kraft, M.E. 2006. Sustainability and water quality policy evolution in Wisconsin's Fox-Wolf River basin. *Public Works Management and Policy*. 10:202-213.

Kohler, E.A., V.L. Poole, Z.J. Reicher, and R.F. Turco. 2004. Nutrient, metal, and pesticide removal during storm and nonstorm events by a constructed wetland on an urban golf course. *Ecological Engineering*. 23: 285-298.

Kutser, T., 2009. Passive optical remote sensing of cyanobacteria and other intense phytoplankton blooms in coastal and inland waters. International Journal of Remote Sensing. 30: 4401-4425.

LaBuhn, S. and J.V. Klump. 2016. Estimating summertime epilimnetic primary production via in situ monitoring in an eutrophic freshwater embayment, Green Bay, Lake Michigan. *Journal of Great Lakes Research*. 42: 1026-1035.

Land, M., W. Graneli, A. Grimvall, C.C. Hoffman, W.J. Mitsch, K.S. Tonderski, J.T.A. Verhoeven. 2016. How effective are created or restored freshwater wetlands for nitrogen and phosphorus removal? A systematic review. *Environmental Evidence*. 5:9.

Larson, J.H., M.A. Evans, R.J. Kennedy, S.W. Bailey, K.A. Loftin, Z.R. Laughrey, R.A. Femmer, J.S. Schaeffer, W.B. Richardson, T.T. Wynne, J.C. Nelson, and J.W. Duris. 2017. Associations between cyanobacteria and indices of secondary production in the western basin of Lake Erie. *Limnology and Oceanography*. 63: 232-243.

Lee, Z.P., K.L. Carder, T.G. Peacock, C.O. Davis, and J.L. Mueller. 1996. Method to derive ocean absorption coefficients from remote-sensing reflectance. *Applied Optics*. 35: 453-462.

Li, Y., R. He, D.J. McGillicuddy, Jr., D.M. Anderson, and B.A. Keafer. 2009. Investigation of the 2006 *Alexandrium fundyense* bloom in the Gulf of Maine: In situ observations and numerical modeling. *Continental Shelf Research*. 29: 2069-2082.

Lin, P., J. V. Klump, and L. Gao. 2016. Dynamics of dissolved and particulate phosphorus influenced by seasonal hypoxia in Green Bay, Lake Michigan. *Science of the Total Environment*. 541: 1070-1082.

Liu, M., J. Ma, L. Kang, Y. Wei, Q. He, X. Hu, and H. Li. 2019. Strong turbulence benefits toxic and colonial cyanobacteria in water: A potential way of climate change impact on the expansion of Harmful Algal Blooms. *Science of the Total Environment*. 670: 613-622.

Ludsin, S.A., M.W. Kershner, K.A. Blocksom, R.L. Knight, and R.A. Stein. 2001. Life after death in Lake Erie: nutrient controls drive fish species richness, rehabilitation. *Ecological Applications*. 11: 731–746.

Lunetta, R.S., B.A. Schaeffer, R.P. Stumpf, D.L. Keith, S.A. Jacobs, and M.S. Murphy. 2015. Evaluation of cyanobacteria cell count detection derived from MERIS imagery across the eastern USA. *Remote Sensing of Environment*. 157: 24-34.

Lurling, M.., G. Waajen, and L.N. de Senerpont Domis. 2016. Evaluation of several end-of-pipe measures proposed to control cyanobacteria. *Aquatic Ecology*. 50: 499-519.

Margalef, R. 1978. Life-forms of phytoplankton as survival alternatives in an unstable environment. *Oceanologica Acta*. 1: 493-509.

Margalef, R., M. Estrada, and D. Blasco. 1979. Functional morphology of organisms involved in red tides, as adapted to decaying turbulence. In D. Taylor and H. Seliger (eds.), *Toxic Dinoflagellate Blooms.* Elsevier, New York, pp 89-94.

Matisoff, G., and J.H. Ciborowski. 2005. Lake Erie trophic status collaborative study. *Journal of Great Lakes Research*. 31: 1-10.

Michalak, A.M., E.J. Anderson, D. Beletsky, S. Boland, N.S. Bosch, T.B. Bridgeman, J.D. Chaffin, K. Cho, R. Confesor, I. Daloglu, J.V, DePinto, M.A. Evans, G.L. Fahnenstiel, L. He, J.C. Ho, L. Jenkins, T.H. Johnengen, K.C. Kuo, E. LaPorte, X. Liu, M.R. McWilliams, M.R. Moore, D.J. Posselt, R.P. Richards, D. Scavia, A.L. Steiner, E. Verhamme, D.M.Wright, and M.A. Zagorski. 2012. Record-setting algal bloom in Lake Erie caused by agricultural meteorological trends consistent with expected future conditions*. Proceedings of the National Academy of Sciences*. 110: 6448-6452.

Michigan Department of Environmental Quality Water Bureau (MDEQB). 2010. Update of phosphorus load data for Saginaw Bay. MI/DEQ/WB-10/006. Accessed online September 20, 2018. https://www.michigan.gov/documents/deq/Rathbun_watershed_P_loading_report_443718_7.pdf

Miller, G.S. and J.H. Saylor. 1985. Currents and temperatures in Green Bay, Lake Michigan. *Journal of Great Lakes Research*. 11: 97-109.

Millie, D.F., G.L. Fahnenstiel, J. Dyble Bressie, R.J. Pigg, R.R. Rediske, D.M. Klarer, P.A. Tester, and R.W. Litaker. 2008. Influence of environmental conditions on late-summer cyanobacterial abundance in Saginaw Bay, Lake Huron. *Aquatic Ecosystem Health and Management*. 11: 196-205.

Millie, D.F., G.L. Fahnenstiel, J. Dyble Bressie, R.J. Pigg, R.R. Rediske, D.M. Klarer, P.A. Tester, and R.W. Litaker. 2009. Late-summer phytoplankton in wester Lake Erie (Laurentian Great Lakes): bloom distributions, toxicity, and environmental influences. *Aquatic Ecology*. 43: 915-934.

Millie, D.F., R.J. Pigg, G.L. Fahnenstiel, and H.J. Carrick. 2010. Algal chlorophylls: A synopsis of analytical methodologies, pp 92-122. IN: Algae: Source to treatment. *American Water Works Association*. Manual M57. AWWA, Denver, Co.

Mitsch, W.J., and N. Wang. 2000. Large-scale coastal wetland restoration on the Laurentian Great Lakes: Determining the potential for water quality improvement. *Ecological Engineering*. 15: 267-282.

Mitsch, W.J., 2017. Solving Lake Erie's harmful algal blooms by restoring the Great Black Swamp in Ohio. *Ecological Engineering*. 108: 406-413.

NASA. 2016. http://seadas.gsfc.nasa.gov/. Accessed 3 February 2017.

NASA. 2019. https://giovanni.gsfc.nasa.gov/giovanni/

National Park Service (NPS). 2018. Cuyahoga River Watershed. Accessed online 19 October, 2018 at: https://www.nps.gov/cuva/learn/nature/watersheds.htm

National Sea Grant Library. 2017. Green Bay Portrait of a waterway. Accessed online 7 December, 2017. http://nsgl.gso.uri.edu/wiscu/wiscuu79001.pdf

Neilan, B.A., L.A. Pearson, J. Muenchhof, M.C. Moffitt, and E. Dittmann. 2013. Environnmental conditions that influence toxin biosynthesis in cyanobacteria. *Environmental Microbiology*. 15: 1239-1253.

Nguyen, T.D., P. Thupaki, E.J. Anderson, and M.S. Phanikumar. 2014. Summer circulation and exchange in the Saginaw Bay-Lake Huron system. *Journal of Geophysical Research: Oceans*. 119:2713-2734.

NOAA. 2012. http://www.noaanews.noaa.gov/stories2012/20120705_habs.html. Accessed March 4, 2015.

NOAA. 2013. http://www.noaanews.noaa.gov/stories2013/20130702_lakeeriehabs.html. Accessed March 4, 2015.

NOAA. 2014. http://www.noaanews.noaa.gov/stories2014/20140710_erie_hab.html. Accessed March 4, 2015.

NOAA. 2016. Available online: https://coastalscience.noaa.gov/research/habs/forecasting#season (accessed on 25 January 2017)

NOAA. 2017. Available online: https://www.glerl.noaa.gov/res/HABs_and_Hypoxia/lakeErieHABArchive/ (accessed 25 January 2017.

NOAA. 2017b. https://www.glerl.noaa.gov/res/HABs_and_Hypoxia/lakeErieHABArchive/bulletin_2016-30.pdf. (Accessed on 27 January 2017)

NPR. 2017. Algae toxins in drinking water sickened people in 2 outbreaks. https://www.npr.org/sections/health-shots/2017/11/09/563073022/algae-contaminates-drinking-water. Accessed online March 30, 2020.

Nurnberg, G., 1988. Prediction of phosphorus release rates from total and reductant soluble phosphorus in anoxic lake sediment. *Canadian Journal of Fisheries and Aquatic Sciences*. 45: 453-462.

Obenour, D.R., A.D. Gronewold, C.A. Stow, and D. Scavia. 2014. Using a Bayesian hierarchical model to improve Lake Erie cyanobacteria bloom forecasts. *Water Resources Research*. 50: 7847-7860.

OEPA, 2010, Ohio Lake Erie Phosphorus Task Force Final Report. Ohio Environmental Protection Agency. http://www.epa.ohio.gov/dsw/lakeerie/index.aspx#126087070-phase-i-information, accessed March 3, 2015.

Ohio Environmental Protection Agency (Ohio EPA)., 2008. Evaluation of lLand use/land Cover characteristics in Ohio drainages to Lake Erie. Ohio Phosphorus Task Force. Accessed online May 2, 2016 http://www.epa.ohio.gov/portals/35/lakeerie/ptaskforce/OPTF_Landuse_20081001_hres.pdf

Paerl, H.W., 1988. Nuisance phytoplankton blooms in coastal, estuarine, and inland waters. *Limnology and Oceanography*. 33: 823-847.

Paerl, H.W., and J. Huisman. 2008. Blooms like it hot. *Science*. 320:57–58.

Paerl, H.W. and J. Huisman. 2009. Climate change: A catalyst for global expansion of harmful cyanobacterial blooms. *Environmental Microbiology Reports*. 1: 27-37.

Paerl, H.W., and V.J. Paul. 2012. Climate change: Links to global expansion of harmful cyanobacteria. *Water Research*. 46: 1349-1363.

Paerl, H.W., and T.G. Otten. 2013. Harmful cyanobacterial blooms: causes, consequences, and controls. *Microbial Ecology*. 65: 995-1010.

Phillips, G., A. Kelly, J.A. Pitt, R. Sanderson, and E. Taylor. 2005. The recovery of a very shallow eutrophic lake, 20 years after the control of effluent derived phosphorus. *Freshwater Biology*. 50: 1628-1638.

Pick, R.R., and D.R.S. Lean. 1987. The role of macronutrients (C,N,P) in controlling cyanobacterial dominance in temperate lakes. *New Zealand Journal of Marine and Freshwater Research*. 21: 425-434.

Pillsbury, R.W., R.L. Lowe, Y.D. Pan, J.L. Greenwood. 2002. Changes in the benthic algal community and nutrient limitation in Saginaw Bay, Lake Huron, during the invasion of the zebra mussel (*Dreissena polymorpha*). *Journal of the North American Benthological Society*. 21: 238-252.

Pope, R.M. and E.S. Fry, 1997. Absorption spectrum (380–700 nm) of pure water. II. Integrating cavity measurements. *Applied Optics*. 36: 8710–8723.

Qualls, T.M., D.M. Dolan, T. Reed, M.E. Zorn, and J. Kennedy. 2007. Analysis of the impact of the zebra mussel *Dreissena polymorpha* on the nutrients, water clarity, and the chlorophyll-phosphorus relationship in lower Green Bay. *Journal of Great Lakes Research*. 33: 617-626.

Qualls, T., H.J. Harris, and V. Harris. 2013. The State of the Bay. University of Wisconsin Sea Grant Institute. Accessed online 28 June 2017. http://www.seagrant.wisc.edu/Home/Topics/HabitatsandEcosystems/Details.aspx?PostID=1840

Reynolds, C.S., R.L. Oliver, and A.E. Walsby. 1987. Cyanobacterial dominance: the role of buoyancy regulation in dynamic lake environments. *New Zealand Journal of Marine and Freshwater Research*. 21: 379-390.

Roberts, J.R., T.O. Hook, S.A. Ludsin, S.A. Pothoven, H.A. Vanderploeg, S.B. Brandt. 2009. Effects of hypolimnetic hypoxia on foraging and distributions of Lake Erie yellow perch. *Journal of Experimental Marine Biology and Ecology*. 381: S132-S142.

Romo, S., J. Soria, F. Fernandez, Y. Ouahid, and A. Baron-Sola. 2013. Water residence time and the dynamics of toxic cyanobacteria. *Freshwater Biology*. 58: 513-522.

Sager, P.E. and J.H. Wiersma. 1975. Phosphorus sources for lower Green Bay, Lake Michigan. *Water Pollution Control Federation.* 46: 504-514.

Sager, P.E., G. Banta, and J. Kirk. 1984. The relation between areal and volumetric expressions of 14C productivity in Green Bay, Lake Michigan. *Internationale Vereinigung fuer Theoretische und Angewandte Limnologie Verhandlungen*. 22:470-474.

Sarada, R., M.G. Pillai, and G.A. Ravishankar. 1999. Phycocyanin from *Spirulina* sp: influence of processing of biomass on phycocyanin yield, analysis of efficacy of extraction methods and stability studies on phycocyanin. *Process Biochemistry*. 34, 795-801.

Saran, S., N. Puri, N.D. Jusaja, M. Kumar, and G. Sharma. 2016. Optimization, purification and characterization of phycocyanin from Spirulina platensis. *International Journal of Applied and Pure Science and Agriculture*. 2: 15-20.

Sayers, M., G.L. Fahnenstiel, R.A. Shuchman, and M. Whitley. 2016. Cyanobacteria blooms in three eutrophic basins of the Great Lakes: a comparative analysis using remote sensing. *International Journal of Remote Sensing*. 37: 4148-4147.

Scavia D., J.D. Allan, K.K. Arend, S. Bartell, D. Beletsky, N.S. Bosch, S.B. Brandt, R.D. Briland, I. Daloğlu, J.V. DePinto, D.M. Dolan, M.A. Evans, T.M. Farmer, D. Goto, H. Han, T.O. Höök, R. Knight, S.A. Ludsin, D. Mason, A.M. Michalak, R.P. Richards, J.J. Roberts, D.K. Rucinski, E. Rutherford, D.J. Schwab, T.M. Sesterhenn, H. Zhang, Y. Zhou. 2014. Assessing and addressing the re-eutrophication of Lake Erie: Central basin hypoxia. *Journal of Great Lakes Research*. 40: 226-246.

Scavia, D., J.V. DePinto, I. Bertani. 2016. A multi-model approach to evaluating target phosphorus loads for Lake Erie. *Journal of Great Lakes Research*. 42: 1130–1150.

Scavia, D., M. Kalcic, R.L. Muenich, J. Read, N. Aloysius, I. Bertani, C. Boles, R. Confessor, J. DePinto, M. Gildow, J. Martin, T. Reddar, D. Robertson, S. Sowa, Y. Wang, and H. Yen. 2017. Multiple models guide strategies for agricultural nutrient reductions. *Frontiers in Ecology and the Environment*. 15: 126–132.

Schaeffer, B. A., K. Loftin, R.P. Stumpf, and P.J. Werdell. 2015. Agencies collaborate, develop a cyanobacteria assessment network. *EOS* 96. doi:10.1029/2015EO038809.

Schaeffer, B.A., S.W. Bailey, R.N. Comney, M. Galvin, A.R. Ignatius, J.M. Johnston, D.J. Keith, R.S. Lunetta, R. Parmar, R.P. Stumpf, E.A. Urquhart, P.J. Werdell, and K. Wolfe. 2018. Mobile device application for monitoring cyanobacteria harmful algal blooms using Sentinel-3 satellite Ocean and Land Colour Instruments. *Environmental Modelling and Software*. 109, 93-103.

Schiller, H., and R. Doerffer. 1999. Neural network for emulation of an inverse model operational derivation of Case II water properties from MERIS data. *International Journal of Remote Sensing*. 20: 1735-1746.

Schindler, D.W., R.E. Hecky, D.L. Findlay, M.P. Stainton, M.J. Paterson, K.G. Baety, M. Lyng, and S.E.M. Kasian. 2008. Eutrophication of lakes cannot be controlled by reducing nitrogen input: Results of a 37-year whole-ecosystem experiment. *Proceedings of the National Academies of Sci*ence. 105: 11254-11258.

Schirrmeister, B.E., M. Gugger, and P.C.J. Donoghue. 2015. Cyanobacteria and the great oxidation event: evidence from genes and fossils. *Paleontology*. 58: 769-785.

Seppälä, J., P. Ylöstalo, S. Kaitala, S. Hällfors, M. Raateoja, and P. Maunula. 2007. Ship-of-opportunity based phycocyanin fluorescence monitoring of the filamentous cyanobacteria bloom dynamics in the Baltic Sea. *Estuarine Coastal and Shelf Science*. 73: 489-500

Sharpley, A., H.P. Jarvie. A. Buda, L. May, B. Spears, and P. Kleinman. 2013. Phosphorus legacy: overcoming the effects of past management practices to mitigate future water quality impairment. *Journal of Environmental Quality*. 42: 1308-1326.

Sigleo, A., W. Frick. 2003. Seasonal Variations in River Flow and Nutrient Concentrations in a Northwestern USA Watershed. pp. 370-376. In: K.G. Renard, S.A. McElroy, W.J. Gburek, H.E. Canfield, and R.L. Scott [eds.], First interagency conference on research in the watersheds. U.S. Department of Agriculture.

Smayda, T.J. 1990. Novel and nuisance phytoplankton blooms in the sea: Evidence for a global epidemic. pp 29-40. In: Graneli E. [ed.] *Toxic Marine Phytoplankton*, Elsevier, NY, NY, USA.

Smith, D.R., K.W. King, L. Johnson, W. Francesconi, P. Richards, D. Baker, and A.N. Sharpley. 2015a. Surface Runoff and Tile Drainage Transport of Phosphorus in the Midwestern United States. *Journal of Environmental Quality.* 44: 495.

Smith, D.R., K.W. King, and M.R. Williams. 2015b. What is causing harmful algal blooms in Lake Erie? *Journal of Soil Water Conservation*. 70: 27A–29A.

Smith, D.R., R.S. Wilson, K.W. King, M. Zwonitzer, J.M. McGrath, R.D. Harmel, R.L. Haney, and L.T. Johnson. 2018. Lake Erie, phosphorus, and microcystin: is it really the farmer's fault? *Journal of Soil Water Conservation*. 73: 48–57.

Smith, V.H., 1983. Low nitrogen to phosphorus ratios favor dominance by blue-green algae in lake phytoplankton. *Science.* 221: 669–671.

Sondergaard, M., J.P Jensen, and E. Jeppesen. 2003. Role of sediment and internal loading of phosphorus in shallow lakes. *Hydrobiologia*. 506-509: 135-145.

Sonzogni, W.C., W.M. Repavich, J.H. Standridge, R.E. Wedepohl, and J.G. Vennie. 1988. A note on algal toxins in Wisconsin waters experiencing blue-green algal blooms. *Lake and Reservoir Management.* 4: 281-285.

Steffen, M.M., T.W. Davis, J.M.A. Stough, R.M.L. Mckay, G.S. Bullerjahn, L.E. Krausfeldt, M.L. Neitzey, G.L. Boyer, T.H. Johengen, D.C. Gossiaux, A.M. Burtner, D. Palladino, M.D. Rowe, G.J. Dick, S. Levy, B. Boone, R.P. Stumpf, T.T. Wynne, and S.W. Wilhelm. 2017. Ecophysiological examination of the Lake Erie *Microcystis* bloom in 2014: linkages between biology and the water supply shutdown of Toledo, OH. *Environmental Science and Technology*. 51: 6745-6755.

Steffensen D.A. (2008) Economic cost of cyanobacterial blooms. In: Hudnell H.K. (eds) Cyanobacterial Harmful Algal Blooms: State of the Science and Research Needs. Advances in *Experimental Medicine and Biology*, vol 619. Springer, New York, NY

Stow, C.A., J. Dyble, D.R. Kashian, T.H. Johengen, K.P. Winslow, S.D. Peacor, S.N. Francour, A.M. Burtner, D. Palladino, N. Morehead, D. Gossiaux, Y.K. Cha, S.S. Qian, and D. Miller. 2014. Phosphorus targets and eutrophication objectives in Saginaw Bay: A 35 year assessment. *Journal of Great Lakes Research*. 40: 4-10.

Stumpf, R.P., M.E. Culver, P.A. Tester, M. Tomlinson, G.J. Kirkpatrick, B.A. Pederson, E. Truby, V. Ransibrahmanakul, and M. Soracco. 2003. Monitoring *Karenia brevis* blooms in the Gulf of Mexico using satellite ocean color imagery and other data. *Harmful Algae*. 2: 147-160.

Stumpf, R.P., and P.J. Werdell. 2010. Adjustment of ocean color sensor calibration through multi-band statistics. *Optics Express.* 18: 401-412.

Stumpf, R.P., T.T. Wynne, D.B. Baker, and G.L. Fahnenstiel. 2012. Interannual variability of cyanobacterial blooms in Lake Erie. *PLoS ONE*. 7(8): e42444. doi:10.1371/journal.pone.0042444.

Stumpf, R.P. T.W. Davis, T.T. Wynne, J.L. Graham, K.A. Loftin. T.H. Johengen, D. Gossiaux, D. Palladino, and A. Burtner. 2016a. Challenges for mapping cyanotoxin patterns from remote sensing of cyanobacteria. *Harmful Algae*. 54:160-173.

Stumpf, R.P., L.T. Johnson, T.T. Wynne, and D.B. Baker. 2016b. Forecasting annual cyanobacterial bloom biomass to inform management decisions in Lake Erie. *Journal of Great Lakes Research.* 42: 1174-1183.

Tarczynska, M., Z. Romanowska-Duda, T. Jurczak, M. Zalewski. 2001. Toxic cyanobacterial blooms in a drinking water reservoir-causes, consequences and management strategy. *Water Supply*. 1: 237-246.

Thomas, D.J., S.L. Sullivan, A.L. Price, and S.M. Zimmerman. 2005. Common freshwater cyanobacteria grow in 100% CO_2. *Astrobiology*. 5: 66-74.

Trainer, V.L. and B.M. Hickey. 2003. The challenges of forecasting and managing toxigenic *Pseudo-nitzschia* blooms on the U.S. west coast. p. 55-60. In D.Scavia and N.Valetta-Silver [eds], *Ecological forecasting: New Tools for Coastal and Marine Ecosystem Management*. NOAA Technical Memo, NOS NCCOS 1

U.S. Fish and Wildlife Service (USFWS), 2019. Michigan Wetland Resources. Accessed 25 July 2019 at https://www.fws.gov/wetlands/data/Water-Summary-Reports/National-Water-Summary-Wetland-Resources-Michigan.pdf

Urquhart, E.A., B.A. Schaeffer, R.P. Stumpf, K.A. Loftin, and P.J. Werdell. 2017. A method for examining temporal changes in cyanobacteria harmful algal bloom spatial extent using satellite remote sensing. *Harmful Algae*. 67: 144-152.

Vanderhoef, L.N., C.Y. Huang, R. Musil, and J. Williams. 1974. Nitrogen-fixing by phytoplankton in Green Bay, Lake Michigan in relation to nutrient concentrations. *Limnology and Oceanography*. 19:119-125.

Vanderploeg, H.A., J.R. Jiebig, W.W. Carmichael, M.A. Agy, T.H. Johengen, G.L. Fahnenstiel, and T.F. Nalepa. 2001. Zebra Mussel (*Dreissena polymorpha*) selective filtration promoted toxic *Microcystis* blooms in Saginaw Bay (Lake Huron) and Lake Erie. *Canadian Journal of Fisheries and Aquatic Sciences*. 58: 1208-1221.

Verhamme, E.M., T.M. Redder, D.A. Schlea, J. Grush, J., J.F. Bretton, and J.V. DePinto. 2016. Development of the Western Lake Erie Ecosystem Model (WLEEM): application to connect phosphorus loads to cyanobacteria biomass. *Journal of Great Lakes Research*. 42: 1193–1205.

Vincent, R.K., X. Quin, R.M.L. McKay, and J. Miner. 2004. Phycocyanin detection from LANDSAT TM data for mapping cyanobacterial blooms in Lake Erie. *Remote Sensing of Environment*. 89: 381–392.

Wang, M. and W. Shi. 2007. The NIR-SWIR combined atmospheric correction approach for MODIS ocean color data processing. *Optics Express*. 15: 15722.

Wang, M., J. Tang, and W. Shi. 2007. MODIS-derived ocean color products along the China east coastal region. *Geophysical Research Letters*. 34:L06611.

Watson, S.B., J. Ridal, and G.L. Boyer. 2008. Taste and odor can cyanobacterial toxins: Impairment, prediction, and management in the Great Lakes. *Canadian Journal of Fisheries and Aquatic Sciences*. 65: 1779-1796.

Waybright, T.J., D.E. Terlizzi, and M.D. Ferrier. 2009. Chemical characterization of the aqueous algistic fraction of barley straw (*Hordeum vulgare*) inhibiting *Microcystis aeruginosa*. *Journal of Applied Phycology*. 21:333-340.

Welch, E.B., and G.D. Cooke. 1995. Internal phosphorus loading in shallow lakes: importance and control. *Lakes and Reservoirs Research Management*. 11: 273-281.

Wikipedia. 2015. http://en.wikipedia.org/wiki/List_of_rivers_by_discharge. Accessed March 4, 2015.

Williams, M.R., K.W. King, W. Ford, A.R. Buda, and C.D. Kennedy. 2016. Effect of tillage on macropore flow and phosphorus transport to tile drains. *Journal of Environmental Quality*. 46: 1306–1313.

Wilson, A.E., W.A. Wilson, M.E. Hay. 2006. Intraspecific variation in growth and morphology on the bloom-forming cyanobacterium *Microcystis aeruginosa*. *Applied and Environmental Microbiology*. 72: 7386-7389.

Wilson, R.S., M.A. Beetstra, J.M. Reutter, G. Hesse, K.M. DeVanna-Fussell, L.T. Johnson, K.W. King, G.A. LaBarge, J.F. Martin, and C. Winslow. 2018. Commentary: Achieving phosphorus reduction targets for Lake Erie. *Journal of Great Lakes Research*. 45: 4-11.

Wisconsin Department of Natural Resources. 2017. Healing the Lower Green Bay and Fox River Area. http://dnr.wi.gov/wnrmag/2013/08/aocinsert_10-11.pdf. Accessed online 7 December, 2017.

Wynne, T.T., R.P. Stumpf, M.C. Tomlinson, V. Ransibrahmanakul, T.A. Villareal. 2005. Detecting *Karenia brevis* blooms and algal resuspension in the western Gulf of Mexico with satellite ocean color imagery. *Harmful Algae.* 4: 992-1003.

Wynne, T.T., R.P. Stumpf, M.C. Tomlinson, R.A. Warner, P.A. Tester, J. Dyble, and G.L. Fahnenstiel. 2008. Relating spectral shape to cyanobacterial blooms in the Laurentian Great Lakes. *International Journal of Remote Sensing.* 29: 3665-3672.

Wynne, T.T., R.P. Stumpf, M.C. Tomlinson, and J. Dyble. 2010. Characterizing a cyanobacterial bloom in western Lake Erie using satellite imagery and metrological data. *Limnology and Oceanography* 55: 2025-2036.

Wynne, T.T., R.P. Stumpf, M.C. Tomlinson, D.J. Schwab, G.Y. Watabayashi, and J.D. Christensen. 2011. Estimating cyanobacterial bloom transport by coupling remotely sensed imagery and a hydrodynamic model. *Ecological Applications*. 21: 2709-2721.

Wynne, T.T., R.P. Stumpf, and T.O. Briggs. 2013a. Comparing MODIS and MERIS spectral shapes for cyanobacterial bloom detection. *International Journal of Remote Sensing.* 34: 6668-6678.

Wynne, T.T., R.P. Stumpf, M.C. Tomlinson, G.L. Fahnensteil, D.J. Schwab, J. Dyble, and S. Joshi. 2013b. Evolution of a cyanobacterial bloom forecast system in western Lake Erie: Development and initial evaluation. *Journal of Great Lakes Research.* 39:90-99.

Wynne, T.T., Meredith, A., Stumpf, R.P., Briggs, T.O., Litaker, R.W., 2018. Harmful algal bloom forecasting branch ocean color satellite imagery processing guidelines. NOAA Technical Memorandum NOS NCCOS 252. Accessed online e23 July, 2019 at https://coastalscience.noaa.gov/project/harmful-algal-bloom-hab-forecasting/

Xu, H., H.W. Paerl, B. Qin, G. Zhu, and G. Gaia. 2009. Nitrogen and phosphorus inputs control phytoplankton growth in eutrophic Lake Taihu, China. *Limnology and Oceanography*. 55: 420-432.

You, J., K. Mallery, J. Hong, and M. Hondzo. 2018, Temperature effects on growth and buoyancy of *Microcystis aeruginosa*. *Journal of Plankton Research*. 40: 16–28.

Young, T.C., J.V. DePinto, S.C. Martin, and J.S. Bonner. 1985. Algal-available particulate phosphorus in the Great Lakes Basin. *Journal of Great Lakes Research*. 11: 434–446.

Zorn, M.E., J.T. Waples, T.J. Valenta, J. Kennedy, and J.V. Klump. 2018. *In situ* high-resolution time series of dissolved phosphate in Green Bay, Lake Michigan. *Journal of Great Lakes Research*. 44: 875-882.

Zou, H., G. Pan, H. Chen, and X. Yuan. 2006. Removal of cyanobacterial blooms in Taihu Lake using local soils II. Effective removal of *Microcystis aeruginosa* using local soils and sediments modified by chitosan. *Environmental Pollution*. 141:201-205.